STRUCTURES AND EVALUATION OF BIOLOGICALLY ACTIVE CONSTITUENTS OF *CUSSONIA ZIMMERMANNII* HARMS

INAUGURALDISSERTATION

zur

Erlangung der Würde eines Doktors der Philosophie

vorgelegt der

Philosophisch-Naturwissenschaftlichen Fakultät

der Universität Basel

von

Martin W. Senn

aus

Buus (BL)

Basel 2006

Genehmigt von der Philosophisch-Naturwissenschaftlichen Fakultät
auf Antrag der Herren

Prof. Dr. U. Séquin
Prof. Dr. R. Brun
Prof. Dr. M. Hamburger

Basel, den 24. Januar 2006

Prof. Dr. H.-J. Wirz, Dekan

The following work was carried out from September 2000 to December 2004 at the Department of Chemistry of the University of Basel under the supervision of Prof. Dr. U. Séquin, and at the Swiss Tropical Institute, Basel under the supervision of Prof. Dr. R. Brun.

I would like to thank Prof. Dr. U. Séquin for the interesting topics, his guidance, supervision and support he gave me during the chemical part of my work.

I thank Prof. Dr. R. Brun for his guidance, supervision, support and encouragement he gave me during the biological part of my work, the friendly work atmosphere, many fruitful discussions and for enabling my trip to Dar Es Salaam, Tanzania.

I thank Prof. Dr. M. N. N. Nkunya for enabling the collection of plant material in Tanzania and Mr. L. B. Mwasumbi for the botanical identification of the plant species and the good time on field trips. I also thank the staff of the Department of Chemistry of the University of Dar Es Salaam for their support with collecting and processing of plant material.

I thank Dr. S. Gunzenhauser for his help and support regarding MPLC techniques and Dr. K. Kulicke for his assistance in NMR work.

I would like to thank Dr. U. Simmen for his broad interest in my work, enabling the perfomance of the receptor binding assays and for many fruitful discussions.

I thank Prof. Dr. E. Sigel for enabling the electrophysiological investigations.

I would like to express my gratitude for their kind help regarding the performance of antiparasitic assays to E. Gobright, Ch. Scheurer, and N. Schild.

I would also like to thank all my collegues at the Department of Chemistry and the Swiss Tropical Institute, M. Nydegger, A. Martin-Kohler, Ch. Liechti, G. Grossmann and S. Bernhard for the good working environment and the fruitful discussions.

CONTENTS

STRUCTURES AND EVALUATION OF BIOLOGICALLY ACTIVE CONSTITUENTS OF *CUSSONIA ZIMMERMANNII* HARMS

Abbreviations

^{13}C-NMR	Carbon Nuclear Magnetic Resonance
COSY	Correlation Spectroscopy
CPRG	Chlorophenol red-β-D-galactopyranoside
DEPT	Distortionless Enhancement by Polarization Transfer
DMAP	4-(Dimethylamino)pyridine
EC_{50}	Enhancement Concentration (half maximal receptor stimulation)
EI-MS	Electron Ionization Mass Spectrometry
FAB-MS	Fast Atom Bombardment Mass Spectrometry
FBS	Foetal Bovine Serum
FCS	Foetal Calf Serum
GABA	γ-Aminobutyric acid
$GABA_A$ receptor	γ-Aminobutyric acid type A receptor
HEPES	*N*-(2-Hydroxyethyl)piperazine-*N*'-2-ethanesulphonic acid
HMBC	Heteronuclear Multiple Bond Correlation
HMQC	Heteronuclear Multiple Quantum Coherence
^{1}H-NMR	Proton Nuclear Magnetic Resonance
HPLC	High Performance Liquid Chromatography
HR-EI-MS	High Resolution Electron Ionization Mass Spectrometry
IC_{50}	Concentration at which the parasite growth is inhibited by 50 %
IR	Infrared Spectroscopy
LD_{50}	Dosis at which 50 % of the experimental animals are killed
MEM	Minimum Essential Medium
MEM NEAA	Minimum Essential Medium Non Essential Amino Acids
MES	Equal volumes of Medium 199 in EBSS (Earle's Balanced Salt Solution) and MCDB 110 Medium
MOPS	4-Morpholinepropanesulphonic acid
MPLC	Medium Pressure Liquid Chromatography
MS-1 (**25**)	8-Hydroxyheptadeca-4,6-diyn-3-yl acetate
MS-2 (**26**)	8-Hydroxyheptadeca-1-ene-4,6-diyn-3-yl acetate
MS-4 (**27**)	16-Acetoxy-11-hydroxyoctadeca-17-ene-12,14-diynyl acetate
MS-5 (**28**)	11,16-Diacetoxyoctadeca-17-ene-12,14-diynyl acetate
n	Number of experiments

NBA	3-Nitrobenzyl alcohol
PBS	Phosphate Buffered Saline
(*R*)-MTPA-Cl	(*R*)-(-)-α-Methoxy-α-trifluoromethylphenylacetyl chloride
RP	Reversed Phase
RPMI	Roswell Park Memorial Institute
r.t.	Room temperature
SDM	Semi-Defined Medium
SI	Selectivity Index (IC_{50} cytotoxicity / IC_{50} activity)
SM	Cunningham's Medium
(*S*)-MTPA-Cl	(*S*)-(+)-α-Methoxy-α-trifluoromethylphenylacetyl chloride
spp.	species
t_R	Retention time
UV/VIS	Ultraviolet/Visible Spectroscopy

A. Theoretical Part

1. Introduction

1.1 Drug discovery

1.1.1 History of important drugs derived from plants

In 1785, Whitering published the use of *Digitalis purpurea*, and this eventually led to the isolation of digoxin, a cardiotonic agent [1]. In 1816, Sertürner isolated the analgesic, morphine, from *Papaver somniferum*, and the isolation of the antimalarial drug, quinine, from the bark of *Cinchona pubescens* was reported in 1820. Some other discovery highlights were the isolation of atropine from *Atropa belladona* in 1831, cocaine from *Erythroxylum coca* in 1860, and ephedrine from *Ephedra sinica* in 1887 [2]. The alkaloids vinblastine and vincristine from the Madagascar periwinkle *Catharanthus roseus* became available in the 1960's and are now extensively used in the treatment of different cancer disease types [3]. Another promising anticancer drug is taxol, which was isolated from *Taxus brevifolia* in 1971. In the early 1970's artemisinin, a potent and essentially non-toxic antimalarial agent was isolated from *Artemisia annua*, a Chinese medicinal plant [4].

1.1.2 Strategy in the search of new biologically active plant constituents

Of the estimated 250.000-500.000 plant species around the globe, only a small percentage has been investigated phytochemically and the fraction subjected to biological or pharmacological screening is even lower [5]. The approach to obtain an exploitable pure plant constituent involves interdisciplinary work in botany, pharmacognosy, pharmacology, chemistry and toxicology and can be formulated as follows [6] :

1) Selection, collection, proper botanical identification and drying of the plant material
2) Preparation of appropriate extracts
3) Biological screening (*in vitro* assays) of the crude extracts

4) Chromatographic separation of pure bioactive constituents (bioassay-guided fractionation)
5) Verification of the purity of the isolated compounds
6) Structure elucidation by chemical and physicochemical methods
7) Partial or total synthesis
8) Preparation of derivatives/analogues for the investigation of structure-activity relationships
9) Large-scale isolation for further pharmacological and toxicological tests

The work presented in the present thesis involved the steps 1) to 6); the procedure is summarized in scheme 1.

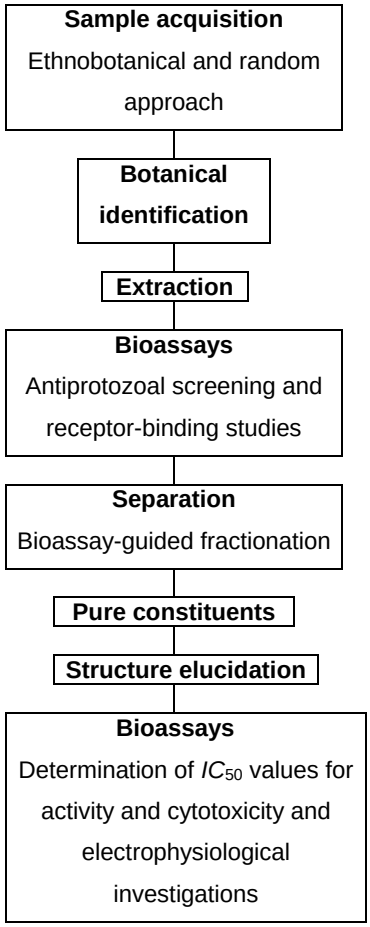

Scheme 1 : Procedure to obtain biologically active plant constituents.

One of the most delicate steps in any drug discovery program from higher plants is the selection of plant species to be collected for investigation. Possible approaches are described in the following :

Random approach

This involves collection of plants in a given locality to generate a large number of plant materials. This will provide a great chemical diversity, which increases the chance of obtaining a biologically active molecule [7].

Chemotaxonomic approach

In the chemotaxonomic approach, the plant is chosen based on taxonomic relationships to plants which have already been reported to contain compounds of biological interest [8].

Ecological approach

The survival of any organism depends on its ability to adapt to its ecosystem. It is believed, that some of the essential plant constituents have been produced by the plants either for their own physiological process or as a defense against predators. Careful observations of plant-animal interaction within a given ecosystem can serve as indicator for possible activity [7].

Ethnopharmacological approach

Ethnopharmacology can be defined as the interdisciplinary scientific exploration of biologically active agents traditionally employed or observed by man [9]. The idea of this approach is that the indigenous use of medicinal plants can offer indications to the biological activities of those plants.

1.2 Medicinal plants

Medicinal plants also known as herbs, herbal medicines, pharmacologically active plants or phytomedicinals, are the dominant form of medicine in most countries. Upwards of three-fourths of the population of the planet is primarily dependent on raw plant products to meet daily health care needs [10].

1.2.1 Reports on medicinal plants in Tanzania

Although various plants from the local flora of Tanzania are used as remedies, only a small number of these plants have been identified. *Haerdi* [11] identified 625 plants used by healers in villages around the town of Ifakara in central Tanzania. *Kokwaro* [12] listed over 1000 East African medicinal plants which are used by traditional healers in Kenya and/or Tanzania. *Hedberg et al.* [13-15] listed 153 plants which are used in the northeastern part of Tanzania. *Chhabra et al.* [16, 17] mentioned 146 plants used by healers in five regions of eastern Tanzania, Coast, Dar Es Salaam, Kilimanjaro, Morogoro and Tanga. Some Tanzanian medicinal plants have been screened for antiprotozoal activity and active plant extracts have been investigated phytochemically [18-22].

1.2.2 Antiprotozoal natural products from medicinal plants

There is a need to develop new antiprotozoal drugs which have novel structures and novel mode of action. Protozoa are responsible for several diseases which are of world wide importance, including amoebiasis, giardiasis, leishmaniasis, malaria and trypanosomiasis [23]. A selection of natural products with antiprotozoal activity is shown in table 1.

Table 1 : Natural products with antiprotozoal activity.

Natural product class	**Compound**	**Protozoa/Disease**	**Isolated from Medicinal plant/References**
A. Terpenoids			
Sesquiterpenes	Artemisinin	*Plasmodium falciparum* / Malaria	*Artemisia annua* [24]
	Yingzaosu A, C	*Plasmodium falciparum* / Malaria	*Artobotrys unicatus* [25, 26]
	Parthenin	*Plasmodium falciparum* / Malaria	*Parthenium hysterophorus* [27, 28]
	Dehydrozaluzanin C	*Leishmania* promastigotes / Leishmaniasis *Trypanosoma cruzi* / American trypanosomiasis	*Munnozia maronii* [29]

Table 1 (continued)

Natural product class	Compound	Protozoa/Disease	Isolated from Medicinal plant/References
Quassinoids	Brusatol Bruceine D	*Plasmodium falciparum* / Malaria	*Brucea javanica* [30]
B. Alkaloids			
Isoquinolines	Tetrandrine	*Plasmodium falciparum* / Malaria	*Cylea barbata* [31]
Indoles	Vinblastine	*Trypanosoma cruzi* / American trypanosomiasis	*Catharanthus roseus* [32]
C. Quinones	Jacaranone	*Leishmania amazonensis* / Leishmaniasis	*Jacaranda copaica* [33]
D. Flavonoids	Artemetin Casticin	*Plasmodium falciparum* / Malaria	*Artemisia annua* [34]

1.3 Traditional medicine

Traditional medicine is a medical system based on cultural beliefs and practices handed down from generation to generation. In many rural communities of developing countries, the use of remedies based on traditional medicine form the basic core of health care. The concept includes mystical and magical rituals, herbal therapy, and other treatments, which may not be explained by modern medicine. Traditional systems in general have had to meet the needs of local communities for many centuries.

Over the years, the World Health Assembly has adopted a number of resolutions drawing attention to the fact that most of the populations in various developing countries around the world depend on traditional medicine for primary health care, that the work force represented by practitioners of traditional medicine is a potentially important resource of the delivery of health care and the medicinal plants are of great importance to the health of individuals and communities [35].

The reasons for inclusion of traditional healers in primary health care are manifold : the healers know the sociocultural background of the people; they are highly respected and experienced in their work; economic considerations; the distances to

be covered in some countries; the strength of traditional beliefs, the shortage of health professionals, particularly in rural areas [36].

1.3.1 Traditional African medicine

Traditional African medicine can be characterised as by the following attributes [37] :

a) *Unwritten knowledge*. The body of knowledge pertaining to traditional African medicine is largely unwritten. Until recently, most of the practitioners were illiterate and the ideas upon which its practice is based have never been subjected to systematic critical evaluation.

b) *Empiricism*. The system is not based on any recognised scientific framework, but rather on the accumulated experience of what has proved effective. Empirical knowledge thus derived has been handed down from generation to generation through apprenticeship or family lineage.

c) *The role of supernatural forces*. The practice of traditional African medicine assumes the existence and participation of supernatural forces – gods, spirits etc. – in the causation of disease or other human misfortune.

1.3.2 Traditional medicine in Tanzania

Traditional medicine is an important part of the health-care system of Tanzania. In spite of an extensive program to create health centers and to train Rural Medical Aids and Medical Assistants, the traditional healer is still the only medical practitioner available, within reasonable distance, to many Tanzanians living in the rural part of the country. The number of traditional healers has been estimated to about 30.000 to 40.000, in comparison with about 600 Western-trained doctors, most of whom are working in hospitals in the big cities [13].

1.4 Tropical diseases with special reference to Africa

Epidemic diseases are not new to mankind, yet outbreaks continue to pose a threat. Reasons which attributed to Africa's current situation include : poverty, urbanization, civil strife, mass movements leading to overcrowding, collaps of public health infrastructure and environmental disasters.

The most important parasites under which Africa moans are summarised in table 2. However, the numbers listed are often underestimated due to poor availability or applicability of data. Some diseases like tuberculosis and malaria break out with so far unknown ferocity, others are resistant to drugs and almost untreatable and new deadly diseases like *Ebola haemorrhagie* fever emerge [38, 39].

Table 2 : African infectious diseases [38, 39].

Parasites	**Disease**	**Occurence**	**Mortality**
Plasmodium spp.	Malaria	23 million	0.5-3 million
Trypanosoma spp.	Trypanosomiasis	300.000	
Leishmania spp.	Leishmaniasis	12 million	
Entamoeba histolytica	Amoebiasis	5 million	5000
Onchocerca volvulus	Filariasis	18 million	
Ascaris lumbricoides	Ascariasis	> 200 million	
Schistosoma spp.	Schistosomiasis	100 million	

1.4.1 Trypanosomiasis

1.4.1.1 Introduction

Trypanosomes are classified under the subkingdom of Protozoa and the phylum Sarcomastigophora. They belong to the order Kinetoplastida and the family Trypanosomatidae. Common features of trypanosomatids are a flagellum and a kinetoplast, a small organelle consisting of a condensed network of circular DNA. All members of the Trypanosomatidae family parasitise a very diverse range of hosts, including vertebrates, invertebrates, plants and other protists [40].

1.4.1.2 African trypanosomiasis (sleeping sickness)

1.4.1.2.1 Introduction

African trypanosomiasis, also known as sleeping sickness, ranks among the top contenders for title of greatest neglected disease of mankind [41]. There are two forms of African trypanosomiasis caused by two morphologically identical parasites : *Trypanosoma brucei gambiense* causes primarily a human chronic disease and is endemic in west and central African countries, *T. b. rhodesiense* has a huge animal reservoir and is primarily zoonotic. It causes acute illness in people in eastern and southern African countries [42]. The disease was largely controlled in the 1960's, but it re-emerged in the 1980's and today 60 million people are exposed to it. 36.000 cases were reported in 1998, but only 3-4 million people are under surveillance and it is estimated that 300.000 people are infected [43].

1.4.1.2.2 The parasite

T. b. gambiense and *T. b. rhodesiense* are morphologically indistinguishable. It is a highly pleomorphic organism, frequently showing in a single blood smear a variety of forms ranging from slender-bodied organisms with a long free flagellum, reaching a length of 30 μm or more, to fatter, stumpier forms without a free flagellum which average about 15 μm in length [44].

1.4.1.2.3 Transmission and infection

The life cycle of *T. b. rhodesiense* is similar to that of *T. b. gambiense*. The infective stage is the metacyclic trypomastigote, which lives within the salivary gland of the tsetse fly. Infection occurs when an individual is bitten by an infected tsetse fly. Important vectors include *Glossina morsitans*, *G. pallidipes*, *G. fuscipes* and *G. palpalis*. The metacyclic trypomastigotes rapidly transform into bloodstream trypomastigotes within the extracellular spaces in the subcutaneous tissue. The trypomastigotes eventually find their way into the bloodstream and the lymphatics,

where they continue the replication cycle. Invasion of the cerebrospinal fluid also occurs, but does not contribute to the life cycle. The tsetse fly becomes infected when it ingests the trypomastigote while taking a blood meal from an infected individual. The trypomastigote transform into the procyclic trypomastigote and after several cycles of cell division it migrates to the insect's salivary glands, where it differentiates further into the epimastigote form. Epimastigotes develop within the salivary gland into metacyclic trypomastigotes, the infective stage for the mammalian host. Wild animals and cattle are important reservoir hosts for *T. b. rhodesiense*. For *T. b. gambiense* the main reservoir are humans [45].

1.4.1.2.4 Clinical manifestation

Initially the trypanosomes are present extracellularly in the subcutaneous tissue at the site of the bite of the tsetse fly and give rise to papular and later ulcerating lesion, often called a chancre. In the first stage trypanosomes enter the bloodstream and multiply there. This stage is accompanied by fever and lymphoid hyperplasia leading to enlargement of the spleen and especially of the cervical lymph nodes. The second stage involves central nervous invasion associated with intermittent fever. Trypanosomes in the cerebrospinal fluid produce diffuse meningoencephalitis. The central nervous system lesions are accompanied by headache, apathy, wasting of musculature, tremors, inability to walk and eventually to somnolescence, paralysis, coma and death, usually after a course of 1-3 years [46].

1.4.1.2.5 Treatment and its limitations

The drugs currently used for the treatment of sleeping sickness are suramin (**1**), pentamidine (**2**), melarsoprol (**3**), eflornithine (**4**), and nifurtimox (**5**).

Suramin (**1**) was introduced in the early 1920's and to this day remains the drug of choice for treatment of the early phase of *T. b. rhodesiense* infections. The mode of action is still a complete mystery [47].

Pentamidine (**2**) was first introduced in 1949. The drug is only used as the second-line drug when therapy with suramin (**1**) is contraindicated [48]. The mechanism of

action is not well understood. It is known that the drug is taken up by at least three transporters [49, 50] and then binds to negative-charged cellular components, and disrupts the structure of kinetoplasts DNA [51].

Melarsoprol (**3**) was introduced in 1949 for the treatment of late-stage sleeping sickness. The drug causes a serious reactive encephalopathy in 5-10 % of the cases, half of which are fatal [48]. Other common side effects include vomiting, abdominal colic and peripheral neuropathy. The mechanism of action could be the combination of trypanothione depletion and the inhibition of trypanothione reductase [47].

Eflornithine (**4**) is the drug of choice for treatment of late-stage sleeping sickness caused by *T. b. gambiense*. The drug is not recommended for *T. b. rhodesiense* infections. The inhibition of polyamine biosynthesis by eflornithine (**4**) triggers a wide range of downstream biochemical effects, but opinion is divided as to which of these are responsible for the trypanocidal effect [52].

Nifurtimox (**5**) is currently registered for the treatment of chagas disease. Side-effects are extremly common and 50 % of patients are unable to complete a full course of treatment. Nevertheless, nifurtimox (**5**) has been used in the treatment of late-stage sleeping sickness where eflornithine (**4**) or melarsoprol (**3**) are ineffective [53]. For the mode of action see chapter 1.4.1.3.5

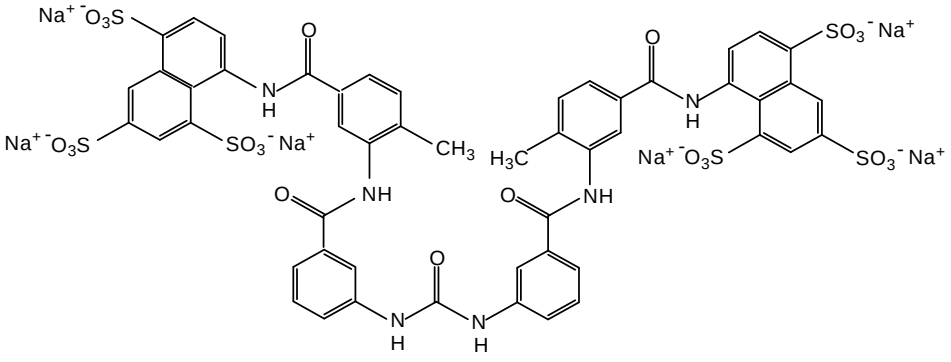

1, suramin

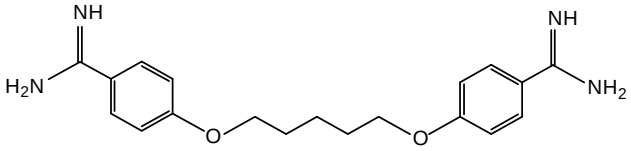

2, pentamidine

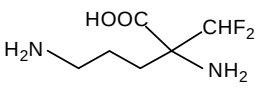

4, eflornithine

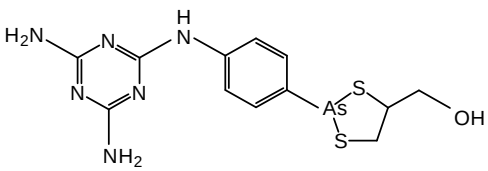

3, melarsoprol

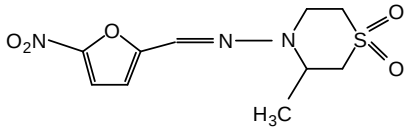

5, nifurtimox

1.4.1.3 American trypanosomiasis (chagas disease)

1.4.1.3.1 Introduction

Chagas disease, caused by *Trypanosoma cruzi*, is a major public health problem in Latin America [54]. The disease is a zoonosis, which afflicts a large variety of small mammals. The parasite is transmitted among its hosts by hematophagus reduviid bugs. Human disease occurs, when the bugs establish a habitat in human dwellings [55]. Currently, there are 18-20 million people infected and another 40 million people are at risk of aquiring the disease [56, 57].

1.4.1.3.2 The parasite

T. cruzi is an organism which differs from other trypanosomes infecting man in that it has an intracellular amastigote stage in cardiac muscle and other tissues, as well as trypomastigote forms in the circulating blood. The trypomastigotes average 20 μm in length. The nucleus is usually positioned centrally and the large oval kinetoplast is located posteriorly. In stained blood films they characteristically assume a C or U shape [44].

1.4.1.3.3 Transmission and infection

The infective stage of *T. cruzi* is the metacyclic trypomastigote. It is 15 μm in length and possesses a single nucleus and flagellum [45]. The most frequent way of transmission is by reduviid bugs (*Rhidnius* spp.; *Triatoma* spp.) [46]. Infection occurs shortly after an infected bug takes a blood meal. Its feces contain the infective trypomastigotes. The host experiences a mild itching sensation and rubs the trypomastigotes into the bite wound. Trypomastigotes enter a wide variety of cells and transform into amastigotes. The amastigote is 3-5 μm in diameter and does not possess an external flagellum. The host becomes hypersensitive to the parasite as the result of the cellular destruction at the site of initial infection. Some amastigotes transform into trypomastigotes, and after being released into the peripheral blood,

they infect other sites in the body. The bug becomes infected, when it takes a blood meal from an individual harbouring trypomastigotes. Trypomastigotes transform into epimastigotes within the midgut of the bug. Epimastigotes differentiate into metacyclic trypomastigotes within the hindgut. This is the infective stage of the parasite [45].

1.4.1.3.4 Clinical manifestation

Acute disease manifestation

T. cruzi may mark its point of entry into human body by inflammation, and when this occurs in the eye there may be conjunctivitis, unilateral palpebral oedema, and satellite adenopathy. Manifestations of generalised infection occur with fever, tachycardia, lymphadenopathy, and oedema. The acute congenital phase may be symptomless or may be associated with jaundice, skin haemmorrhages, and neurological signs.

Chronic disease manifestation

After 2-4 months the acute clinical manifestation disappears and the disease enters the chronic phase, generally starting with a long period of clinical latency, which lasts 10-30 years or throughout life. After this period many infected patients present manifestations related to the involvement of certain organs such as heart, oesophagus, colon, and nervous system.

Cardiac involvement

Heart involvement is the major aspect of chagas disease because of its characteristics, frequency, and consequences, and is also the source of most controversies. About 20-30 % of the total chagasic population in endemic areas has symptomless heart disease and these patients may live for many years. Heart disease worsens in some of them, with increasing arrythmias or heart failure [58].

1.4.1.3.5 Treatment and its limitations

The drugs used for the treatment of chagas disease are nitroheterocyclic compounds, a nitrofuran, nifurtimox (**5**) and benznidazole (**6**), a nitroimidazole derivative.

Nifurtimox (**5**) acts via the reduction of the nitro group to unstable nitroanion radicals, which in turn react to produce highly toxic, reduced oxygen metabolites [59].

Benznidazole (**6**) seems to act via a different mechanism (reductive stress), which involves covalent modification of macromolecules by nitroreduction intermediates [60]. Both nifurtimox (**5**) and benznidazole (**6**) have significant activity in the acute phase, with up to 80 % parasitological cures in treated patients [61]. However their efficacy varies according to the geographical area, probably due to differences in drug susceptibility among different *T. cruzi* strains [62, 63].

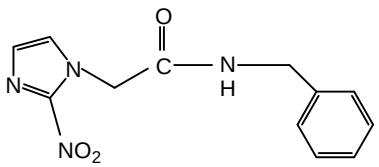

6, benznidazole

1.4.2 Malaria

1.4.2.1 Introduction

Malaria is the world's most important parasitic infection, ranking among the major health and developmental challenges for the poor countries of the world [64]. Four parasite species of the genus *Plasmodium* infect human beings. Nearly all malaria deaths are caused by *Plasmodium falciparum* [65], which is transmitted by the most efficient of the malaria vector mosquitos, *Anopheles gambiae* [66]. More than a third of the world's population live in malaria-endemic areas, and 1 billion people are estimated to carry parasites at any one time. In Africa alone, there are an estimated 200-450 million cases of fever in children infected with malaria parasites each year [67]. Estimates for annual malaria mortality range from 0.5 to 3.0 million people [68].

1.4.2.2 The parasite

The agents of human malaria are members of the genus *Plasmodium* and the suborder Haemosporina [69]. The problem with the definition is the unusual biology of these organisms. *P. falciparum*, the agent of malaria tropica, is an exceedingly small, haploid, but genomically complicated eukaryote, able to constantly change its gene expression [70].

1.4.2.3 Transmission and infection

Natural transmission is dependent on a complex interaction between host, vector, parasite and environment. The anopheline mosquito is infected via blood from an infected host (human); the parasite then matures to the sporozoit stage in the vector, and invades its salivary glands. The mosquito infects other people by injecting sporozoites in the salvia while feeding on their blood [71]. The sporozoites are then carried to the liver, where they leave the blood circulation system. Each sporozoite penetrates a “building block” cell of the liver tissue and invades hepatocytes. Whithin the liver cell, the sporozoite rounds up and transforms into a “spore”-like form. During the succeeding two weeks, this spore replicates into thousands of merozoites (cyst-like structures) and the host liver cell is destroyed in the process. The merozoites then invade the red blood cells and increase in a series of two- to three-day cycles. The first clinical attack of intense rigour and sweating with high fever develops when a large number of red cells are infected and burst. As they continue to flood into the blood stream, the resulting merozoites attach to the surface of other red blood cells and create a continuous cycle of replication [72].

1.4.2.4 Clinical manifestation

It is important to distinguish between the disease caused by malaria parasites and the frequently asymptomatic infection caused by the same parasites. It is important to recognize that one may be infected without having the disease [73]. The clinical manifestations of malaria are extremly diverse in terms of onset of signs and

symptoms, severity and complications. However, common characteristic symptoms are alternating episodes of fever and asymptomatic phases associated with symptoms like chills, headache, myalgia, joint pains, sweating and anaemia. Rigors are common and splenomegaly is a frequent consequence. Almost exclusively people infected with *P. falciparum* malaria may develop severe and complex symptoms which will usually lead to death if not treated [74].

1.4.2.5 Treatment and its limitations

Currently ten drugs are available for the treatment of malaria. These are artemisinin (**7**) and derivatives, atovaquone (**8**), benflumetol (**9**), chloroquine (**10**), halofantrine (**11**), mefloquine (**12**), primaquine (**13**), proguanil (**14**) (and chloroproguanil (**15**)), pyrimethamine (**16**) and quinine (**17**).

Artemisinin (**7**) and derivatives are used for both uncomplicated and severe *P. falciparum* malaria. The most commonly used compounds are artemether and artesunate. Artemisinins probably work by generation of free radicals in parasitised red blood cells, followed by alkylation of parasite proteins [75].

Atovaquone (**8**) is thought to inhibit mitochondrial respiration in the parasite [76] and is used orally in synergistic combination with proguanil (**14**) to treat uncomplicated *P. falciparum* malaria [77].

Benflumetol (**9**) is exclusively used in combination with artemether to treat uncomplicated *P. falciparum* malaria. Its mode of action is unknown [78].

Chloroquine (**10**) remains the most widely used antimalarial drug world wide. It works by joining with the ferriprotoporphyrin IX in the parasite, thereby antagonising the polymerisation of this toxic metabolic product into inert crystals of haemozoin [79].

Halofantrine (**11**) seems to have a mechanism of action similar to that of chloroquine (**10**). It is used for uncomplicated cases of multiresistant *P. falciparum* malaria [78].

Mefloquine (**12**) is also thought to work in much the same way as chloroquine (**10**) [80].

Primaquine (**13**) is given orally to eradicate the liver hypnozoites of *P. vivax* and *P. ovale*; it is normally given when the treatment with chloroquine (**10**) has been completed and the patient is recovering.

Proguanil (**14**) (and chloroproguanil (**15**)) are metabolised to active metabolites which inhibit parasite dihydrofolate reductase (DHFR).

Pyrimethamine (**16**) is a selective, competitive inhibitor of parasite DHFR, and is only used in synergistic combination with a sulfonamide [78].

Quinine (**17**) is reliable in the face of chloroquine-resistant *P. falciparum*. World wide, quinine (**17**) is used mainly as a parenteral drug for severe *P. falciparum* malaria.

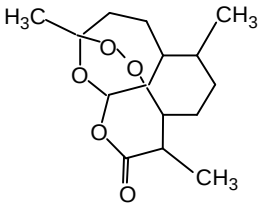

7, artemisinin

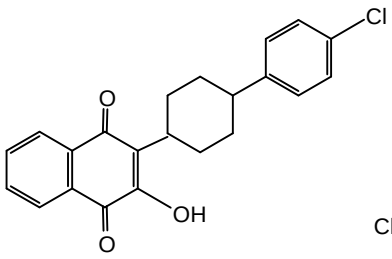

8, atovaquone

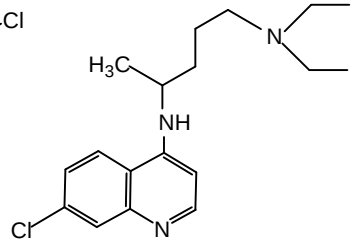

10, chloroquine

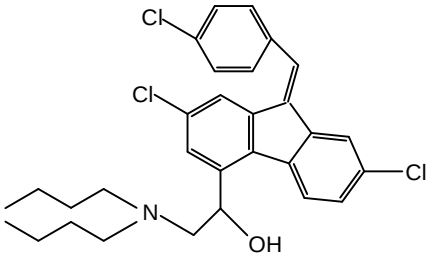

9, benflumetol

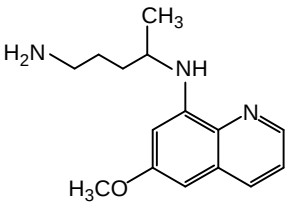

13, primaquine

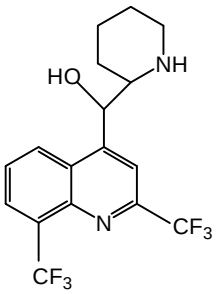

12, mefloquine

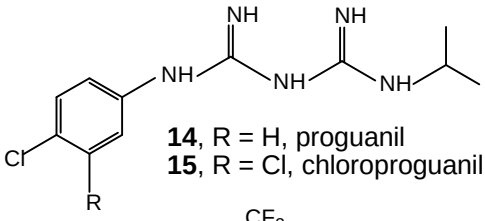

14, R = H, proguanil
15, R = Cl, chloroproguanil

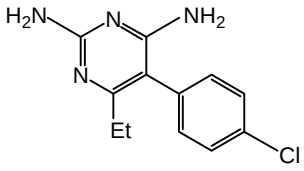

16, pyrimethamine

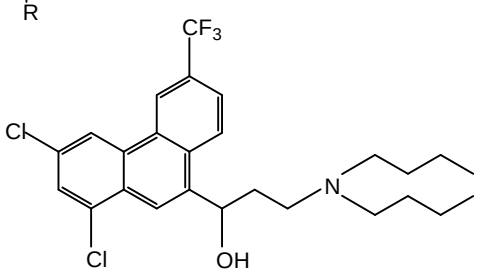

11, halofantrine

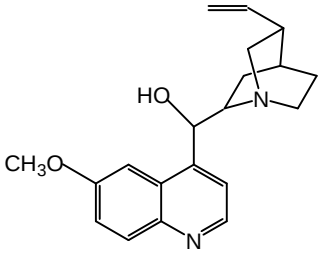

17, quinine

1.4.3 Leishmaniasis

1.4.3.1 Introduction

Leishmaniasis is a group of infections caused by the trypanosomid parasites, *Leishmania* spp. There are 350 million people residing in regions endemic to the disease. Annually, 12 million people, in at least 74 countries, are infected by the parasites [81]. The number of new cases of cutaneous leishmaniasis each year in the world is thought to be about 1.5 million. The number of new cases of visceral leishmaniasis is thought to be about 500.000 [82]. Leishmaniasis is endemic to many densely populated regions of the world including the Persian Gulf, the Mediterranean, Northern Africa, Asia, and Central and South America [83].

1.4.3.2 The parasite

Leishmaniasis is caused by hemoflagellated intracellular parasites belonging to the genus *Leishmania*. Basic anatomy and physiology include a single free flagellum, rod-shaped kinetoplasts, a single nucleus, mitochondrion and rough endoplasmatic reticulum. The size of the parasite varies not only between species, but also between amastigote and promastigote forms. The size of promastigotes (form in the insect vector) ranges from 10 to 20 μm long and 2 to 5 μm in major diameter. Amastigote cells are smaller, generally 2-3 μm in diameter and obligate intracellular [84].

1.4.3.3 Transmission and infection

Transmission begins with either the female *Phlebotomus* spp. or the *Lutzomyia* spp. sandfly taking up the pathogenic *Leishmania* spp. from an infected vertebrate host. These host reservoirs include sloths, horses, dogs, rats and other rodents [85]. Once the sandfly has been infected, the amastigote migrates to the alimentary canal of the insect where it attaches to local epidermal cells. The parasites mature and differentiate into motile promastigotes. Then they transit away from the midgut region to the pharynx and/or the proboscis of the sandfly. Upon a subsequent blood meal,

the promastigotes are injected into the blood stream of the victim and there they will be phagocytized [86]. The parasite is equipped to evade the digestive enzymes present in the vacuole. *Leishmania* spp. have a membrane bound molecule known as the lipophosphoglycan (LPG). The LPG permits intracellular survival [87, 88]. Once inside the macrophage, the parasite resides in the phagolysosomal or the parasitophorous vacuole. Here it transforms back into the infectious amastigote. Amastigotes replicate and are released back into the blood stream where similar cycles commence. Parasites are known to infect macrophages within the skin, viscera and blood tissues. Dissemination of the disease is local or systemic depending on the distinct *Leishmania* spp. involved [89].

1.4.3.4 Clinical manifestation

Three common clinical manifestations and two rare forms of leishmaniasis exist :

Cutaneous leishmaniasis (oriental sore)
The manifestation results in external lesions in the outer epidermal layers. The infection cures itself spontaneously in 4-6 months, except in the case of diffuse cutaneous leishmaniasis, which is incurable. Cutaneous leishmaniasis is primarily associated with the *L. mexican* complex, *L. tropica* and *L. major* [90].

Mucocutaneous leishmaniasis (espundia, chicler's ulcer)
This form results in ulcers within the pharyngeal and nasal mucosa and also self cures in a matter of months. The extensive scarring and degradation of tissues never completely heal. Mucocutaneous leishmaniasis is most commonly encountered in the forested areas of Central and South America and is primarily associated with the *L. braziliensis* complex [91].

Visceral leishmaniasis (kala-azar, black fever, black sickness)
This manifestation effects the lymph nodes and the internal mesentery of the liver and spleen and results in inflammation of local visceral tissues. Anemia, portal hypertension and ascites are all symptomatic of advanced infection. *L. chagasi* and *L. donovani* are responsible for this form of leishmaniasis. The disease is fatal unless

treated early. Many parasites causing visceral leishmaniasis are known to be resistant to modern chemotherapy [90].

There are two other rare forms of leishmaniasis. Recidua leishmaniasis (chronic relapsing) is a cutaneous manifestation that is responsible for the presence of chronic lesions in the epidermis. *L. tropica* is most often associated with this disease. Post-Kala Azar Dermal leishmaniasis is often encountered after a successful recovery from visceral leishmaniasis [89].

1.4.3.5 Treatment and its limitations

The drugs recommended for the treatment of leishmaniasis include the pentavalent antimonials sodium stibogluconate (pentostam), the structure of which is still not known, despite its use for over 50 years [92], and meglumine antimoniate (glucantime (**18**)), amphotericin B (**19**), and pentamidine (**2**). A more modern drug is miltefosine (**20**) [93].

The **antimonials** remain effective treatments, but the requirement for up to 28 days of parenteral administration, the variable efficacy against visceral and cutaneous leishmaniasis, and the emergence of significant resistance are all factors underlining the limitations of these drugs.

The polyene antibiotic **amphotericin B** (**19**) has proved to be highly effective for the treatment of antimonial-resistant *L. donovani* visceral leishmaniasis [94], but is an unpleasant drug because of its toxicity and the need for slow infusion parenteral administration over four hours.

The usefulness of the diamidine **pentamidine** (**2**) has been limited by its toxicity.

Perhaps the most significant recent advance has been the effective oral treatment of visceral leishmaniasis by using **miltefosine** (**20**), an alkylphosphocholine orginally developed as an anticancer drug [92].

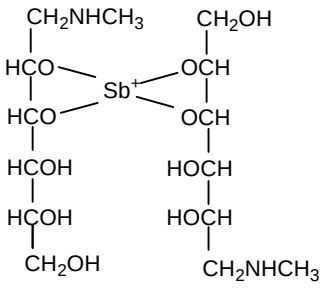

18, glucantime

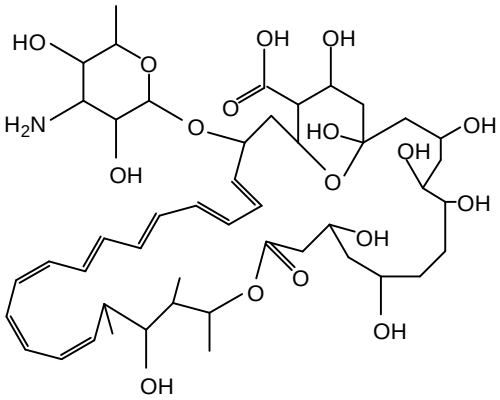

19, amphotericin B

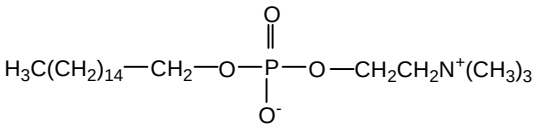

20, miltefosine

1.5 The $GABA_A$ receptor

1.5.1 Introduction

The γ-aminobutyric acid type-A ($GABA_A$) receptor is a ligand-gated anion-selective ion channel, that exists as a pentameric complex of structurally homologous subunits [95, 96]. Four families of subunits, termed α, β, γ, and δ, whose members may co-assemble to create $GABA_A$ receptors with differential biophysical and pharmacological properties, are currently recognized [97-99]. $GABA_A$ receptor isoforms mediate the majority of the inhibitory action of GABA within the central nervous system (CNS), the activation of postsynaptically located $GABA_A$ receptors resulting in an increase in membrane conductance, predominantly to chloride ions, which shunts the influence of excitatory neurotransmitters, such as glutamate [100]. $GABA_A$ receptor-mediated inhibition represents a key process in which information transfers within the CNS can be modulated by therapeutic agents. Facilation of $GABA_A$-ergic transmission by drugs from diverse chemical classes can produce a broad spectrum of behavioral effects that include anxiolytic, anticonvulsant, sedative, and most profundly, general anaesthetic actions [95].

1.5.2 GABA

γ-Aminobutyric acid (GABA) is an inhibitory neurotransmitter and present in the brain abundantly. The major pathway of GABA synthesis is decarboxylation of glutamate catalyzed by L-glutamate decarboxylase (GAD), while GABA degradation is catalyzed by GABA-α-ketoglutarase transaminase (GABA-T). The activity of GAD is also high in the neuronal tissues. Some non-neuronal tissues also have high concentration of GABA and high GAD activity, which are comparable to those of the brain. One of such tissues is the pancreatic islet. Especially B cells of the islet possess extremly high concentration of GABA and GAD activity [101, 102].

1.5.3 Molecular structure of $GABA_A$ receptors

As members of the ligand-gated ion channel family, $GABA_A$ receptors share structural and functional similarities with the nicotinic acetylcholine receptor, the glycine receptor and the $5\text{-}HT_3$ receptor, which include a pentameric pseudosymmetrical transmembrane subunit structure with a central pore. Each subunit is composed of a large N-terminal putatively extracellular domain, thought to mediate ligand-channel interactions, and four putative transmembrane domains with a large intracellular loop [103-105]. *In vivo*, fully functional $GABA_A$ receptors generally are assembled from a combination of α-, β-, and γ2- subunits [106, 107]. The subunit stochiometry has been proposed to be two α-subunits, one β-subunit, and two γ-subunits [108, 109].

1.5.4 Drugs acting at the $GABA_A$ receptor

$GABA_A$ receptors are the site of action of a variety of pharmacologically important drugs, including benzodiazepines, barbiturates, neurosteroids and ethanol [110, 111]. The clinically used **benzodiazepines**, e.g. valium (diazepam (**21**)), act as positive allosteric modulators and have sedative, hypnotic, anxiolytic, muscle-relaxant and anticonvulsant effects. Benzodiazepines act by increasing the frequency of channel openings [112]. The benzodiazepine-binding site is located at the interface between

the α and the γ subunit [113]. A great diversity in benzodiazepine pharmacology is generated by the existence of receptor isoforms containing different α and γ subunit forms. **Barbiturates**, e.g. phenobarbital (**22**), enhance the actions of GABA by increasing the average channel open time [112], in addition, at high concentrations, they directly increase channel openings, even in the absence of GABA.

Several **steroids**, among them the anaesthetic alfaxalone (**23**), have been described to enhance receptor function, whereas others, e.g. pregnanolone (**24**), inhibit the GABA response. Neurosteroids might be endogenous modulators of the $GABA_A$ receptor [114]. Whether or not **ethanol** can directly act on the $GABA_A$ receptor is discussed very controversially. It was shown to enhance receptor function [115] as well as not altering it [116].

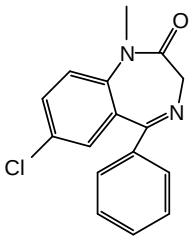

21, diazepam

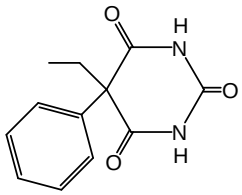

22, phenobarbital

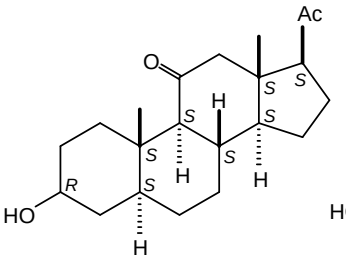

23, alfaxalone

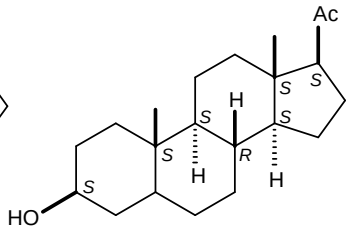

24, pregnanolone

2. Aim of the thesis

The aim of the present thesis was to isolate, identify, elucidate and evaluate antiparasitic and $GABA_A$ receptor stimulating constituents from African medicinal plants. The aim was divided into three parts :

1. Biological screening of plant extracts

Extracts of selectively collected African medicinal plants were screened for antitrypanosomal (African trypanosomes) and antiplasmodial activity and for cytotoxicity. In addition, the extracts were tested for $GABA_A$ receptor stimulation using receptor binding assays. The goal of this screening was the evaluation of the most promising plant extracts in regard to the subsequent isolation of bioactive constituents.

2. Chemical investigation of selected active plant extracts

The second part was the bioassay-guided fractionation of those plant extracts which showed significant antiparasitic activity and/or $GABA_A$ receptor stimulation in the preliminary screening and the structure elucidation of the isolated compounds.

3. Further biological investigation of the isolated compounds

In addition to the mentioned tests the isolated compounds were tested for further antiparasitic activity including antitrypanosomal (American trypanosomes) and antileishmanial activity. The cytotoxicity was determined and the compounds were investigated electrophysiologically.

3. Plant species

3.1 Selection

The selection of the plant species was based on the information obtained from two Ph.D. theses [20, 21], the availability of the plant species in Tanzania and on the information obtained from the search in the Chemical Abstracts. In addition, some plant species were selected randomly based on availability.
Gessler [20] obtained ethnobotanical information by interviewing traditional healers in Tanzania and by analyzing ethnobotanical literature regarding antimalarial plants. *Freiburghaus* [21] selected some rare Tanzanian medicinal plants randomly. Samples of the appropriate plants were collected, extracts produced and screened for antitrypanosomal or antiplasmodial activity.

Based on the obtained results, plant species were selected for the present thesis, whose extracts fulfilled the following criterions :

a) antitrypanosomal activity (*T. b. rhodesiense*) : $IC_{50} \leq 10$ µg/ml
b) antiplasmodial activity (*P. falciparum*) : $IC_{50} \leq 5$ µg/ml

Of the plant species where the extracts fulfilled these criterions not all parts have been collected and screened by *Gessler* and *Freiburghaus*. For the present thesis it was decided to collect all available parts of these plants except those whose extracts had shown no activity. It was also decided to screen all plant species for both activities, antitrypanosomal and antiplasmodial.

The Chemical Abstract search, then, provided the necessary chemical knowledge known about the selected plant species, and heavily investigated plants were removed from the selection.

3.2 Collection and identification

Plant species were collected at the end of the wet season in June and July 2001 from Pugu forest (50 km west of Dar Es Salaam) and Chalinze region (100 km west of Dar

Es Saalam) in Tanzania. The plants were botanically identified by Mr. L. B. Mwasumbi of the Institute of Botany of the University of Dar Es Salaam and voucher specimens were deposited at the Herbarium of the University of Dar Es Salaam, Tanzania. The collected plant species are shown in table 3 and 4.

Table 3 : Plant species collected from Pugu forest (*) and Chalinze region (**), selected based on the information obtained from two Ph.D. theses [20, 21].

Plant species	Synonyms	Family	Plant part
Hymenocardia ulmoides Oliv.*/** [117]	*H. poggei* Pax. *H. ulmoides* Oliv. var. *capensis* *H. capensis* (Pax.)	Euphorbiaceae	stembark rootbark root rootbark (Chalinze)
Albizia gummifera (J.F. Gmel.) C.A. Sm.* [118]	*Sassa gummifera* *Inga sassa* Willd. *A. sassa* (Willd.) *A. mearnsi* De Wild. *A. laevicorticata* Zimm.	Mimosaceae	stembark (large tree) stembark (small tree) root (small tree) rootbark (small tree)
Foetidia africana Verdc.** [119]	-	Lecythidaceae	root rootbark stembark
Salacia madagascariensis (Lam.)** [120]	*Hippocratea madagascariensis* Lam. *H. verticillata* Steud var. *madagascariensis* *H. senegalensis* Lam. var. *madagascariensis* *Tonsella madagascariensis* (Lam.) *Salacia simtata* Loes.	Celastraceae	root rootbark stembark leaves
Asteranthe asterias (S. Moore) Engl. & Diels** [121]	*Uvaria asterias* S. Moore *Asteranthopsis asterias* (S. Moore)	Annonaceae	rootbark root stembark leaves
Cussonia zimmermannii Harms* [122]	-	Araliaceae	rootbark stembark
Commiphora eminii Engl.* [123]	*C. puguensis* sensu Wild	Burseraceae	stembark

Table 4 : Plant species collected from Pugu forest (*) and Chalinze region (**), selected randomly, based on availability.

Plant species	Synonyms	Family	Plant part
Bridelia micrantha (Hochst.) Baill.* [117]	*B. speciosa* Muell. Arg. var. *trichoclada* Muell. Arg. *B. stenocarpa* Muell. Arg. *B. zanzibarensis* Vatke & Pax *B. abyssinica* Pax *B. abyssinica* Pax var. *densiflora* Gehrm. *B. mildbraedii* Gehrm. *Candelabria micrantha* Hochst.	Euphorbiaceae	stembark root rootbark
Commiphora fulvotomentosa Engl.* [123]	*C. boiviniana* Engl. *C.* sp. near *C. trollii* Mattick sensu *C. torrei* Mendes	Burseraceae	stembark
Vangueria infausta Burchell* [124]	*V. tomentosa* Hochst.	Rubiaceae	rootbark
Vernonia spp.*	-	Compositae	leaves
Bridelia cathartica Bertol. f.* [117]	*B. melanthesoides* (Baill.) Klotzsch *B. fischeri* Pax *B. lingelsheimii* Gehrm. *B. niedenzui* Gehrm. *B. fischeri* Pax var. *lingelsheimii* (Gehrm.) *B. schlechteri* Hutch. *B. cathartica* Bertol. f. subsp. *Melanthesoides* (Baill.) *Pentameria melanthesoides* Baill.	Euphorbiaceae	stembark rootbark root
Combretum harissii */a)	-	Combretaceae	root stem leaves fruits

a) New plant species [125].

3.3 Extraction

The dried plant material was hackled with a chaffcutter and powdered with a coffee grinder. The ground material was then sequentially extracted with four different solvents, starting with petroleum ether, then dichloromethane, methanol and at the end water. Thereby four extracts of different polarity were obtained from each sample. The extraction procedure is shown in scheme 2 and the yields of the crude extracts are listed in table 5. The crude extracts were then screened for biological activity.

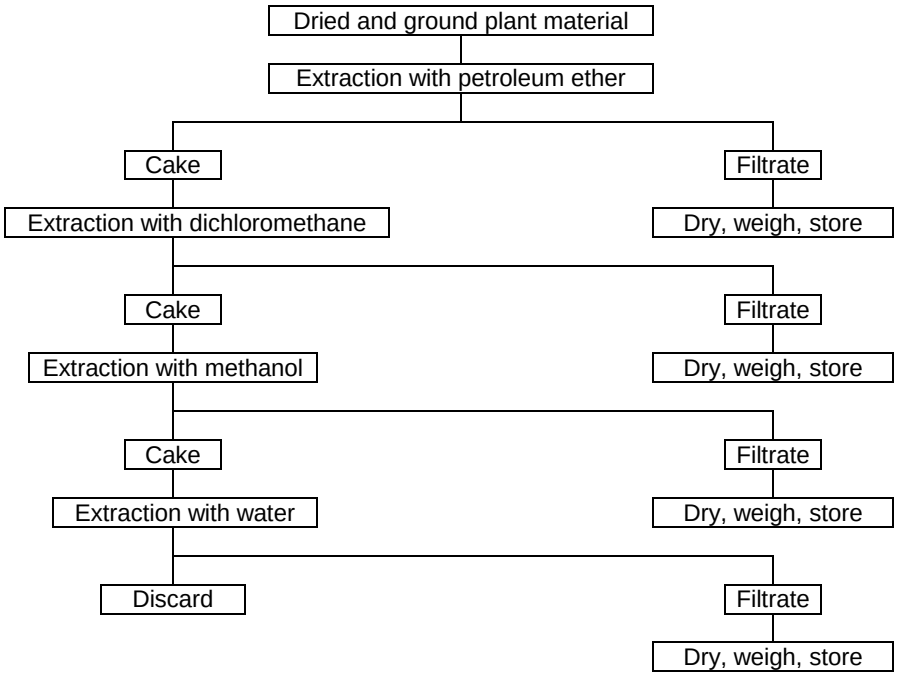

Scheme 2 : Extraction procedure.

Table 5 : Yields of the extracts obtained with different solvents from the ground plant material.

Plant species	**Part**	**Quantity** [g]	**Extracts** [mg]			
			Petroleum ether	**CH_2Cl_2**	**MeOH**	**Water**
Hymenocardia ulmoides	stembark	34.6	207	178	3917	870
	rootbark	34.7	145	119	7783	690
	root	33.3	25	50	1294	460
	rootbark (Chalinze)	34.6	148	110	5746	450
Albizia gummifera	stembark (large tree)	34.4	65	103	1212	1810
	stembark (small tree)	34.0	84	129	1291	2770
	root (small tree)	33.5	172	165	1601	550
	rootbark (small tree)	34.2	74	124	2606	3800
Foetidia africana	root	34.8	59	94	1338	340
	rootbark	34.3	472	185	6804	1600
	stembark	34.6	338	321	4153	1340
Salacia madagascar.	root	34.9	139	1507	3246	430
	rootbark	34.8	523	2350	7415	1250
	stembark	34.9	685	2251	5747	1080
	leaves	35.0	1584	641	8397	2650
Asteranthe asterias	rootbark	34.9	676	688	1476	690
	root	35.1	54	27	1005	490
	stembark	34.9	298	456	1505	1010
	leaves	35.9	1032	648	4146	1810
Cussonia zimmermannii	rootbark	35.1	220	218	3125	3520
	stembark	35.6	129	172	1261	2780
Commiphora eminii	stembark	35.9	697	324	2827	920
Bridelia micrantha	stembark	34.5	173	115	8506	620
	root	35.2	56	66	2045	730
	rootbark	34.9	135	73	7466	790
Commiphora fulvo.	stembark	34.6	197	479	1790	1030
Vangueria infausta	rootbark	35.4	88	128	2289	1670
Vernonia spp.	leaves	37.3	589	1051	3927	3710
Bridelia cathartica	stembark	35.1	150	143	4050	790
	rootbark	35.7	149	103	7020	710
	root	35.1	145	72	2484	650
Combretum harissii	root	28.7	41	52	1951	400
	stem	36.1	48	51	2269	420
	leaves	35.7	2141	487	8537	900
	fruits	35.5	600	385	10900	1210

4. Biological testing

4.1 Methodology

4.1.1 Antitrypanosomal activity testing

The assays for *T. b. rhodesiense* and *T. cruzi* were based on the LILIT (long incubation low inoculation test) [126] with minor modifications. The fluorometric evaluation of the Alamar Blue assay [127] was determined as shown by *Kaminsky* and *Brun* [128] and the concentration at which the parasite growth was inhibited by 50 % (IC_{50}) was estimated by linear interpolation between the two adjacent drug concentrations above and below the 50 % incorporation line [129]. *T*. *cruzi* assays were performed using reporter gene transfected parasites and photometric evaluation.

4.1.2 Antiplasmodial activity testing

The drug sensitivity assay was performed as previously described by *Desjardins et al.* [130]. The assay uses the uptake of [^{3}H]hypoxanthine by parasites as an indicator for viability. The IC_{50} values were calculated according to *Hills et al.* [129].

4.1.3 Antileishmanial activity testing

The assay for *L. donovani* was performed as described by *Neal* and *Croft* [131]. IC_{50} values were calculated by linear regression analysis [128].

4.1.4 Cytotoxicity testing

Cytotoxicity assays were performed using an Alamar Blue assay as described by *Pagé et al.* [132] with the modification of *Ahmed et al.* [133].

4.1.5 $GABA_A$ receptor binding assay

Modulatory effects of the ion channel $GABA_A$ receptor were performed as described by *Karobath* and *Sperk* [134] and *Simmen et al.* [135]. The stimulation of [^{3}H]flunitrazepam binding to rat cortex at a selected extract concentration was determined as a primary screen. Subsequent EC_{50} values of purified compounds were graphically determined.

4.1.6 Electrophysiological investigations

Electrophysiological investigations were performed using *Xenopus laevis* oocytes. The oocytes were prepared, injected, defolliculated and currents recorded as described by *Sigel* [136] and *Sigel et al.* [137].

4.2 Results

4.2.1 Crude plant extracts

4.2.1.1 Antitrypanosomal activity testing (African trypanosomes)

Definition of test score

Active : $IC_{50} \leq 10$ µg/ml

Moderate activity : 1 µg/ml $\leq IC_{50} \leq 10$ µg/ml

High activity : $IC_{50} < 1$ µg/ml

The summary of the results of the *in vitro* testing of the crude plant extracts on STIB 900 strain of *T. b. rhodesiense* is presented in table 6. All samples were tested in duplicate ($n = 2$). The standard drug melarsoprol exhibited an IC_{50} value of 0.0042 µg/ml.

Table 6 : IC_{50} values of the crude extracts. All values as µg/ml.

Plant species	Part	Extracts			
		Petroleum ether	CH_2Cl_2	MeOH	Water
Hymenocardia ulmoides	stembark	49.8	23.1	**6.2**[1]	**6.5**[1]
	rootbark	70.4	19.1	**5.0**[1]	18.5
	root	61.9	15.3	**8.6**[1]	32.5
	rootbark (Chalinze)	> 100	53.3	**6.5**[1]	26.6
Albizia gummifera	stembark (large tree)	88.6	19.5	15.4	48.4
	stembark (small tree)	64.6	22.4	17.8	23.3
	root (small tree)	58.0	**5.0**[1]	**9.8**[1]	52.7
	rootbark (small tree)	55.8	**9.6**[1]	24.1	37.4
Foetidia africana	root	57.2	**7.1**[1]	**3.8**[1]	22.1
	rootbark	59.5	25.1	**7.3**[1]	58.5
	stembark	81.2	27.9	**4.6**[1]	58.8
Salacia madagascariensis	root	**4.0**[1]	16.9	13.2	19.6
	rootbark	**0.15**[2]	**1.7**[1]	18.0	51.0
	stembark	**0.21**[2]	**1.6**[1]	28.9	15.2
	leaves	18.3	45.3	27.7	14.9
Asteranthe asterias	rootbark	**6.2**[1]	**2.9**[1]	14.0	11.4
	root	**2.6**[1]	**5.4**[1]	10.7	42.4
	stembark	**6.2**[1]	**6.5**[1]	13.9	42.0
	leaves	27.8	**4.8**[1]	10.8	38.0
Cussonia zimmermannii	rootbark	**4.8**[1]	21.1	59.6	58.9
	stembark	**8.8**[1]	14.8	23.0	18.0
Commiphora eminii	stembark	**4.3**[1]	**3.9**[1]	16.1	52.7
Bridelia micrantha	stembark	**0.70**[2]	14.6	**2.2**[1]	17.0
	root	**1.2**[1]	**8.2**[1]	**4.5**[1]	11.7
	rootbark	**0.68**[2]	20.1	**4.2**[1]	29.2
Commiphora fulvotomentosa	stembark	**2.1**[1]	**6.5**[1]	13.1	34.1
Vangueria infausta	rootbark	**1.5**[1]	**3.0**[1]	15.4	56.6
Vernonia spp.	leaves	**4.3**[1]	**1.8**[1]	60.3	24.1
Bridelia cathartica	stembark	59.6	10.9	**7.9**[1]	18.3
	rootbark	**5.0**[1]	**2.0**[1]	**5.0**[1]	18.6
	root	**1.5**[1]	**2.2**[1]	**3.9**[1]	17.1
Combretum harissii	root	80.3	**9.6**[1]	26.5	56.2
	stem	19.9	13.6	20.6	52.3
	leaves	76.0	25.5	15.9	**9.7**[1]
	fruits	20.1	22.3	**7.6**[1]	21.9

bold : Active extracts
[1] : Moderate activity
[2] : High activity

From the antitrypanosomal screening of the crude plant extracts it could be found that of a total of 140 extracts from 35 samples of 13 plant species, 89 (64 %) showed no activity and 51 (36 %) exhibited significant activity against *T. b. rhodesiense* STIB 900 strain. Of the 51 active extracts 47 (92 %) showed moderate activity and 4 (8 %) showed high activity. 17 (49 %) of the petroleum ether extracts, 17 (49 %) of the dichloromethane, 15 (43 %) of the methanol and 2 (8 %) of the water extracts were found to be active. The most active extracts were the petroleum ether extracts of the rootbark and the stembark of *Salacia madagascariensis* and the rootbark and the stembark of *Bridelia micrantha.* Their IC_{50} values of 0.15 and 0.21 µg/ml were compared with the standard drug melarsoprol (IC_{50} = 0.0042 µg/ml) and found about 36 respectively 50-fold higher.

4.2.1.2 Antiplasmodial activity testing

Definition of test score

Active : $IC_{50} \leq 5$ µg/ml

Moderate activity : 0.5 µg/ml $\leq IC_{50} \leq 5$ µg/ml

High activity : $IC_{50} < 0.5$ µg/ml

The summary of the results of the *in vitro* testing of the crude plant extracts on K1 strain of *P. falciparum* is presented in table 7. All samples were tested in duplicate (*n* = 2). The standard drugs chloroquine and artemisinin exhibited an IC_{50} value of 0.036 µg/ml and 0.0023 µg/ml, respectively.

Table 7 : IC_{50} values of the crude extracts. All values as µg/ml.

Plant species	Part	Extracts			
		Petroleum ether	CH_2Cl_2	MeOH	Water
Hymenocardia ulmoides	stembark	13.1	7.8	> 20	11.4
	rootbark	13.9	**3.2**[1]	> 20	> 20
	root	> 20	13.4	> 20	> 20
	rootbark (Chalinze)	> 20	5.4	> 20	> 20
Albizia gummifera	stembark (large tree)	15.5	11.0	> 20	6.6
	stembark (small tree)	> 20	15.3	> 20	> 20
	root (small tree)	> 20	**2.6**[1]	**1.6**[1]	> 20
	rootbark (small tree)	> 20	11.2	> 20	> 20
Foetidia africana	root	> 20	17.7	16.1	> 20
	rootbark	> 20	11.0	> 20	> 20
	stembark	16.8	5.4	> 20	> 20
Salacia madagascariensis	root	**0.96**[1]	> 20	> 20	> 20
	rootbark	**0.053**[2]	**0.73**[1]	> 20	> 20
	stembark	**0.087**[2]	**1.0**[1]	> 20	> 20
	leaves	> 20	> 20	> 20	> 20
Asteranthe asterias	rootbark	**2.1**[1]	**0.88**[1]	17.9	> 20
	root	**2.4**[1]	**2.8**[1]	> 20	> 20
	stembark	**1.3**[1]	**1.2**[1]	> 20	> 20
	leaves	> 20	**3.3**[1]	> 20	> 20
Cussonia zimmermannii	rootbark	**3.3**[1]	5.9	> 20	> 20
	stembark	13.6	6.4	> 20	> 20
Commiphora eminii	stembark	6.0	**2.8**[1]	> 20	> 20
Bridelia micrantha	stembark	14.5	13.8	> 20	> 20
	root	> 20	11.5	12.1	> 20
	rootbark	> 20	15.0	> 20	> 20
Commiphora fulvotomentosa	stembark	7.0	9.3	> 20	> 20
Vangueria infausta	rootbark	> 20	8.3	> 20	> 20
Vernonia spp.	leaves	> 20	**3.2**[1]	> 20	> 20
Bridelia cathartica	stembark	> 20	8.3	> 20	> 20
	rootbark	> 20	6.9	> 20	> 20
	root	> 20	> 20	7.4	> 20
Combretum harissii	root	> 20	6.2	> 20	> 20
	stem	> 20	10.9	> 20	> 20
	leaves	> 20	12.4	> 20	> 20
	fruits	17.7	7.6	12.6	> 20

bold : Active extracts
[1] : Moderate activity
[2] : High activity

From the antiplasmodial screening of the crude plant extracts it could be found that of a total of 140 extracts from 35 samples of 13 plant species, 122 (87 %) showed no activity and 18 (13 %) exhibited significant activity against *P. falciparum* K1 strain. Of the 18 active extracts 16 (89 %) showed moderate activity and 2 (11 %) showed high activity. 7 (20 %) of the petroleum ether extracts, 10 (29 %) of the dichloromethane, 1 (3 %) of the methanol and none of the water extracts were found to be active.

The most active extracts were the petroleum ether extracts of the rootbark and the stembark of *Salacia madagascariensis*. Their IC_{50} values of 0.053 and 0.087 µg/ml were compared with the standard drugs chloroquine (IC_{50} = 0.036 µg/ml) and artemisinin (IC_{50} = 0.0023 µg/ml) and found about 1.5 and 23, and 2.4 and 38-fold higher.

4.2.1.3 Summary of the antiparasitic and the cytotoxicity testings

51 crude plant extracts which showed significant activity either in the antitrypanosomal and/or in the antiplasmodial testing were tested for cytotoxicity.

The results of the antiparasitic and the cytotoxicity testings of the active crude extracts and the appropriate selectivity indices are summarised in table 8. All samples were tested in duplicate (*n* = 2).

Table 8 : Summary of the antiparasitic and cytotoxicity test results of the active extracts.

Standard drugs/ Plant species	**Part**	**Extract**	***IC*$_{50}$ *T.b. rhod.* [µg/ml]**	***IC*$_{50}$ *P. falc.* [µg/ml]**	***IC*$_{50}$ Cytotox. [µg/ml]**	**SI *T.b. rhod.***	**SI *P. falc.***
Standard drugs							
Melarsoprol			0.0042				
Mefloquine					1.7		
Chloroquine				0.036			
Artemisinin				0.0023			
Plant species							
Salacia madagascar.	rb	PE	0.15	0.053	0.34	2.3	6.4
Salacia madagascar.	sb	PE	0.21	0.087	0.45	2.1	5.2
Bridelia micrantha	rb	PE	0.68	> 20	40.0	58.8	
Bridelia micrantha	sb	PE	0.70	14.5	12.8	18.3	0.9
Bridelia micrantha	r	PE	1.2	> 20	> 100	> 83	
Vangueria infausta	rb	PE	1.5	> 20	20.7	13.8	
Bridelia cathartica	r	PE	1.5	> 20	12.0	8.0	

Table 8 (continued)

Standard drugs/ Plant species	**Part**	**Extract**	***IC*$_{50}$ *T.b. rhod.* [µg/ml]**	***IC*$_{50}$ *P. falc.* [µg/ml]**	***IC*$_{50}$ Cytotox. [µg/ml]**	**SI *T.b. rhod.***	**SI *P. falc.***
Salacia madagascar.	sb	CH_2Cl_2	1.6	1.0	5.7	3.6	5.7
Salacia madagascar.	rb	CH_2Cl_2	1.7	0.73	2.6	1.5	3.6
Vernonia spp.	l	CH_2Cl_2	1.8	3.2	3.0	1.6	0.94
Bridelia cathartica	rb	CH_2Cl_2	2.0	6.9	0.85	0.43	0.12
Commiphora fulvo.	sb	PE	2.1	7.0	45.0	21.4	6.4
Bridelia cathartica	r	CH_2Cl_2	2.2	> 20	6.0	2.7	
Bridelia micrantha	sb	MeOH	2.2	> 20	60.0	27.1	
Asteranthe asterias	r	PE	2.6	2.4	50.1	19.3	20.9
Asteranthe asterias	rb	CH_2Cl_2	2.9	0.88	17.1	5.9	19.4
Vangueria infausta	rb	CH_2Cl_2	3.0	8.3	33.2	11.1	4.0
Foetidia africana	r	MeOH	3.8	16.1	51.0	13.4	3.2
Commiphora eminii	sb	CH_2Cl_2	3.9	2.8	15.4	3.9	5.5
Bridelia cathartica	r	MeOH	3.9	7.4	23.7	6.1	3.2
Salacia madagascar.	r	PE	4.0	0.96	15.3	3.8	15.9
Bridelia micrantha	rb	MeOH	4.2	> 20	62.0	14.8	
Commiphora eminii	sb	PE	4.3	6.0	29.3	6.8	4.9
Vernonia spp.	l	PE	4.3	> 20	73.8	17.2	
Bridelia micrantha	root	MeOH	4.5	12.1	28.8	6.4	2.4
Foetidia africana	sb	MeOH	4.6	> 20	51.2	11.1	
Asteranthe asterias	l	CH_2Cl_2	4.8	3.3	22.9	4.8	6.9
Cussonia zimmerm.	rb	PE	4.8	3.3	6.9	1.4	2.1
Bridelia cathartica	rb	PE	5.0	> 20	16.1	3.2	
Bridelia cathartica	rb	MeOH	5.0	> 20	8.7	1.7	
Hymenocardia ulmo.	rb	MeOH	5.0	> 20	37.6	7.5	
Albizia gummifera (small tree)	r	CH_2Cl_2	5.0	2.6	57.8	11.6	22.2
Asteranthe asterias	r	CH_2Cl_2	5.4	2.8	26.3	4.9	9.4
Hymenocardia ulmo.	sb	MeOH	6.2	> 20	43.2	7.0	
Asteranthe asterias	rb	PE	6.2	2.1	15.8	2.5	7.5
Asteranthe asterias	sb	PE	6.2	1.3	14.4	2.3	11.1
Hymenocardia ulmo.	sb	MeOH	6.5	11.4	26.4	4.1	2.3
Hymenocardia ulmo. (Chalinze)	rb	MeOH	6.5	> 20	51.2	7.9	
Asteranthe asterias	sb	CH_2Cl_2	6.5	1.2	16.8	2.6	14.0
Commiphora fulvo.	sb	CH_2Cl_2	6.5	9.3	15.4	2.4	1.7
Foetidia africana	r	CH_2Cl_2	7.1	17.7	67.4	9.5	3.8
Foetidia africana	rb	MeOH	7.3	> 20	54.1	7.4	
Combretum harissii	f	MeOH	7.6	12.6	79.0	10.4	6.3
Bridelia cathartica	sb	MeOH	7.9	> 20	1.9	0.24	
Bridelia micrantha	r	CH_2Cl_2	8.2	11.5	> 100	> 12.2	

Table 8 (continued)

Standard drugs/ Plant species	**Part**	**Extract**	***IC*$_{50}$ *T.b. rhod.* [µg/ml]**	***IC*$_{50}$ *P. falc.* [µg/ml]**	***IC*$_{50}$ Cytotox. [µg/ml]**	**SI *T.b. rhod.***	**SI *P. falc.***
Hymenocardia ulmo.	r	MeOH	8.6	> 20	64.3	7.5	
Cussonia zimmerm.	sb	PE	8.8	13.6	88.4	10.0	6.5
Albizia gummifera (small tree)	rb	CH_2Cl_2	9.6	11.2	77.7	8.1	6.9
Combretum harissii	r	CH_2Cl_2	9.6	6.2	11.8	1.2	1.9
Combretum harissii	l	Water	9.7	15.0	75.2	7.8	5.0
Albizia gummifera (small tree)	r	MeOH	9.8	1.6	49.7	5.1	31.1

SI : selectivity index = *IC*$_{50}$ cytotoxicity / *IC*$_{50}$ activity
rb : rootbark
sb : stembark
r : root
l : leaves
f : fruits
PE : petroleum ether

The selectivity indices (SI) of the extracts with antitrypanosomal activity were in the range from 0.24 to > 83 and the SI of the extracts with antiplasmodial activity were in the range from 0.12 to 31.1.

4.2.1.4 $GABA_A$ receptor binding assay

Definition of test score

Enhanced binding : relative specific binding ≥ 120 %
Moderate enhanced binding : 120 % ≤ relative specific binding ≤ 140 %
High enhanced binding : relative specific binding > 140 %

The summary of the results of the crude plant extracts in the [^{3}H]flunitrazepam binding assay to rat cortex membranes is presented in table 9. The extract concentration tested was 50 µg/ml. All samples were tested in triplicate (*n* = 3). The standard compound GABA exhibited a relative specific binding of 124 % at a concentration of 10 µM.

Specific binding : Total binding – non specific binding
Relative specific binding : Specific binding (%) = 100 %

Table 9 : Relative specific binding of the crude plant extracts. All values as %.

Plant species	Part	Extracts			
		Petroleum ether	CH_2Cl_2	MeOH	Water
Hymenocardia ulmoides	stembark	89	93	74	95
	rootbark	92	100	98	115
	root	84	98	102	**120**[1]
	rootbark (Chalinze)	82	75	**141**[2]	116
Albizia gummifera	stembark (large tree)	104	117	**120**[1]	93
	stembark (small tree)	**142**[2]	92	118	86
	root (small tree)	118	58	115	97
	rootbark (small tree)	104	96	92	67
Foetidia africana	root	96	103	107	105
	rootbark	107	108	82	117
	stembark	91	97	87	107
Salacia madagascar.	root	87	72	102	104
	rootbark	100	93	89	**121**[1]
	stembark	96	96	116	112
	leaves	109	89	**124**[1]	**133**[1]
Asteranthe asterias	rootbark	**143**[2]	105	**135**[1]	107
	root	100	89	70	90
	stembark	103	65	**130**[1]	**141**[2]
	leaves	**124**[1]	103	107	119
Cussonia zimmermannii	rootbark	**151**[2]	**143**[2]	116	**120**[1]
	stembark	**148**[2]	81	100	87
Commiphora eminii	stembark	94	81	**129**[1]	103
Bridelia micrantha	stembark	86	72	103	99
	root	**123**[1]	83	103	98
	rootbark	87	92	98	118
Commiphora fulvo.	stembark	90	104	93	105
Vangueria infausta	rootbark	100	74	84	81
Vernonia spp.	leaves	54	81	112	72
Bridelia cathartica	stembark	99	91	100	88
	rootbark	88	79	101	97
	root	95	63	93	85
Combretum harissii	root	82	**122**[1]	96	91
	stem	108	93	112	101
	leaves	86	84	91	97
	fruits	45	69	101	72

bold : Extracts with enhanced binding at the $GABA_A$ receptor
[1] : Moderate enhanced binding
[2] : High enhanced binding

From the $GABA_A$ receptor binding assay of the crude plant extracts it could be found that of a total of 140 extracts from 35 samples of 13 plant species, 121 (86 %) showed no effect on the relative specific binding, while 19 (14 %) exhibited a significant effect on the relative specific binding. Of the 19 active extracts 12 (63 %) showed moderate enhanced binding and 7 (37 %) showed high enhanced binding. 6 (17 %) of the petroleum ether extracts, 2 (8 %) of the dichloromethane, 6 (17 %) of the methanol and 5 (14 %) of the water extracts were found to bind at the $GABA_A$ receptor.

The most active extracts were the petroleum ether extracts of the rootbark and the stembark of *Cussonia zimmermannii* Harms with an enhanced relative specific binding of 151 and 148 %, respectively.

4.2.2 Fractions

4.2.2.1 Rootbark extract of *Cussonia zimmermannii* Harms

The results of the antiparasitic (n = 2) and the $GABA_A$ receptor binding assays (n = 3) of the fractions of the petroleum ether extract of the rootbark of *Cussonia zimmermannii* Harms are presented in table 10. Only those fractions are listed which exhibited an increase or at least the same activity compared to the previous fraction. After two fractionation steps only the main fractions were investigated further. For the procedure of the bioassay-guided fractionation see chapter 5.2.1.

The crude petroleum ether extract exhibited the following antiparasitic avtivities and relative specific binding at the $GABA_A$ receptor :

- *T. b. rhodesiense* : IC_{50} 4.8 µg/ml
- *P. falciparum* : IC_{50} 3.3 µg/ml
- $GABA_A$ receptor : enhanced relative specific binding 151 % (conc. 50 µg/ml)

Table 10 : Results of the antiparasitic and the $GABA_A$ receptor binding assays of the fractions of *Cussonia zimmermannii* Harms rootbark petroleum ether extract.

Fraction	IC_{50} *T.b. rhod.* [µg/ml]	IC_{50} *P. f.* [µg/ml]	rel. spec. binding [%]
F3	1.7	1.0	156
F4	2.7	0.90	173
F5		2.1	
F6		1.7	
F3.4		0.33	
F3.6	0.48	0.91	156
F3.7	1.5		
F4.7	1.1	0.81	172

4.2.2.2 Stembark extract of *Commiphora fulvotomentosa* Engl.

The results of the *in vitro* testing of the fractions of the petroleum ether extract of the stembark of *Commiphora fulvotomentosa* Engl. on STIB 900 strain of *T. b. rhodesiense* are presented in table 11. Only those fractions are listed which exhibited an increase or at least the same activity compared to the previous fraction.

After three fractionation steps the fractions did no longer show any activity, therefore no further investigation was performed. For the procedure of the bioassay-guided fractionation see chapter 5.2.1. All samples were tested in duplicate (n = 2).

The crude petroleum ether extract exhibited the following antitrypanosomal activity :

- *T. b. rhodesiense* : IC_{50} 2.1 µg/ml

Table 11 : IC_{50} values (µg/ml) of the fractions of *C. fulvotomentosa* rootbark petroleum ether extract determined with STIB 900 strain of *T. b. rhodesiense*.

Fraction	IC_{50}
F2	1.5
F3	0.57

4.2.3 Isolated pure compounds of *Cussonia zimmermannii* Harms

4.2.3.1 Antiparasitic and cytotoxicity testing

The results of the antiparasitic (*T. b. rhodesiense, P. falciparum, T. cruzi and L. donovani* axenic and in infected macrophages) and the cytotoxicity testing of the isolated pure compounds MS-1 (**25**), MS-2 (**26**) and MS-4 (**27**) of *Cussonia zimmermannii* Harms (Isolation and structure elucidation see chapter 5.2.1 and 5.2.2) and the selectivity indices of the compounds MS-2 (**26**) and MS-4 (**27**) are summarised in table 12. All samples were tested in duplicate (*n* = 2). The isolated compound MS-5 (**28**) was not tested because of small quantity.

Formulas of the compounds MS-1 (**25**), MS-2 (**26**), and MS-4 (**27**) (see chapter 5.2.2).

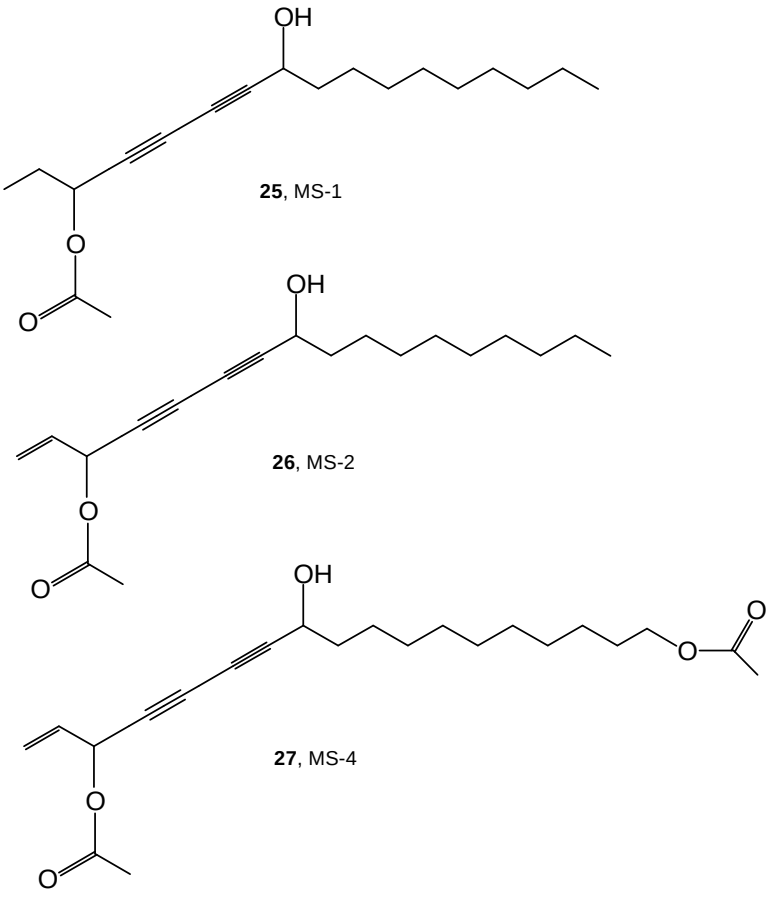

25, MS-1

26, MS-2

27, MS-4

Table 12 : Summary of the antiparasitic and cytotoxic test results of the isolated pure compounds of *Cussonia zimmermannii* Harms.

Standard drugs/ compounds	***IC*$_{50}$ *T. b. rhod.* [µg/ml]**	***IC*$_{50}$ *P. falc.* [µg/ml]**	***IC*$_{50}$ *T. cruzi* [µg/ml]**	***IC*$_{50}$ *L. dono.* axenic [µg/ml]**	***IC*$_{50}$ *L. dono.* inf. mac. [µg/ml]**	***IC*$_{50}$ Cytotox. [µg/ml]**	**SI[1] *T. cruzi***	**SI[1] *L. dono.* inf. mac.**
Standard drugs								
Melarsoprol	0.0023							
Chloroquine		0.027						
Artemisinin		0.0012						
Benznidazole			0.62					
Miltefosine				0.18	0.29			
Mefloquine						1.9		
Compounds								
MS-1 (**25**)	5.4	5.9	7.9	2.4	> 3	16.5		
MS-2 (**26**)	0.14	0.44	**0.2**	**0.039**	**0.098**	3.6	18.0	36.7
MS-4 (**27**)	0.42	0.84	**0.15**	**0.054**	0.85	21.8	145.3	

[1] : SI = Selectivity index : *IC*$_{50}$ cytotoxicity / *IC*$_{50}$ activity

bold : *IC*$_{50}$ values of isolated pure compounds < *IC*$_{50}$ values of standard drugs (higher activity than the standard drug)

4.2.3.2 GABA$_A$ receptor binding assay

The summary of the results of the isolated pure compounds MS-1 (**25**), MS-2 (**26**), and MS-4 (**27**) of *Cussonia zimmermannii* Harms obtained from the [^{3}H]flunitrazepam binding assay to rat cortex membranes are presented in table 13 and figure 1.

The isolated compound MS-5 (**28**) was not tested because of small quantity. The compounds were tested at concentrations from 20 to 0.1 µg/ml. Compound MS-1 (**25**) (*n* = 9) and MS-2 (**26**) and MS-4 (**27**) (*n* = 3). The standard compound GABA led to a relative specific binding of 120 % at a concentration of 10 µM.

Table 13 : Summary of the results of the pure compounds isolated from *Cussonia zimmermannii* Harms obtained from the $GABA_A$ receptor binding assay.

	Rel. spec. binding of [^{3}H]flunitrazepam [%] Compound		
Tested concentrations [µg/ml]	MS-1 (**25**)	MS-2 (**26**)	MS-4 (**27**)
20	138	152	158
10	140	132	132
5	138	137	142
2	126	125	121
1	113	113	113
0.1	101	112	100

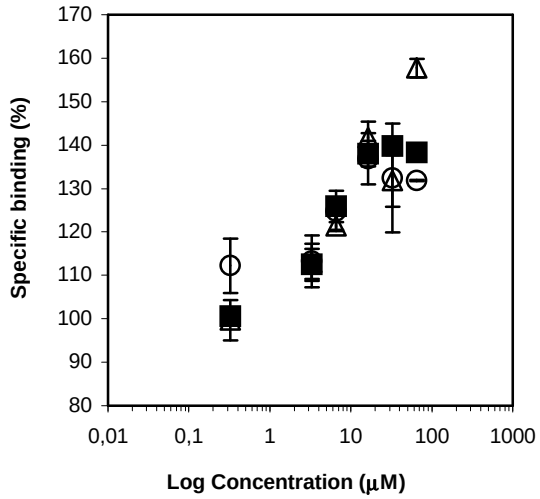

Figure 1 : Stimulation of [^{3}H]flunitrazepam binding by MS-1 (**25**), MS-2 (**26**), and MS-4 (**27**). Specific binding stimulated by MS-1 (**25**) (■), MS-2 (**26**) (○), and MS-4 (**27**) (△) is shown relative to control binding in the absence of drugs. Data are expressed as mean ± SEM of three to nine individual experiments.

4.2.3.3 Electrophysiological investigations

Positive allosteric modulation

Functional effects of the isolated compounds MS-1 (**25**), MS-2 (**26**), and MS-4 (**27**) were investigated in electrophysiological studies at recombinant $GABA_A$ receptors expressed in *Xenopus laevis* oocytes. For reasons of solubility the compounds were only used up to a concentration of 30 µM. GABA was always used at concentrations eliciting 2-6 % of the maximal current amplitude in the corresponding $GABA_A$ receptor type. 30 µM of each tested compound elicited at the $\alpha_1\beta_2\gamma_2$ receptor type by itself tiny currents amounting to < 0.1 % of the maximal current elicited by GABA. But all compounds exhibited a potent positive allosteric modulatory effect by enhancing the GABA-stimulated current at $\alpha_1\beta_2\gamma_2$. This concentration dependent stimulation is documented for MS-1 (**25**) at $\alpha_1\beta_2\gamma_2$ with a GABA concentration of 7 µM (figure 2). Maximum stimulation at $\alpha_1\beta_2\gamma_2$ was achieved with about 10 µM MS-1 (**25**). It was also tested whether 10 µM MS-1 (**25**) stimulated currents elicited by GABA concentrations eliciting near maximal current amplitudes. In the presence of 500 µM GABA, 10 µM MS-1 (**25**) did not significantly affect the current amplitudes (97.7 ± 2.5 % of the control (n = 3)).

*Subunit specificity of MS-1 (**25**)*

Figure 3A shows an averaged concentration response curve of this type of experiment for the $\alpha_1\beta_2\gamma_2$ receptor type. Maximal stimulation was about 450 % and half-maximal stimulation was observed at a concentration (EC_{50}) of about 1.5 µM. Replacement of the α_1 subunit in this combination by one of the other α subunit isoforms (α_2, α_3, α_5, or α_6) resulted in little effect on EC_{50}, that varied between 0.6 and 1.0 µM, but had in some cases a drastic effect on the maximal stimulation. Extent of stimulation was $\alpha_1\beta_2\gamma_2 \approx \alpha_3\beta_2\gamma_2 > \alpha_2\beta_2\gamma_2 > \alpha_5\beta_2\gamma_2 \approx \alpha_6\beta_2\gamma_2$. Figure 3B shows the effect of the β subunit isoform and the lacking effect of omitting γ_2 from $\alpha_1\beta_2\gamma_2$. Replacing β_2 in $\alpha_1\beta_2\gamma_2$ by β_1 or β_3 drastically reduced maximal stimulation from 450 % to 80 % and 150 %, respectively. Introducing the point mutation β_2N265S, which is known to strongly reduce stimulatory effects by loreclezole [138] into $\alpha_1\beta_2\gamma_2$, had only a relatively weak effect in this case, reducing maximal stimulation to about 65 %.

*Subunit specificity of MS-2 (**26**) and MS-4 (**27**)*

Figures 4 and 5 show subunit specificities of MS-2 (**26**) and MS-4 (**27**), respectively. Again replacement of the α_1 subuniț in $\alpha_1\beta_2\gamma_2$ by one of the other α subunit isoforms (α_2, α_3, α_5, or α_6) resulted in little effect on EC_{50}, that varied between 0.8 and 1.3 μM for MS-2 (**26**) and 1.4 and 3.5 μM for MS-4 (**27**), but had in some cases a drastic effect on the maximal stimulation. Maximal stimulation was about 300 % for MS-2 (**26**) and about 110 % for MS-4 (**27**). The following specificity in this respect was observed for MS-2 (**26**) $\alpha_1\beta_2\gamma_2 \approx \alpha_3\beta_2\gamma_2 \approx \alpha_1\beta_2 > \alpha_2\beta_2\gamma_2 \approx \alpha_6\beta_2\gamma_2 \approx \alpha_5\beta_2\gamma_2 > \alpha_1\beta_1\gamma_2$, and for MS-4 (**27**) $\alpha_1\beta_2\gamma_2 \approx \alpha_1\beta_2 \approx \alpha_5\beta_2\gamma_2 \approx \alpha_3\beta_2\gamma_2 \approx \alpha_2\beta_2\gamma_2 > \alpha_6\beta_2\gamma_2 \gg \alpha_1\beta_1\gamma_2$.

Lack of inhibition by the benzodiazepine antagonist Ro15-1788

It was tested whether MS-1 (**25**) would act at a known site on the $GABA_A$ receptor. Currents elicited by 2-7 μM GABA were stimulated by 10 μM MS-1 (**25**) 361 ± 117 % (*n* = 6). When 1 μM of the benzodiazepine antagonist Ro15-1788 was co-applied, stimulation was not significantly altered with 391 ± 156 % (*n* = 3). In contrast the antagonist of the ROD site [139], ROD178B, significantly reduced stimulation to 134 ± 16 % (*n* = 3) at a concentration of 100 μM (figure 6).

*Effect of MS-1 (**25**) on the apparent affinity of picrotoxin*

Currents elicited by 3 or 4 μM GABA were inhibited by increasing concentrations of the channel pore blocker picrotoxin. The half-maximal concentration of picrotoxin for current inhibition was 1.2 ± 0.3 μM (*n* = 3) in the absence and 3.3 ± 0.9 μM in the presence of 10 μM MS-1 (**25**) (*n* = 3). MS-1 (**25**) seems to decrease apparent picrotoxin affinity about three-fold (figure 7).

Ion selectivity is maintained and stimulation is potential independent

The reversal potential and the potential dependence of the current elicited by GABA were both not altered in the presence of 10 μM MS-1 (**25**). The reversal potential was –29 ± 1 mV (*n* = 3) in the absence of 10 μM MS-1 (**25**) and was not altered in its presence (not shown).

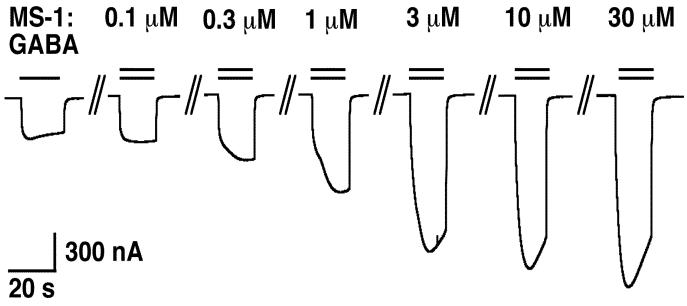

Figure 2 : Concentration dependence of allosteric stimulation by MS-1 (**25**) at $\alpha_1\beta_2\gamma_2$ $GABA_A$ receptors. Recombinant $\alpha_1\beta_2\gamma_2$ $GABA_A$ receptors were expressed in *Xenopus leavis* oocytes and exposed to either 7 μM GABA alone or in combination with increasing concentrations of MS-1 (**25**). The experiment was repeated twice on oocytes of two different batches with similar results.

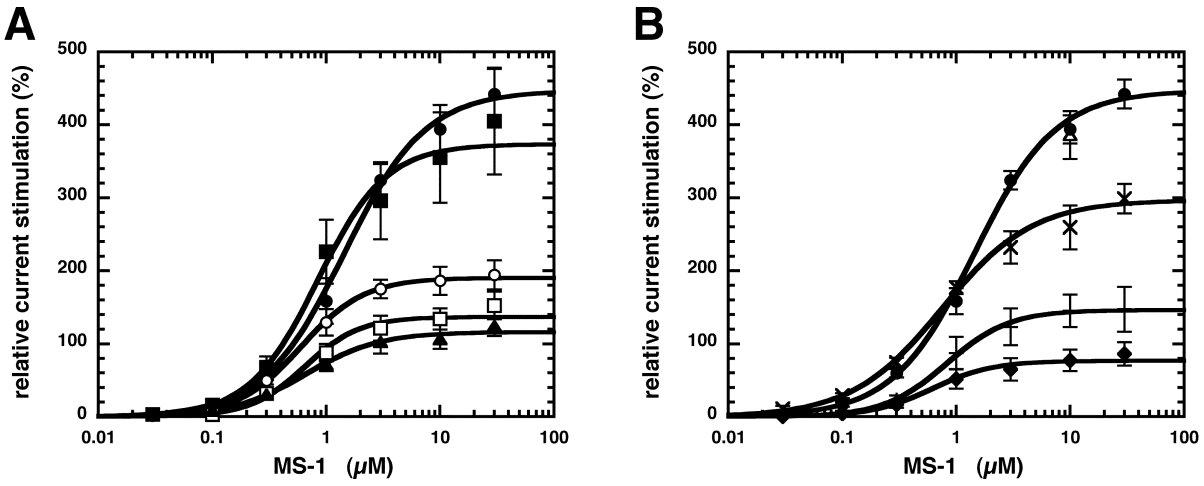

Figures 3A/B : Subunit isoform specificity of MS-1 (**25**). (**A**) Recombinant $\alpha_1\beta_2\gamma_2$ (●), $\alpha_2\beta_2\gamma_2$ (○), $\alpha_3\beta_2\gamma_2$ (■), $\alpha_5\beta_2\gamma_2$ (□) and $\alpha_6\beta_2\gamma_2$ (▲) and (**B**) $\alpha_1\beta_2\gamma_2$ (●), $\alpha_1\beta_2$ (△), $\alpha_1\beta_2$N265Sγ_2 (x), $\alpha_1\beta_3\gamma_2$ (+), and $\alpha_1\beta_1\gamma_2$ (◆). $GABA_A$ receptors were expressed in *Xenopus leavis* oocytes and exposed to either GABA alone or in combination with increasing concentrations of MS-1 (**25**). Data are given as mean ± SEM (≤ 3 oocytes from two different batches).

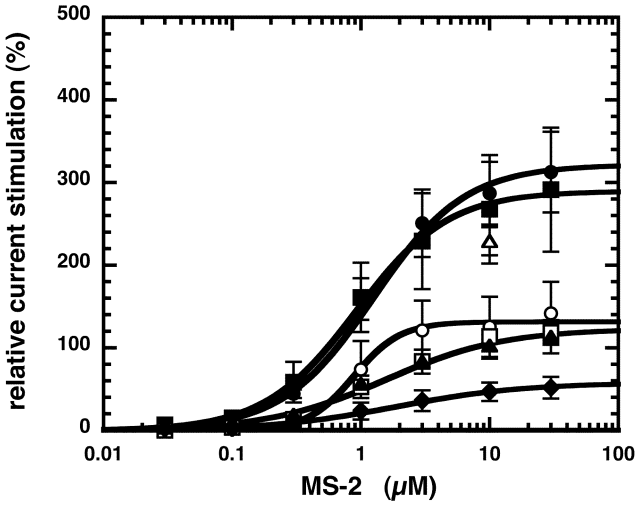

Figure 4 : Subunit isoform specificity of MS-2 (**26**). Recombinant $\alpha_1\beta_2\gamma_2$ (●), $\alpha_1\beta_2$ (△), $\alpha_2\beta_2\gamma_2$ (○), $\alpha_3\beta_2\gamma_2$ (■), $\alpha_5\beta_2\gamma_2$ (□), $\alpha_6\beta_2\gamma_2$ (▲) and $\alpha_1\beta_1\gamma_2$ (◆). $GABA_A$ receptors were expressed in *Xenopus leavis* oocytes and exposed to either GABA alone or in combination with increasing concentrations of MS-2 (**26**). Data are given as mean ± SD (≥ 3 oocytes from two different batches).

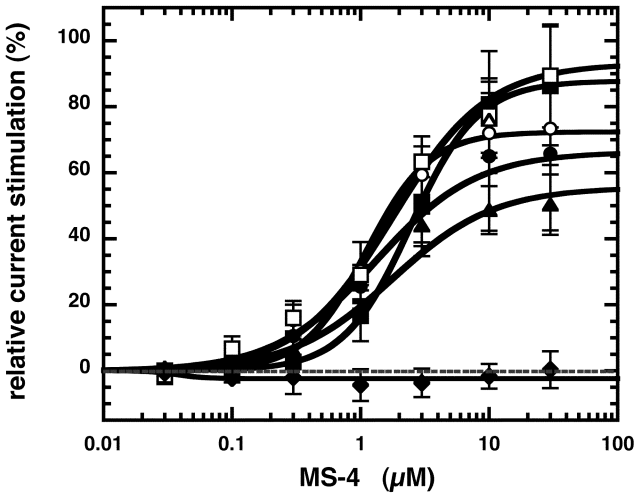

Figure 5 : Subunit isoform specificity of MS-4 (**27**). Recombinant $\alpha_1\beta_2\gamma_2$ (●), $\alpha_1\beta_2$ (△), $\alpha_2\beta_2\gamma_2$ (○), $\alpha_3\beta_2\gamma_2$ (■), $\alpha_5\beta_2\gamma_2$ (□), $\alpha_6\beta_2\gamma_2$ (▲) and $\alpha_1\beta_1\gamma_2$ (◆). $GABA_A$ receptors were expressed in *Xenopus leavis* oocytes and exposed to either GABA alone or in combination with increasing concentrations of MS-4 (**27**). Data are given as mean ± SEM (≥ 3 oocytes from two different batches).

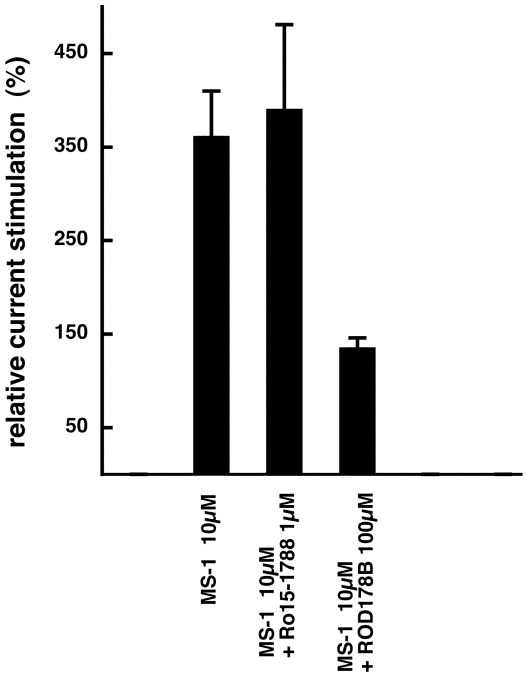

Figure 6 : Lack of inhibition by the benzodiazepine antagonist Ro15-1788 and reduction of the stimulation by the ROD site antagonist ROD178B. Recombinant $\alpha_1\beta_2\gamma_2$ $GABA_A$ receptors were exposed to either GABA in combination with 10 μM MS-1 (**25**), to GABA in combination with 10 μM MS-1 (**25**) and 1 μM Ro15-1788, or to GABA in combination with 10 μM MS-1 (**25**) and 100 μM ROD178B. Data are given as mean ± SEM (≥ 3 oocytes from two different batches).

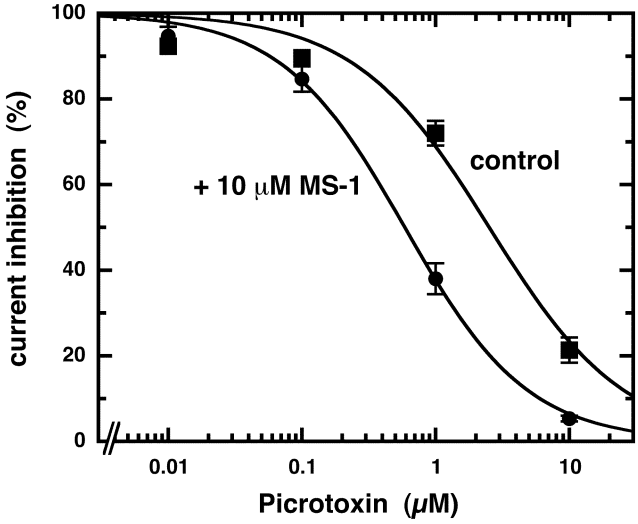

Figure 7 : MS-1 (**25**) affects inhibition by picrotoxin. Recombinant $\alpha_1\beta_2\gamma_2$ $GABA_A$ receptors were exposed to either GABA alone (■) or in combination with 10 μM MS-1 (**25**) (●). Currents were inhibited by increasing concentrations of picrotoxin. Data are given as mean ± SEM (3 oocytes from two different batches).

4.3 Discussion and conclusions of the results of the crude plant extracts

Summary of the antiparasitic and the cytotoxicity testings

The most active extracts in both antiparasitic assays were the petroleum ether extracts of the rootbark and the stembark of *Salacia madagascariensis*. But the cytotoxicity was also high and the selectivity indices in a moderate range of 2-6. Promising results showed the petroleum ether extract of the rootbark of *Bridelia micrantha* with an IC_{50} value of 0.68 µg/ml against *T. b. rhodesiense* and a SI of about 60. Other parts of this plant showed also interesting results. Some constituents of this plant are known. Also promising results showed the petroleum ether extract of the stembark of *Commiphora fulvotomentosa* with an IC_{50} value of 2.1 µg/ml against *T. b. rhodesiense* and a SI of 21.4. Of this plant no consituents are known. Also the petroleum ether extract of the rootbark of *Vangueria infausta* with an IC_{50} value of 1.5 µg/ml against *T. b. rhodesiense* and a SI of 13.8 was interesting, unfortunately only a small quantity of about 200 g of plant material could be collected.

$GABA_A$ receptor binding assay

The most promising results showed the petroleum ether and the dichloromethane extract of the rootbark and the petroleum ether extract of the stembark of *Cussonia zimmermannii*. Interesting was the fact that the plant is used in traditional medicine for the treatment of epilepsy [11] and mental illness [16]. Also remarkable was that in contrast to the antiparasitic results many water extracts exhibited a significant enhanced relative specific binding at the $GABA_A$ receptor.

Selection of the extracts for bioassay-guided fractionation

Many extracts showed promising activities in the antiparasitic and $GABA_A$ receptor binding testings. Because not all of them could be investigated phytochemically, a selection had to be made. The selected plant extract should show high activities in the preliminary screening and of the plant, from which it was extracted, no constituents should be known. Therefore *Salacia madagascariensis*, *Bridelia micrantha* and *Vangueria infausta* were excluded from further investigation.

For the bioassay-guided fractionation the petroleum ether extract of the stembark of *Commiphora fulvotomentosa* and the petroleum ether extract of the rootbark of *Cussonia zimmermannii* were selected because of the following reasons :

Petroleum ether extract of the stembark of C. fulvotomentosa :

- low IC_{50} value of 2.1 µg/ml against *T. b. rhodesiense*
- high selectivity index of 21.4
- no known constituents
- enough plant material at hand (1039 g)

Petroleum ether extract of the rootbark of C. zimmermannii :

- acceptable IC_{50} value of 4.8 µg/ml against *T. b. rhodesiense*
- good IC_{50} value of 3.3 µg/ml against *P. falciparum*
- high relative specific binding at the $GABA_A$ receptor of 151 %
- traditionally used for the treatment of epilepsy and mental illness
- no known constituents
- enough plant material at hand (717 g)

The main reason for the selection of *Cussonia zimmermannii* for further investigation was the fact, that its rootbark extract showed activity in all three performed assays and that the plant is known to be used in traditional medicine not only for the treatment of malaria but also for epilepsy and mental illness. This could be due to constituents with $GABA_A$ receptor stimulating properties, because benzodiazepines which also act at the $GABA_A$ receptor are used as antiepileptics.

5. Constituents of *Cussonia zimmermannii* Harms

5.1 Introduction

5.1.1 Botany

Cussonia zimmermannii Harms belongs to the genus *Cussonia* of the family Araliaceae. Local names are msopole (Kihehe, Kisagara), mtumbitumbi (Kingindo) and mutolondo. No synonyms are known [11]. It is a tree to 25 m tall with greenish-grey fissured bark. Leaves digitately compound; petiole up to 53 cm long and 5 mm diameter, but generally considerably smaller, glabrous apart from some crisped hairs in stipular region and at junction with leafets; leafets 5-7 (-9), sessile, chartaceous to

coriaceous, lanceolate to oblanceolate, narrowly ovate and narrowly obovate, up to 25 cm long by 8 cm wide, but generally considerably less, caudate to acute, with a narrowly cuneate to much attenuated base with crenate to subentire margins, glabrous above, glabrous to slightly puberulous beneath. Flowering spikes up to about 12 together, up to 34 cm long [122]. It blooms from October to November [11]. The plant occurs in Kenya (Kwale- and Tana River District) and Tanzania (Tanga-, Uzaramo- and Lindi District). It grows in lowland rain forest, lowland dry evergreen forest and woodlands of 0 - 400 m [122].

5.1.2 Use in traditional medicine

In traditional medicine a decoction of the root of *Cussonia zimmermannii* Harms is used to treat **malaria**. The marrow of the stem and branches are eaten to treat **epilepsy** and a decoction of the root is taken as a remedy for labour pain [11]. An infusion of the leaves is used as a wash for people suffering from **fever** or the ague. A decoction of the roots is taken as a remedy for gonorrhoea [12]. Roots of *Cussonia zimmermannii* Harms along with roots of *Deinbollia borbonica* Scheff. f. are cooked with chicken and the resulting soup is ingested for hypertensive encephalopathy, post-partum haemorrhage and **mental illness** [16].

5.1.3 Known constituents of the genus *Cussonia*

Of the genus *Cussonia* 51 compounds from 10 different species are described in literature. They belong to eight classes of natural products. Most compounds belong to the classes of triterpenoid saponins and diterpenoid glycosides. There is only one species which is known to contain polyacetylenes and from another species stigmasterol has been isolated.

The known constituents of the genus *Cussonia* are summarised in table 14. The structures of the known polyacetylenes from the genus *Cussonia* are shown in scheme 3.

Table 14 : Known constitutents of the genus *Cussonia*.

Class of natural products	Constituent	Plant species/ References
Polyacetylenes	(+)-9(*Z*),17-Octadecadiene-12,14-diyne-1,11(*S*), 16(*S*)-triol (**29**) (+)-9(*Z*),17-Octadecadiene-12,14-diyne-1,11(*S*), 16(*S*)-triol-1-acetate (**30**)	*C. barteri* [140]
Quinic acid esters	1'-*O*-Chlorogenoylchlorogenic acid 1'-*O*-Chlorogenoylneochlorogenic acid	*C. barteri* [141]
Triterpenoid saponins	3-*O*-(α-L-Arabinopyranosyl)-23-hydroxyursolic acid 3-*O*-(β-D-Glucopyranosyl)-23-hydroxyursolic acid	*C. bancoensis* [142]
	28-*O*-[α-L-Rhamnopyranosyl-(1→4)-β-D-glucopyranosyl-(1→6)-β-D-glucopyranosyl]-23-hydroxyursolic acid ester	*C. bancoensis* [143]
	Cussosaponins A-E	*C. racemosa* [144]
	[(α-L-Arabinofuranosyl-(1→4)-β-D-glucuronopyranosyl-(1→3)]-3β-hydroxyolean-12-en-28-oic acid [(α-L-Arabinofuranosyl-(1→4)-β-D-galactopyranosyl-(1→2)]-β-D-glucuronopyranosyl-(1→3)]-3β-hydroxyolean-12-en-28-oic acid	*C. spicata* [145]
	Cussonoside A and B	*C. barteri* [146]
Steroids	Stigmasterol	*C. bancoensis* [142]
Triterpenoid carbocyclic acids and esters	Ursolic acid 23-Hydroxyursolic acid 3β-Hydroxylup-20(29)-en-28-oic acid	*C. bancoensis* [142]
	23-Hydroxy-3-oxo-urs-12-en-28-oic acid	*C. natalensis* [147]
	Hederagenin	*C. holstii* [148] *C. bojeri* [149] *C. corbisieri* [150]
	Oleanolic acid Oleanolic acid methyl ester acetate	*C. corbisieri* [150]
Diterpenoid glycosides	Paniculoside IV	*C. vantsilana* [151] *C. bojeri* [152] *C. racemosa* [153]

Table 14 (continued)

Class of natural products	Constituent	Plant species/ References
Diterpenoid glycosides	Cussovantoside A-D Suavioside E Cussovacoside C	*C. vantsilana* [151]
	β-D-Glucopyranosyl,17-hydroxy-ent-kauran-19-oate-16-O-β-D-glucopyranoside β-D-Glucopyranosyl 16β,17-dihydroxy-(–)-kauran-19-oate	*C. bojeri* [153]
	Cussoracosides A-F	*C. racemosa* [153]
	β-D-Glucopyranosyl-ent-16β,17-dihydroxykauran-19-oate Cussosides A-D (cleorodane glycosides) Cussoside E (labdane glycoside)	*C. racemosa* [154]
Diterpenoid carbocyclic acids	Cussovantonin A and B Kaur-16-en-18-oic acid	*C. vantsilana* [151]
	16β,17-Dihyroxy-kauran-19-oic acid	*C. bojeri* [153]
Flavonoids	Rutin	*C. vantsilana* [151] *C. bojeri* [153] *C. barteri* [141]
	Kaempferol rutinoside	*C. vantsilana* [151]

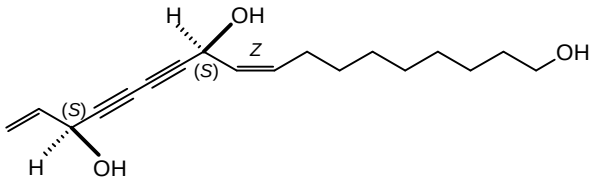

29, (+)-9(*Z*),17-Octadecadiene-12,14-diyne-1,11(*S*),16(*S*)-triol

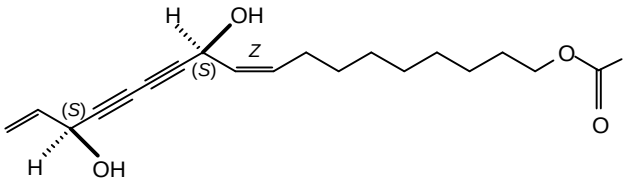

30, (+)-9(*Z*),17-Octadecadiene-12,14-diyne-1,11(*S*),16(*S*)-triol-1-acetate

Scheme 3 : Structures of the known polyacetylenes (**29**) and (**30**) from the genus *Cussonia*.

5.2 The polyacetylenes and stigmasterol

The polyacetylenes

Polyacetylenes (polyynes) are compounds with very diverse structures containing several C/C triple bonds. In addition they often also contain C/C double bonds, allene units, thiophene and furan rings. "Polyacetylenes" is used as a collective name even when only one C/C triple bond is present in the molecule. They are produced mainly by fungi (basidomycetes) and plants of the families Asteraceae, Apiaceae, and Araliaceae [155]. In some species they are not constitutively present, but were induced after fungal attack, for example in certain Fabaceae and Solanaceae (e.g. falcarindiol (**31**) production by *Cladosporium*-infected tomatoes). More than one thousand natural polyacetylenes are known in higher plants [156]. Naturally occurring polyacetylenes are formed biogenetically from unsaturated fatty acids such as oleic and linoleic acids by further dehydrogenation of their *cis*-alkene bonds and subsequent shortening of the carbon chain. Compounds with an odd number of carbon atoms develop by decarboxylation and α-oxydation. They can occur in all plant organs and are localized in oil channels [157].

For the isolation of polyacetylenes generally, careful solvent extraction at room temperature is performed. They normally are concentrated in oil channels, therefore, extractions with ether-petroleum ether mixtures are sufficient. Repeated column chromatography and finally TLC are usually successful in isolation of the acetylenes. Structure elucidation methods are mostly spectroscopic, important is the infrared spectroscopy, although the acetylenic stretching frequency is usually weak. Important is also mass spectroscopy but the most important method has become NMR spectroscopy. The position of the signals of triple bond-methyl groups is located around 2 ppm, which is very little changed by the number of triple bonds and the couplings across triple bonds are unusually large [158] :

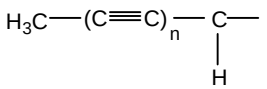

n = 1 : *J* = ~ 3 Hz
n = 2 : *J* = ~ 1 Hz
n = 3 : *J* = 0.3 Hz

Polyacetylenes are known to possess antifungal, insecticidal, antibiotic (e.g. *Helicobacter pylori*), molluscicidal and local anaesthetic activities. Further biological properties are inhibition of 5-lipoxygenase, phototoxicity, neurotoxicity and hemolytic activity. Some polyacetylenes can also cause allergic and irritant contact dermatitis. It has been shown that the antifungal activity of e.g. falcarindiol (**31**) is due to destruction of the plasma membrane of dermatophytes.

The trivial names, biological activities and origin of some typical polyacetylenes from plant species of the families Apiaceae and Asteraceae and from basidomycete cultures are shown in table 15, their structures and molecular folmulas are shown in scheme 4.

Table 15 : Trivial names, biological activities and origin of some typical polyacetylenes from Apiaceae, Asteraceae and basidomycete cultures.

Trivial names	Biological activties	Origin	Ref.
Mycomycin (**32**)	antibiotic	Basidomycete cultures	[155]
Cicutoxin (**33**)	highly toxic (neurotoxicity)	*Cicuta virosa* (Apiaceae)	[156]
Œanthotoxine (**34**)	highly toxic (neurotoxicity)	*Œanthus crocata* (Apiaceae)	[156]
Wyerone (**35**)	antifungal, phytoalexin	*Vicia faba* (Asteraceae)	[159]
Tonghaosu (**36**)	antifeedant activity towards insects	*Chrysanthemum segetum* (Asteraceae)	[155]

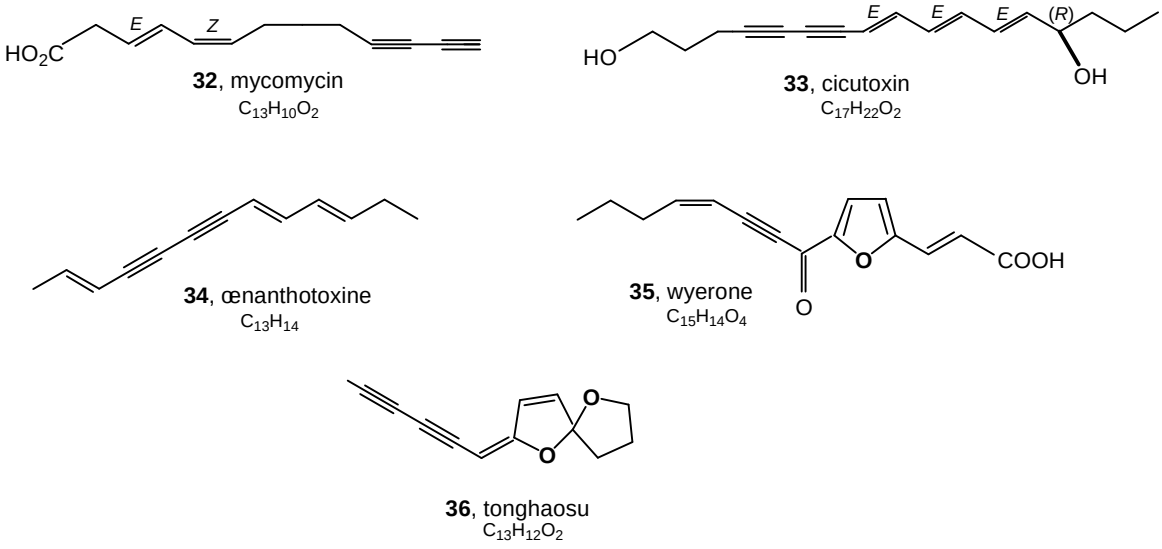

Scheme 4 : Structures and molecular formulas of some typical polyacetylenes.

From the family Araliaceae (where *Cussonia zimmermannii* Harms belongs to) over thirty different polyacetylenes have been isolated. The trivial names, CA index names, biological activities and origin of some selected polyacetylenes closely related to the ones isolated from *Cussonia zimmermannii* are shown in table 16, their structures and molecular formulas are shown in scheme 5.

Table 16 : Names, biological activities and origin of some polyacetylenes, isolated from plants of the family Araliaceae.

Trivial names/CA index names	**Biological activities**	**Origin**	**Ref.**
Falcarinol (**37**, 1,9-Heptadecadiene-4,6-diyn-3-ol (3*R*, 9*Z*))	Causes allergic and irritant contact dermatitis Inhibition of *Helicobacter pylori* growth and vacuolation Antifungal Local anaesthetic	*Panax ginseng* *Hedera helix*	[160] [161] [162] [163]
Falcarindiol (**31**, 1,9-Heptadecadiene-4,6-diyn-3,8-diol (3*S*, 8*S*, 9*Z*))	Inhibitory activity on 5-lipoxygenase Local anaesthetic Destroys the plasma membrane	*Schefflera digitata*	[160] [164]
Heptadeca-1-en-4,6-diyn-3,9-diol (**38**)	n.d.	*Panax ginseng*	[160]
Panaxytriol, Falcarintriol (**39**, 1-Heptadecene-4-6-diyn-3,9,10-triol (3*R*, 9*R*, 10*R*))	Inhibition of *Helicobacter pylori* growth and vacuolation	*Panax ginseng*	[160] [162]
8-Heptadecene-4,6-diyn-3,10-diol, 10 acetate (**40**)	n.d.	*Panax vietnamensis*	[165]
1,9-Heptadecadiene-4,6-diyn-3-ol, acetate [*R*-(*Z*)] (**41**)	n.d	*Didymopanax* spp.	[166]

n.d. : not determined

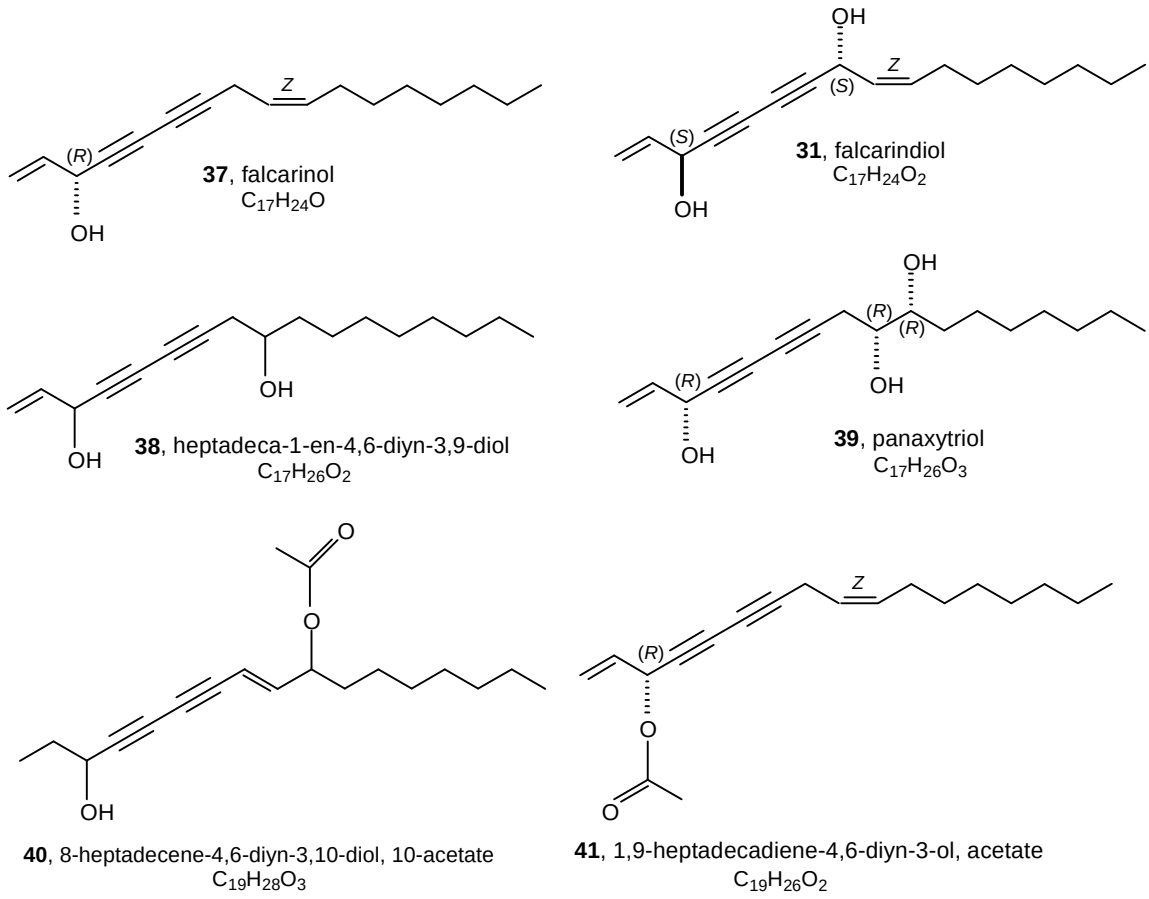

Scheme 5 : Structures and molecular formulas of some polyacetylenes closely related to polyacetylenes isolated from *Cussonia zimmermannii*.

Stigmasterol

Stigmasterol (24-ethyl-cholest-5,22-dien-3β-ol) (**42**) belongs to the sterols, a group of naturallly occurring steroids derived from cholesterol that possess a 3β-hydroxy group and a 17β-aliphatic side chain normally with 8-10 carbon atoms. Sterols are widely distributed in the animal and plant kingdom as cell components either in the free form or as esters or glycosides. Depending on their occurrence, they are distinguished as zoosterols of the animal kingdom or phytosterols of the plant kingdom. The non-saponifiable part of soy bean oil contains 12-25 % stigmasterol (**42**) [167]. Stigmasterol (**42**) is used as starting material for the partial synthesis of hormones [157].

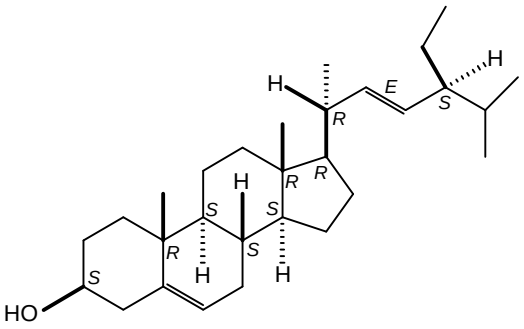

42, stigmasterol

5.2.1 Isolation

The polyacetylenes and stigmasterol were obtained from the petroleum ether extract from 717 g of *Cussonia zimmermannii* Harms rootbark. The extract was subjected to bioassay-guided fractionation by preparative scale chromatography : MPLC and HPLC methods as described in chapter 4.1.1.2. Thus 36.5 mg of MS-1 (**25**), 81.2 mg of MS-2 (**26**), 17.3 mg of stigmasterol (**42**), 221.7 mg of MS-4 (**27**), and 1.4 mg of MS-5 (**28**) were obtained.

For the activities of the crude extract and the fractions see chapter 4.2.1.1, for the activities of the isolated pure compounds see chapters 4.3.1.1, 4.3.1.2, and 4.3.1.3. The procedure of the bioassay-guided fractionation of the petroleum ether extract from *Cussonia zimmermannii* Harms is shown in schemes 6-15**.** The footnotes stand for the following : bold frames : fractions investigated further; [1] : fractions with activity against *T. b. rhodesiense*; [2] : fractions with activity against *P. falciparum* and [3] : tested fractions that stimulate $GABA_A$ receptor binding. For the isolation methods see chapter 4.1.1.2 in the experimental part.

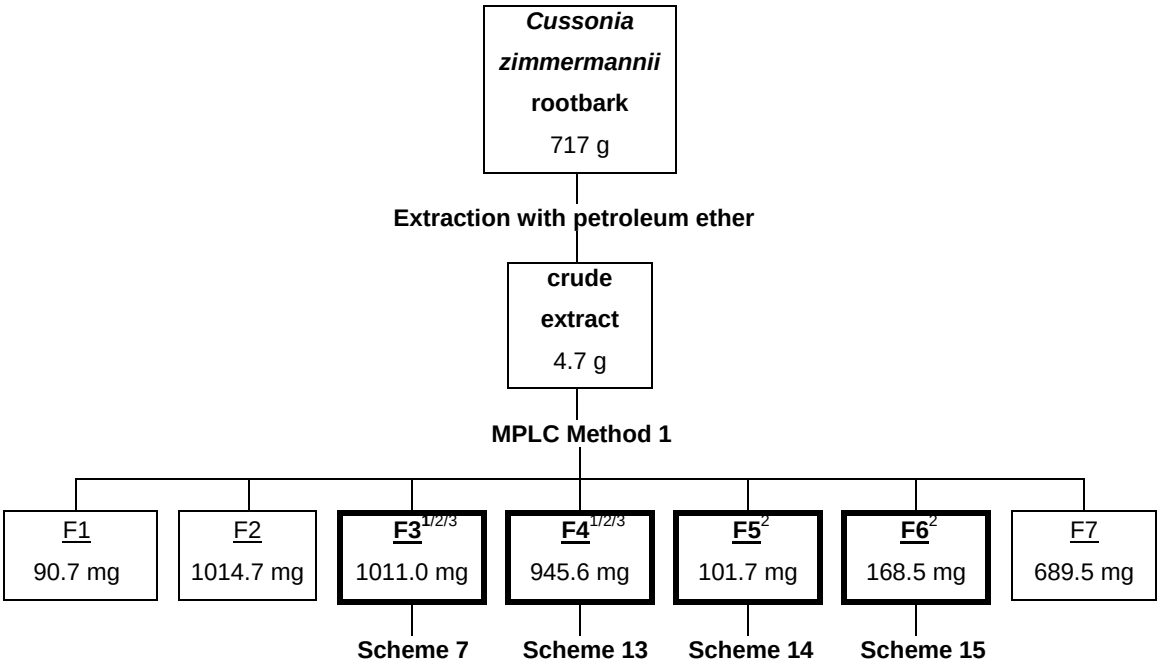

Scheme 6 : Procedure of the bioassay-guided fractionation of the petroleum ether extract from *Cussonia zimmermannii* Harms rootbark (from plant material to fraction F3, F4, F5 and F6).

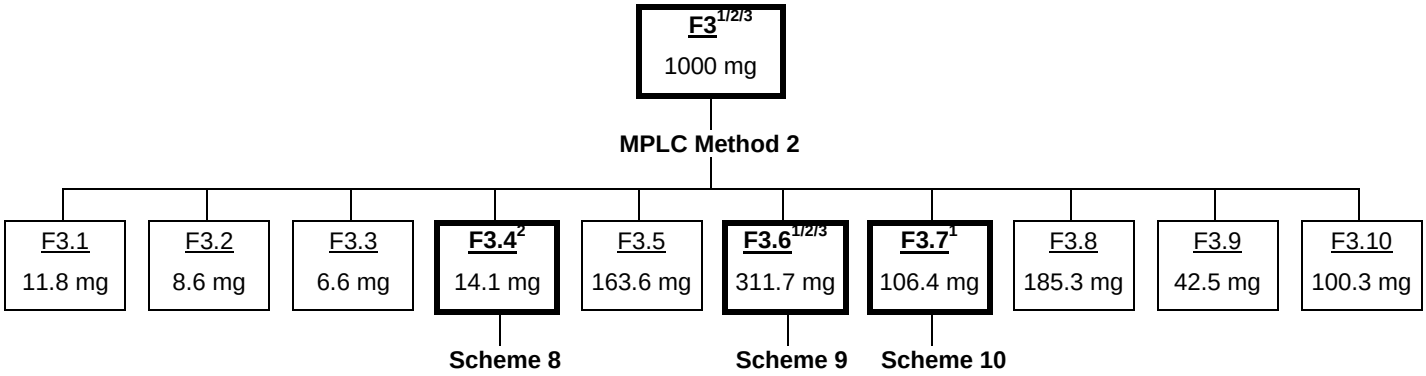

Scheme 7 : Procedure of the bioassay-guided fractionation of the petroleum ether extract from *Cussonia zimmermannii* Harms rootbark (from fraction F3 to fraction F3.4, F3.6 and F3.7).

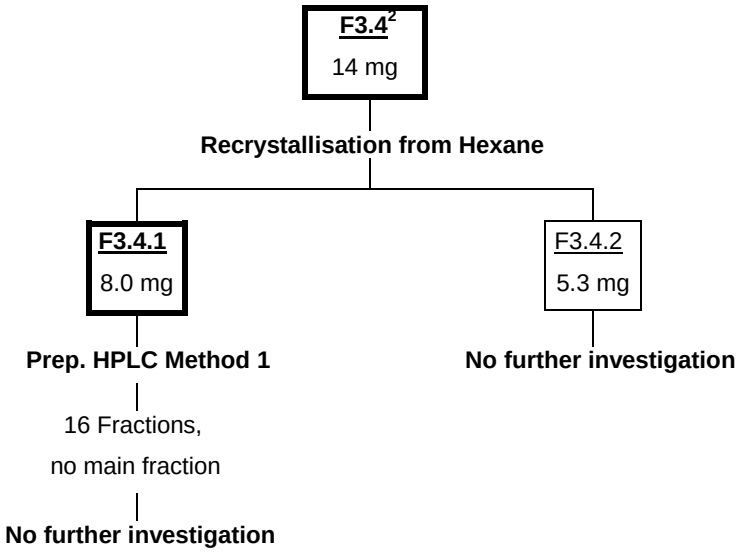

Scheme 8 : Procedure of the bioassay-guided fractionation of the petroleum ether extract from *Cussonia zimmermannii* Harms rootbark (from fraction F3.4 to fraction F3.4.1 and F3.4.2).

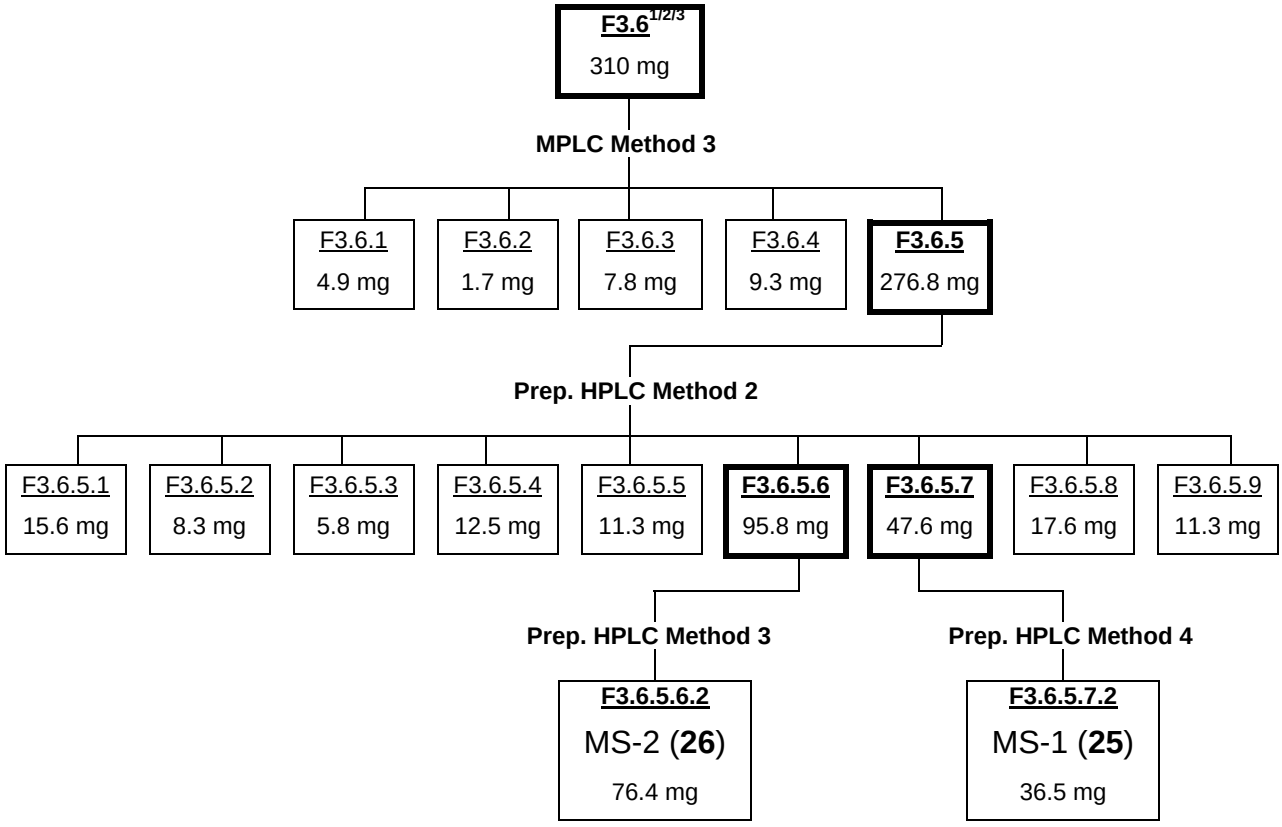

Scheme 9 : Procedure of the bioassay-guided fractionation of the petroleum ether extract from *Cussonia zimmermannii* Harms rootbark (from fraction F3.6 to MS-1 (**25**) and MS-2 (**26**)).

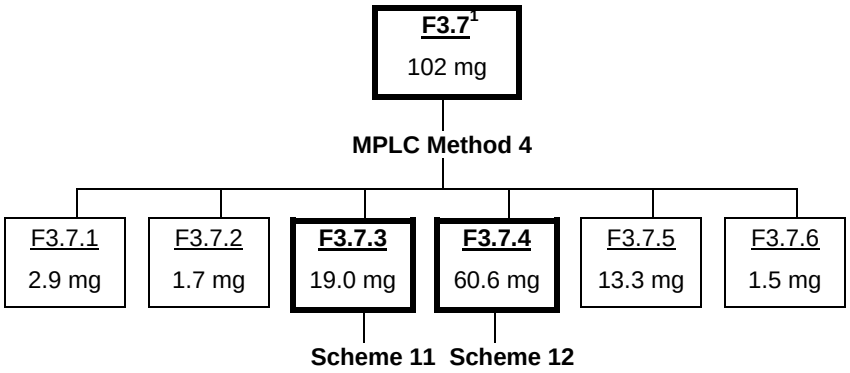

Scheme 10 : Procedure of the bioassay-guided fractionation of the petroleum ether extract from *Cussonia zimmermannii* Harms rootbark (from fraction F3.7 to fraction 3.7.3 and 3.7.4).

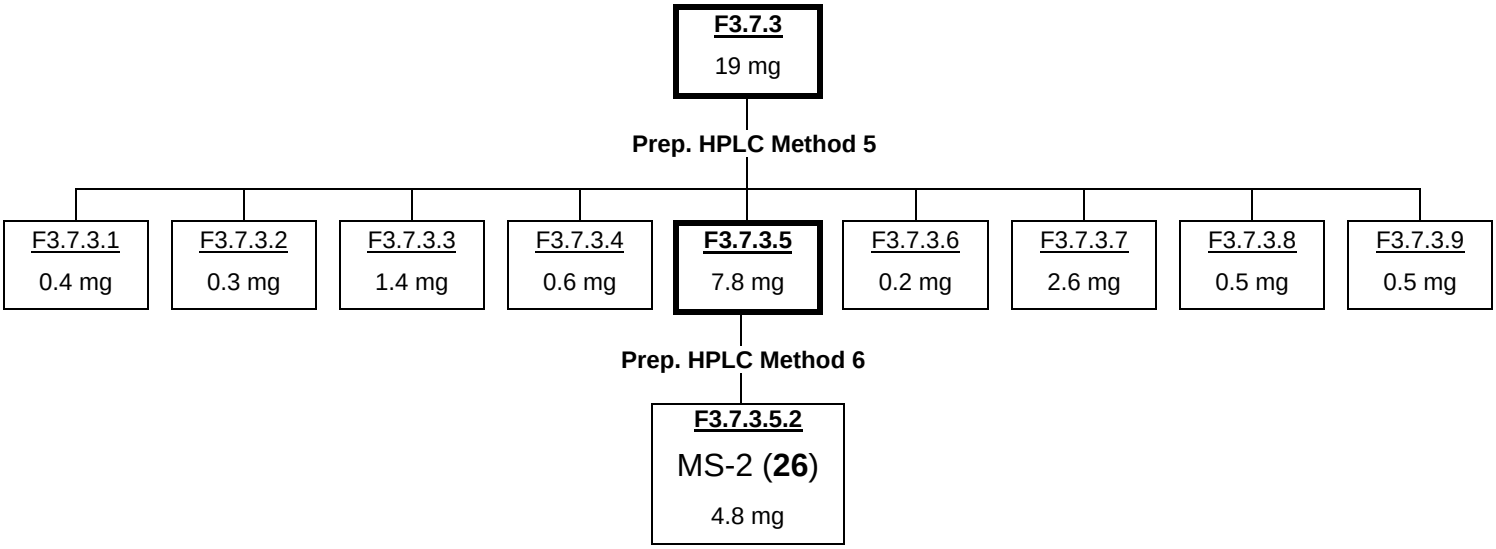

Scheme 11 : Procedure of the bioassay-guided fractionation of the petroleum ether extract from *Cussonia zimmermannii* Harms rootbark (from fraction F3.7.3 to MS-2 (**26**)).

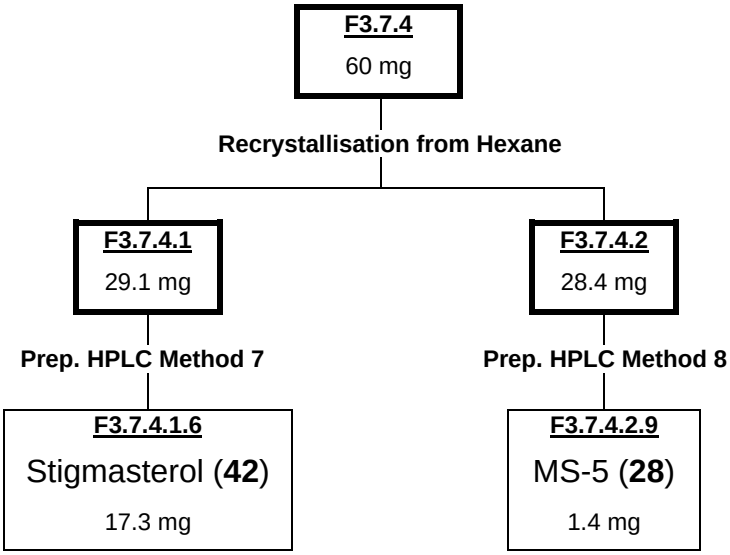

Scheme 12 : Procedure of the bioassay-guided fractionation of the petroleum ether extract from *Cussonia zimmermannii* Harms rootbark (from fraction F3.7.4 to stigmasterol (**42**) and MS-5 (**28**)).

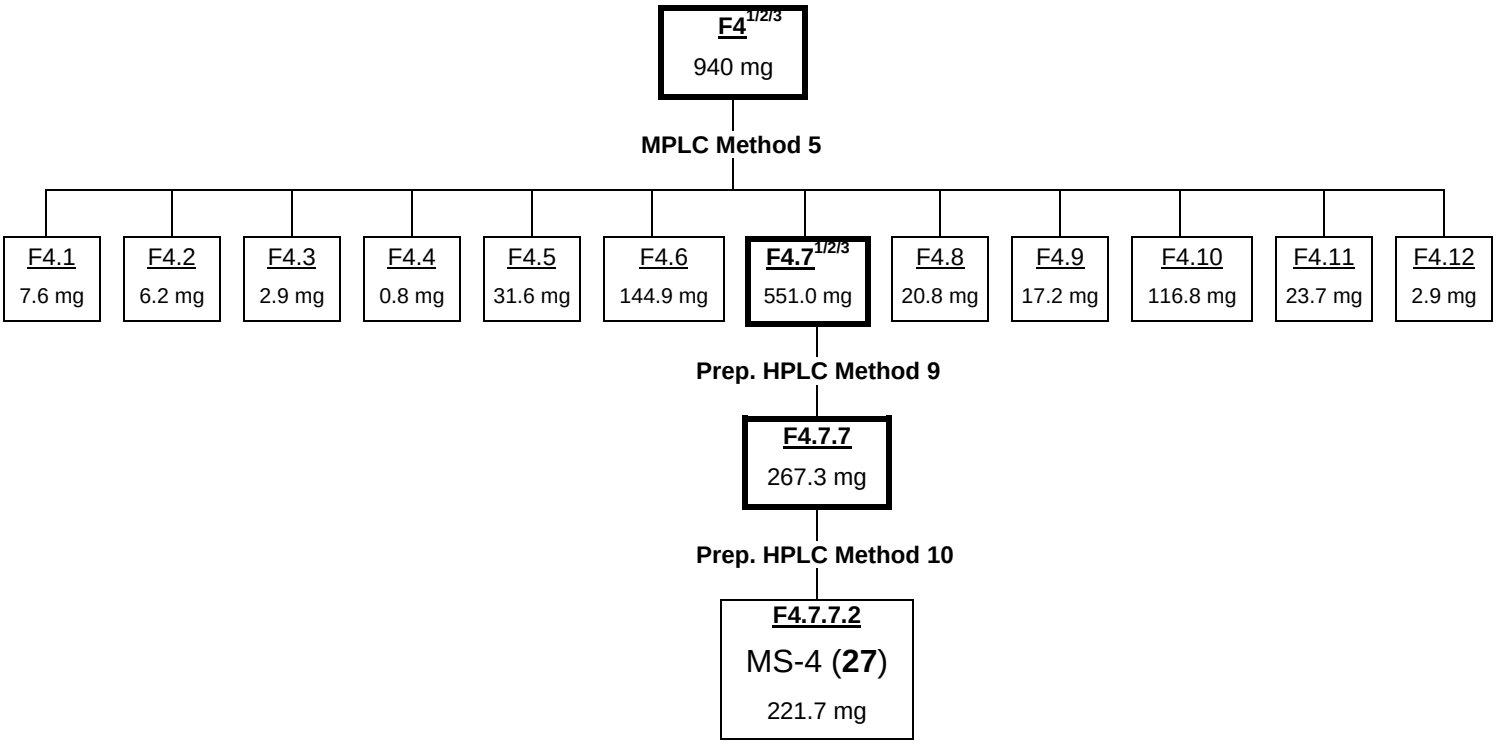

Scheme 13 : Procedure of the bioassay-guided fractionation of the petroleum ether extract from *Cussonia zimmermannii* Harms rootbark (from fraction F4 to MS-4 (**27**)).

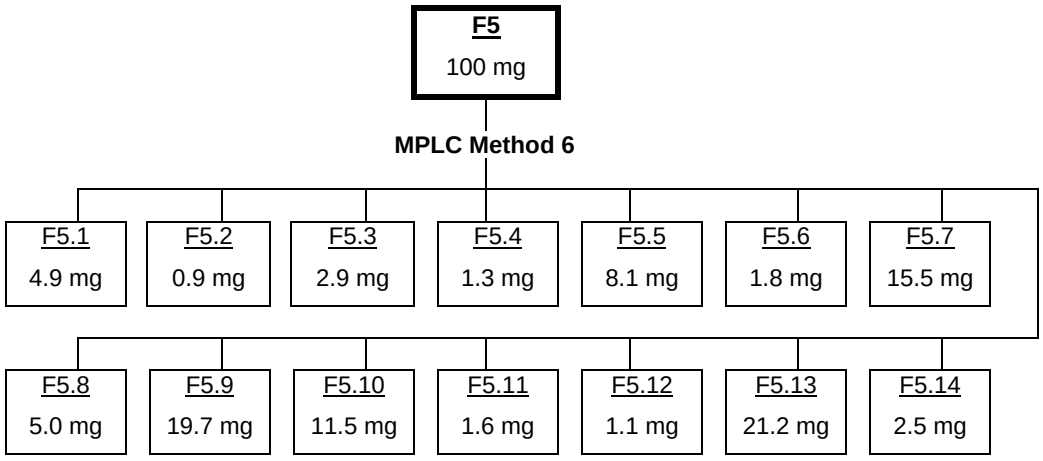

Scheme 14 : Procedure of the bioassay-guided fractionation of the petroleum ether extract from *Cussonia zimmermannii* Harms rootbark (from fraction F5 to fraction F5.1-F5.14).

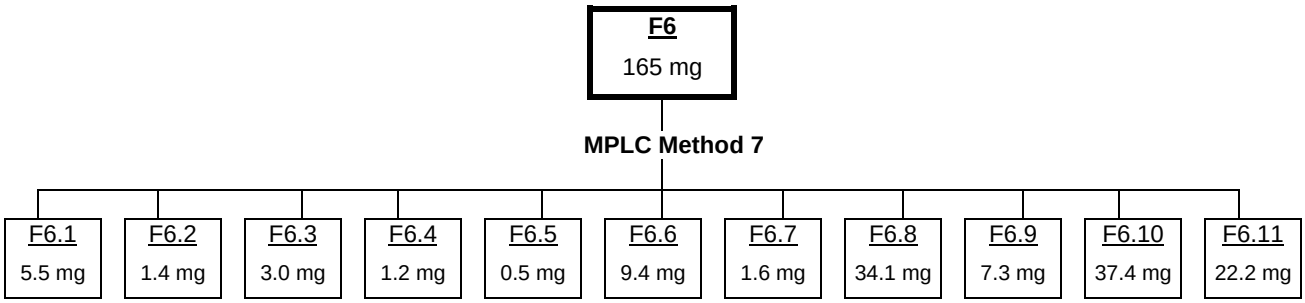

Scheme 15 : Procedure of the bioassay-guided fractionation of the petroleum ether extract from *Cussonia zimmermannii* Harms rootbark (from fraction F6 to fraction F6.1-F6.11).

5.2.2 Structure elucidation of the polyacetylenes

5.2.2.1 8-Hydroxyheptadeca-4,6-diyn-3-yl acetate (MS-1 (**25**)), a novel diyne

Preparative HPLC (see scheme 9) yielded 36.5 mg of a yellowish viscous oil with a negative optical rotation ($[\alpha]_D$ –94.5). The oil was analyzed by EI-MS, HR-EI-MS, UV/VIS- and IR-spectroscopy, ^{1}H-NMR, ^{13}C-NMR, DEPT135, ^{1}H-^{1}H COSY, HMQC and HMBC.

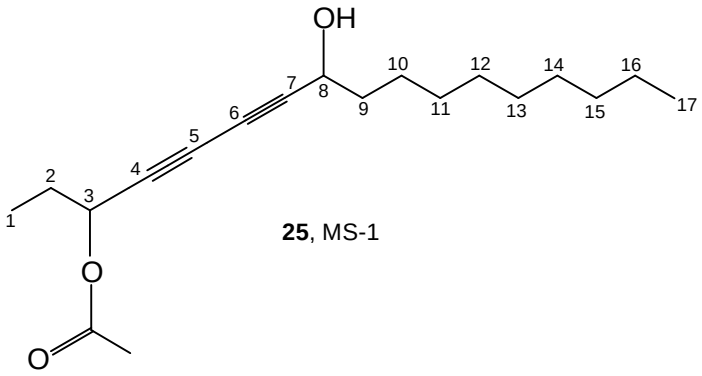

25, MS-1

The EI-MS measurement of MS-1 (**25**) showed a $[M]^+$ peak at *m*/*z* 306 and the molecular formula was determined as $C_{19}H_{30}O_3$ from its HR-EI-MS measurement (*m*/*z* $[M]^+$ calc.: 306.21950; found : 306.21971). The UV spectrum suggested a conjugated diyne [158]. IR absorption bands indicated the presence of hydroxyl groups (3424 cm^{-1}), alkanes (2926 cm^{-1}, 2855 cm^{-1}, 1464 cm^{-1} and 1372 cm^{-1}), acetylenes (2253 cm^{-1} and 2156 cm^{-1}) and esters/acetates (1746 cm^{-1} and 1231 cm^{-1}). The ^{13}C-NMR spectrum (figure 8) showed 19 resonances, which corresponded to the molecular formula derived from HR-EI-MS. The DEPT135 spectrum (figure 8) showed 14 resonances, five methyls or methines (δ_C 65.3, 62.9, 20.9, 14.1 and 9.3) and nine methylenes (δ_C 37.5, 31.9, 29.51, 29.48, 29.29, 29.21, 27.8, 25.0 and 22.7). Therefore it could be concluded that the molecule must contain five quaternary carbon atoms (δ_C 169.9, 80.6, 76.7, 69.3 and 68.8) which was also confirmed by HMQC. The quaternary carbon atom at δ_C 169.9 was identified as that of an ester carbonyl group and the other four had to be connected by conjugated triple bonds. The suggestion of a diyne structure also was in agreement with the acetylene bands in the IR spectrum, the UV bands and the comparison with literature data [140].

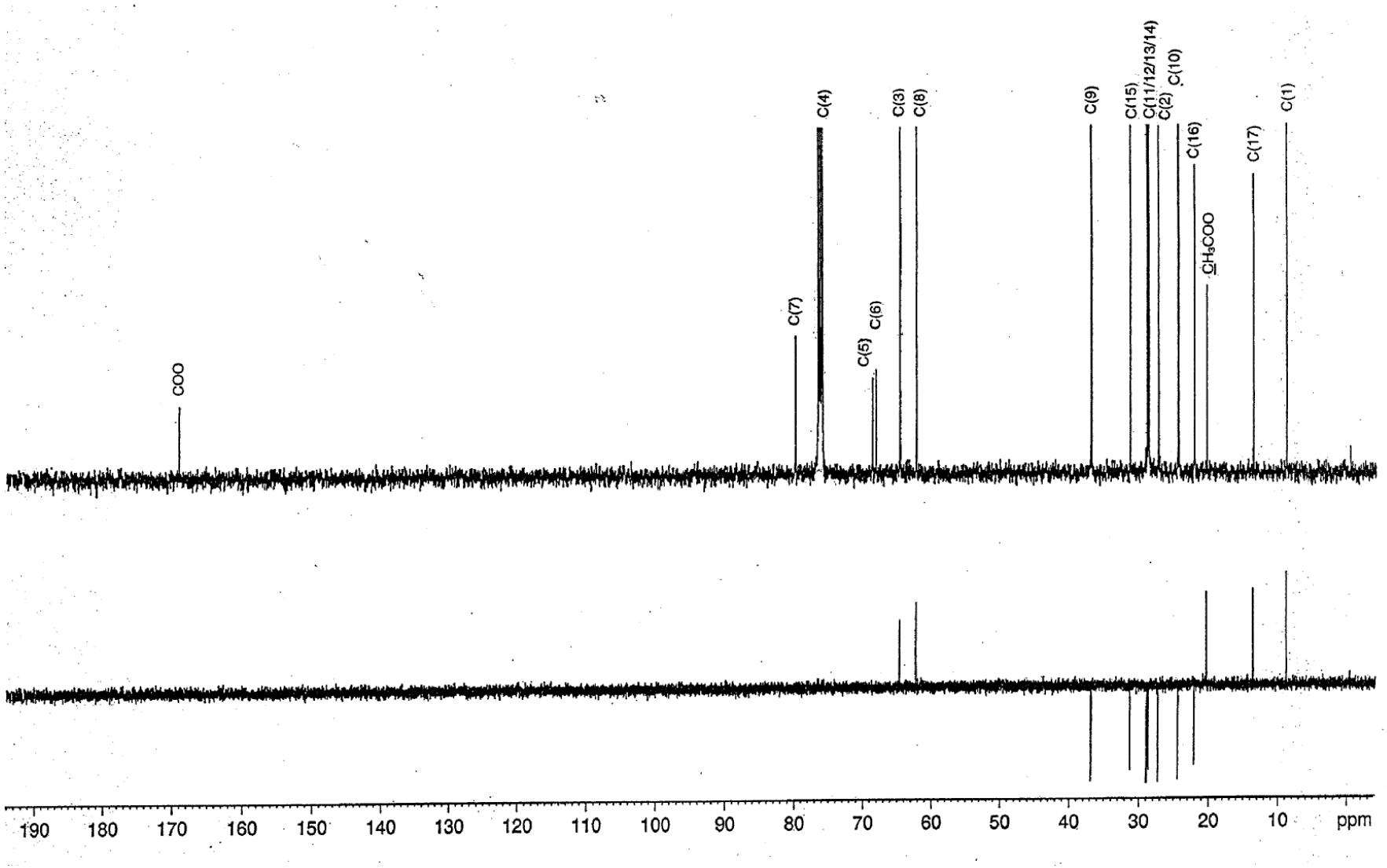

Figure 8 : ^{13}C-NMR and DEPT135 of 8-hydroxyheptadeca-4,6-diyn-3-yl acetate (MS-1 (**25**)) in $CDCl_3$.

The crosspeaks in the HMQC spectrum (figure 9) and the corresponding integrals from the ^{1}H-NMR spectrum (figure 10) showed that the carbon atoms at δ_C 65.3 and 62.9 were methines and those at δ_C 20.9, 14.1 and 9.3 were methyls. Therefore the molecule must contain the following structure components :

1x COO

4x C (conjugated triple bonds)

2x CH

3x CH_3

9x CH_2

= $C_{19}H_{29}O_2$. The difference to the found molecular formula was OH which corresponded to the hydroxyl band in the IR spectrum.

Furthermore the carbon atoms at δ_C 65.3 and 62.9 were identified as oxygen-bearing.

The ^{1}H-NMR spectrum (figure 10) showed two oxygen-bearing methines at δ_H 5.35 (*t*, *J* = 6.5) and 4.42 (*t*, *J* = 6.6), three methyls at δ_H 1.02 (*t*, *J* = 7.4), 0.88 (*t*, *J* = 7.0) and 2.09 (*s*), a hydroxyl at δ_H 1.75 (*d*, *J* = 5.8), and three methylenes at δ_H 1.82-1.77 (*m*), 1.72-1.69 (*m*) and 1.43 (*broad q*, *J* = 7.3) and an overlapped methylene envelope at δ_H 1.31-1.26 (*m*). A ^{1}H-^{1}H COSY experiment (figure 11) showed two separate spin systems. The first showed a methyl at δ_H 1.02 (*t*) that was coupled to a methylene at δ_H 1.82-1.77 (*m*) that was further coupled to an oxygen-bearing methine at δ_H 5.35 (*t*) marking the end of this spin system. The second spin system began at the second oxygen-bearing methine at δ_H 4.42 (*t*) which was coupled to a hydroxyl proton at δ_H 1.75 (*d*) and a methylene at δ_H 1.72-1.69 (*m*) that was coupled to a further methylene at δ_H 1.43 (*broad q*). Beyond this, the spin system extended to the overlapped methylene envelope at δ_H 1.31-1.26 (*m*) and could not be traced further with certainty.

Then the ^{13}C resonances were correlated with the corresponding ^{1}H resonances by HMQC (figure 9) and the structure components were linked using an HMBC experiment (figure 12). Key correlations were that of the carbonyl carbon atom at δ_C 169.9 with the methyl protons at δ_H 2.09 which indicated an acetate. The correlation observed between the carbonyl carbon atom at δ_C 169.9 and the methine proton at δ_H 5.35 indicated an acetoxy group at the C-atom with δ_C 65.3.

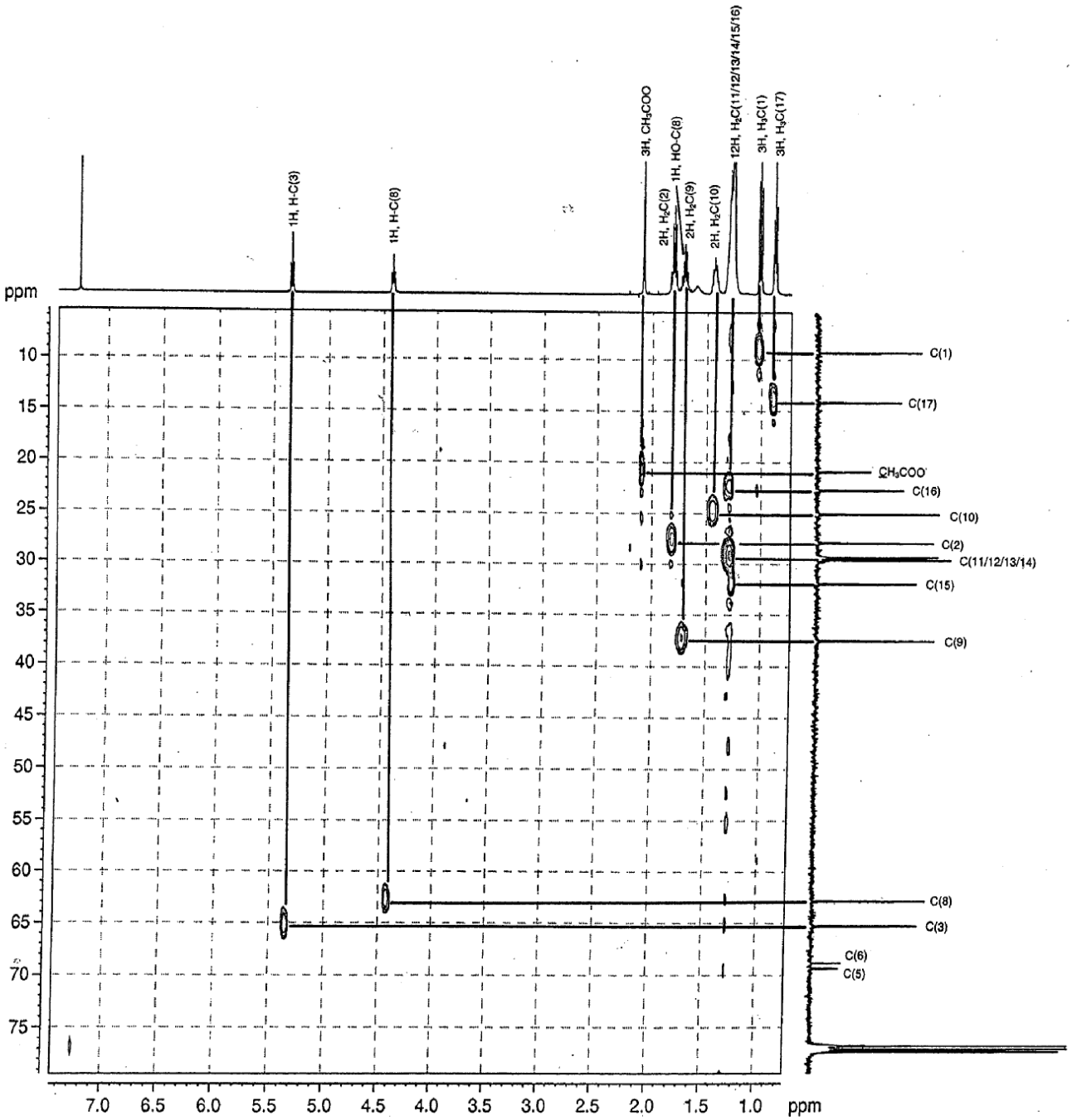

Figure 9 : HMQC of 8-hydroxyheptadeca-4,6-diyn-3-yl acetate (MS-1 (**25**)) in $CDCl_3$.

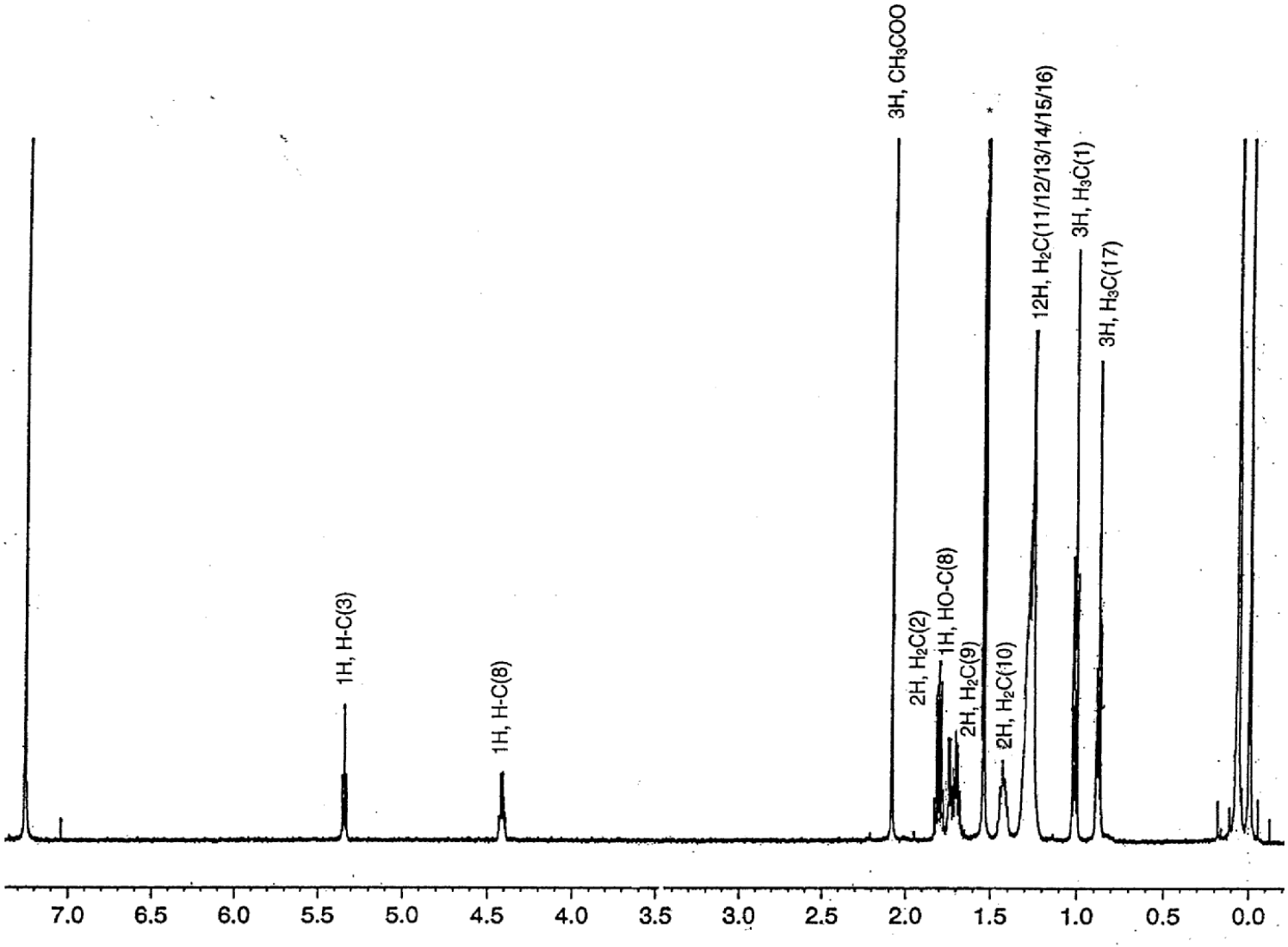

Figure 10 : ^{1}H-NMR of 8-hydroxyheptadeca-4,6-diyn-3-yl acetate (MS-1 (**25**)) in $CDCl_3$. (∗ water).

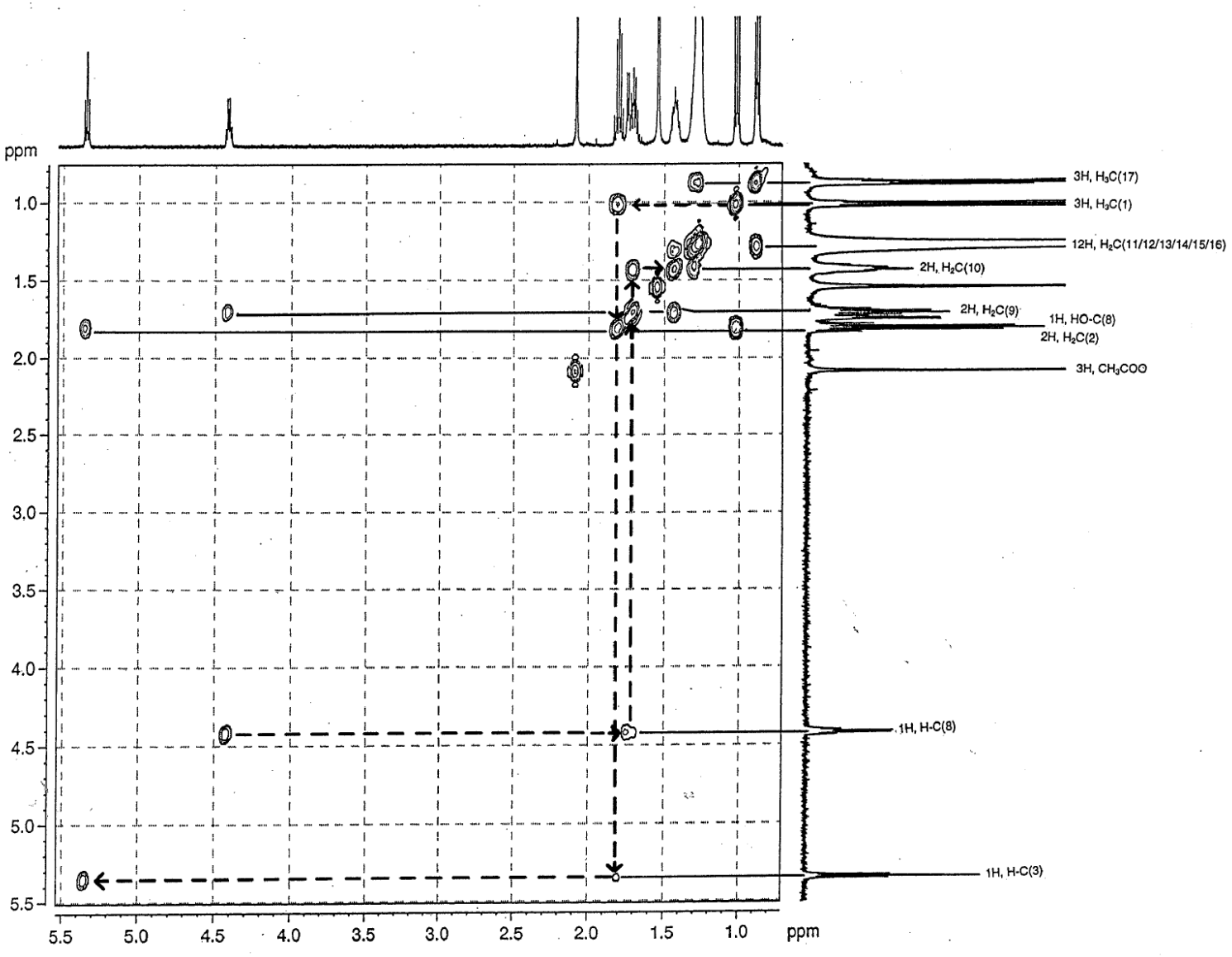

Figure 11 : ^{1}H-^{1}H COSY of 8-hydroxyheptadeca-4,6-diyn-3-yl acetate (MS-1 (**25**)) in $CDCl_3$.

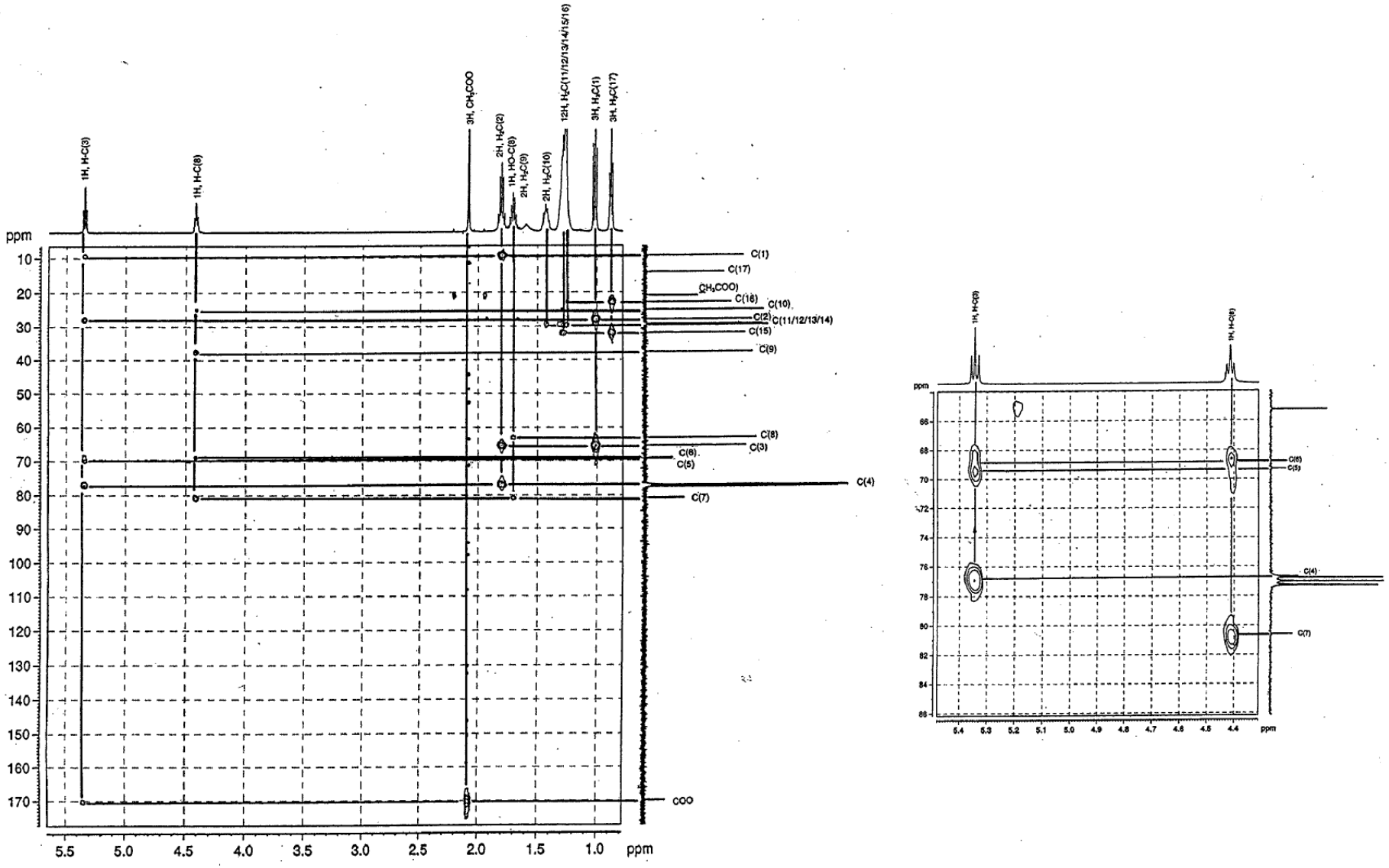

Figure 12 : HMBC of 8-hydroxyheptadeca-4,6-diyn-3-yl acetate (MS-1 (**25**)) in $CDCl_3$ (with detail).

The acetylene carbon atom at δ_C 80.6 showed crosspeaks with the proton of the hydroxyl-bearing methine at δ_H 4.42 and the methylene protons at δ_H 1.72-1.69, which placed the carbinol-C with δ_C 62.9 adjacent to the acetylene-C at δ_C 80.6. On the opposite side of the diyne, a correlation was observed between the acetylene carbon atom at δ_C 76.7 and the methine proton at δ_H 5.35 and the methylene protons at δ_H 1.82-1.77 which placed this acetylene carbon next to the acetoxy-bearing C at δ_C 65.3. A strong correlation between one of the inner alkyne carbon atoms at δ_C 69.3 and the methine proton at δ_H 5.35, and a weak correlation with the methine proton at δ_H 4.42 placed this acetylene carbon next to that at δ_C 76.7. The second inner alkyne carbon atom at δ_C 68.8 correlated strongly with the methine proton at δ_H 4.42 and weakly with the methine proton at δ_H 5.35, which placed it adjacent to the acetylene carbon atom at δ_C 80.6. The crosspeaks between the carbon at δ_C 65.3 and the methylene protons at δ_H 1.82-1.77 and the methyl protons at δ_H 1.02 placed the methylene at δ_C 27.8 next to the acetate and the methyl at δ_C 9.3 next to the methylene. The hydroxyl-bearing methine at δ_C 62.9 showed crosspeaks with the methylene protons at δ_H 1.72-1.69 which placed the methylene-C at δ_C 37.5 next to the carbinol. This methylene-C correlated with the protons of a further methylene at δ_H 1.43, which placed that methylene-C at δ_C 25.0. Finaly the methylene-C at δ_C 31.9 showed strong correlations with the methyl protons at δ_H 0.88 and with methylene protons of the methylene envelope at δ_H 1.28. Another methylene-C at δ_C 22.7 showed also a strong correlation with the methyl protons at δ_H 0.88 but only a weak correlation with the protons of a methylene of the methylene envelope at δ_H 1.26. That placed the methylene-C at δ_C 31.9 next to that at δ_C 22.7 and that next to the terminal methyl group.

The formula of MS-1 (**25**) with C→H correlations obtained from the HMBC experiment is shown in figure 13.

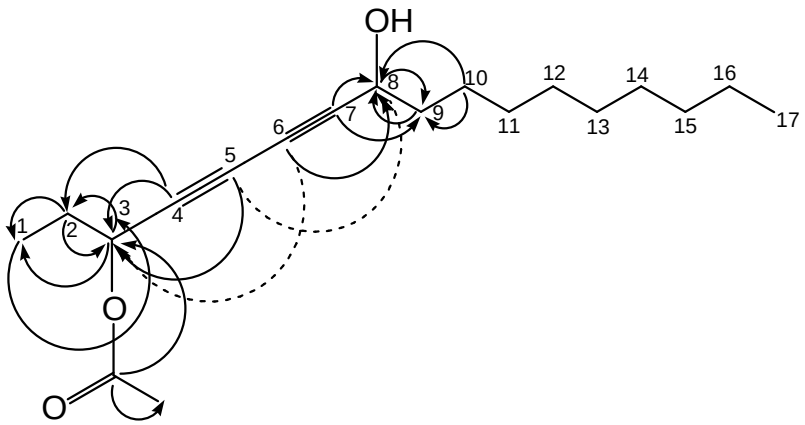

Figure 13 : C→H correlations obtained from the HMBC experiment of MS-1 (**25**) in $CDCl_3$. (Optimized for ${}^{n}J_{CH}$ = 7 Hz (*n* = 2 or 3)).

On the basis of the above data MS-1 (**25**) was identified as 8-hydroxyheptadeca-4,6-diyn-3-yl acetate. The comparison of the spectroscopic data with those of analogous structures from the literature : (+)-9(*Z*),17-octadecadiene-12,14-diyne-1,11,16-triol (**43**) [140]; oplopandiol (**44**), (+)-9(*Z*),17-octadecadiene-12,14-diyne-1,11,16-triol, 1-acetate (**45**); oplopandiol acetate (**46**) [168]; and (9*Z*, 16*S*)-16-hydroxy-9,17-octadecadiene-12,14-diynoic acid (**47**) [169] showed good correspondance.

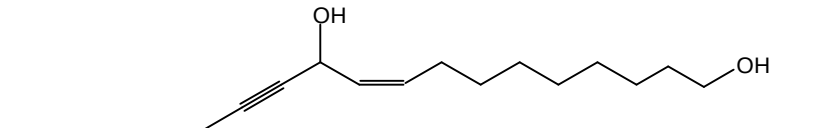

43, (+)-9(*Z*),17-Octadecadiene-12,14-diyne-1,11,16-triol

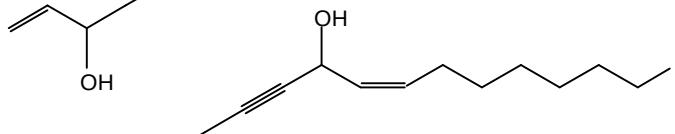

44, oplopandiol

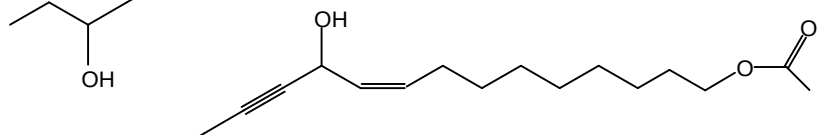

45, (+)-9(*Z*),17-Octadecadiene-12,14-diyne-1,11,16-triol, 1-acetate

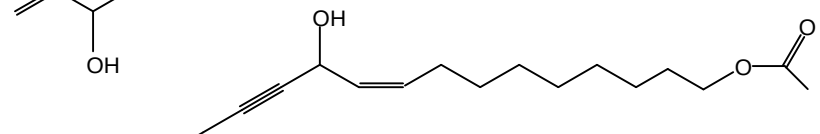

46, oplopandiol acetate

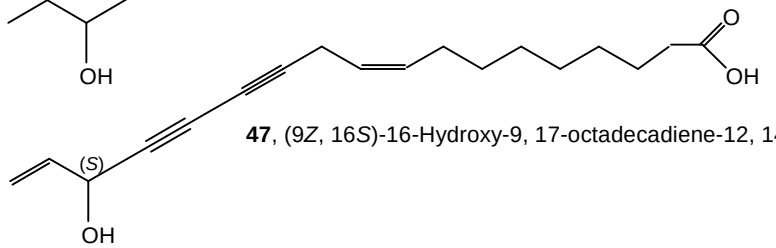

47, (9*Z*, 16*S*)-16-Hydroxy-9, 17-octadecadiene-12, 14-diynoic acid

5.2.2.2 8-Hydroxyheptadeca-1-ene-4,6-diyn-3-yl acetate (MS-2 (**26**)), a novel diyne

Preparative HPLC (see scheme 9 and 11) yielded 76.4 mg and 4.8 mg of a yellowish viscous oil with a negative optical rotation ($[\alpha]_D$ –28.0). The oil was analyzed by FAB-MS (NBA + KCl), EI-MS, HR-EI-MS, UV/VIS- and IR-spectroscopy, ^{1}H-NMR, ^{13}C-NMR, DEPT135, ^{1}H-^{1}H COSY, HMQC and HMBC.

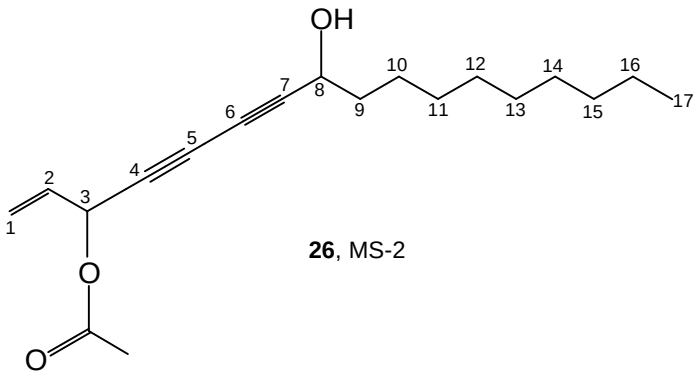

26, MS-2

The FAB-MS (NBA + KCl) measurement of MS-2 (**26**) showed a $[M+K]^+$ peak at *m*/*z* 343, therefore the molecular mass must have been 304. The EI-MS measurement showed an $[M-1]^+$ peak of *m*/*z* 303 and the molecular formula was determined as $C_{19}H_{27}O_3$ from its HR-EI-MS measurement (*m*/*z* $[M-1]^+$ calc.: 303.19602; found : 303.19530). Therefore the correct molecular formula must have been $C_{19}H_{28}O_3$. The UV spectrum suggested a conjugated diyne [158]. IR absorption bands indicated the presence of hydroxyl groups (3426 cm^{-1}), alkenes (3088 cm^{-1} and 1650 cm^{-1}), alkanes (2926 cm^{-1}, 2856 cm^{-1}, 1461 cm^{-1} and 1372 cm^{-1}), acetylenes (2255 cm^{-1} and 2157 cm^{-1}) and esters/acetates (1746 cm^{-1} and 1225 cm^{-1}). The ^{13}C-NMR spectrum (figure 14) showed 19 resonances, which corresponded to the molecular formula derived from HR-EI-MS. The DEPT135 spectrum (figure 14) showed 14 resonances, five methyls or methines (δ_C 131.9, 64.5, 62.9, 20.9 and 14.1) and nine methylenes (δ_C 119.8, 37.4, 31.9, 29.51, 29.48, 29.29, 29.20, 25.0 and 22.7). Therefore it could be concluded that the molecule must contain five quaternary carbon atoms (δ_C 169.5, 81.3, 74.4, 70.8 and 68.6) which also was confirmed by HMQC. The quaternary carbon atom at δ_C 169.5 was identified as that of a ester carbonyl group and the other four had to be connected by conjugated triple bonds due to comparison with MS-1 (**25**).

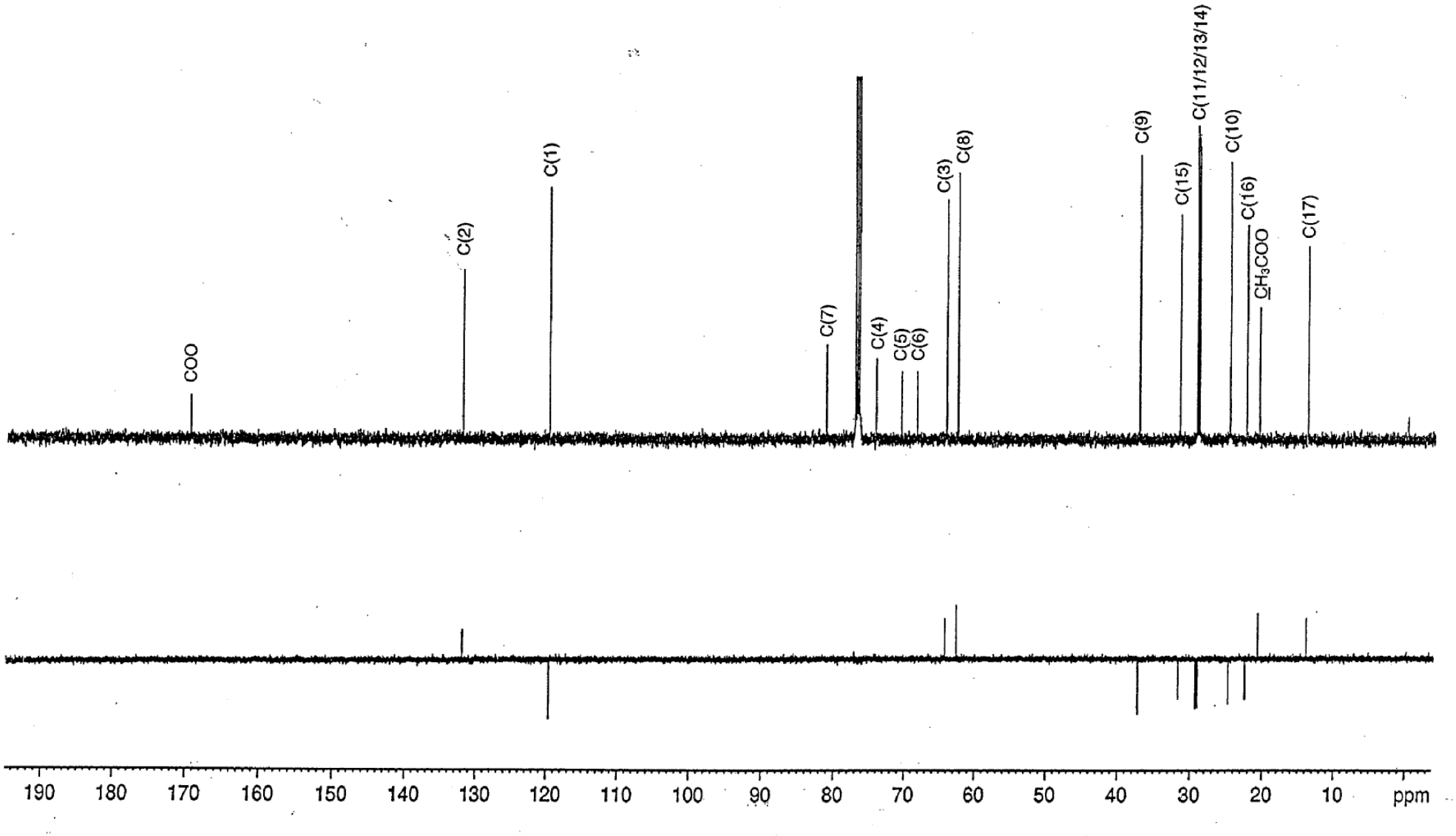

Figure 14 : ^{13}C-NMR and DEPT135 of 8-hydroxyheptadeca-1-ene-4,6-diyn-3-yl acetate (MS-2 (**26**)) in $CDCl_3$.

The suggestion of a diyne structure also was in agreement with the acetylene bands in the IR spectrum, the UV bands and the comparison with literature data [140]. The crosspeaks in the HMQC spectrum (figure 15) and the corresponding integrals from the ^{1}H-NMR spectrum (figure 16) showed that the carbon atoms at δ_C 131.9, 64.5 and 62.9 were methines and those at δ_C 20.9 and 14.1 were methyls. Therefore the molecule must contain the following structure components :

1x COO

4x C (conjugated triple bonds)

3x CH

2x CH_3

9x CH_2

= $C_{19}H_{27}O_2$. The difference to the found molecular formula was OH which corresponded to the hydroxyl band in the IR spectrum.

Furthermore the carbon atoms at δ_C 64.5 and 62.9 were identified as oxygen-bearing and those at δ_C 131.9 and 119.8 as a terminal olefin.

The ^{1}H-NMR spectrum (figure 16) showed signals for three olefinic protons at δ_H 5.89-5.84 (*m*), 5.55 (*d*, *J* = 16.8) and 5.35 (*d*, *J* = 10.0), two oxygen-bearing methines at δ_H 5.93-5.90 (*m*) and 4.43 (*broad t*, *J* = 6.5), a hydroxyl at δ_H 1.81 (*broad s*), two methylenes at δ_H 1.75-1.66 (*m*) and 1.43 (*broad q*, *J* = 7.5), two methyls at δ_H 2.11 (*s*) and 0.88 (*t*, *J* = 7.0) and a methylene envelope at δ_H 1.31-1.22 (*m*). A ^{1}H-^{1}H COSY experiment (figure 17) showed three separate spin systems. The first began with an olefinic methylene at δ_H 5.55 (*d*) and 5.35 (*d*) which was coupled with an olefinic methine at δ_H 5.89-5.84 (*m*) that was further linked to an oxygen-bearing methine at δ_H 5.93-5.90 (*m*) marking the end of this spin system. The second spin system began at the second oxygen-bearing methine at δ_H 4.43 (*broad t*) which was coupled to a hydroxyl at δ_H 1.81 (*broad s*) and a methylene at δ_H 1.75-1.66 (*m*) that was coupled to a further methylene at δ_H 1.43 (*broad q*). Beyond this, the spin system extended to the overlapped methylene envelope at δ_H 1.31-1.22 (*m*) and could not be traced further with certainty.

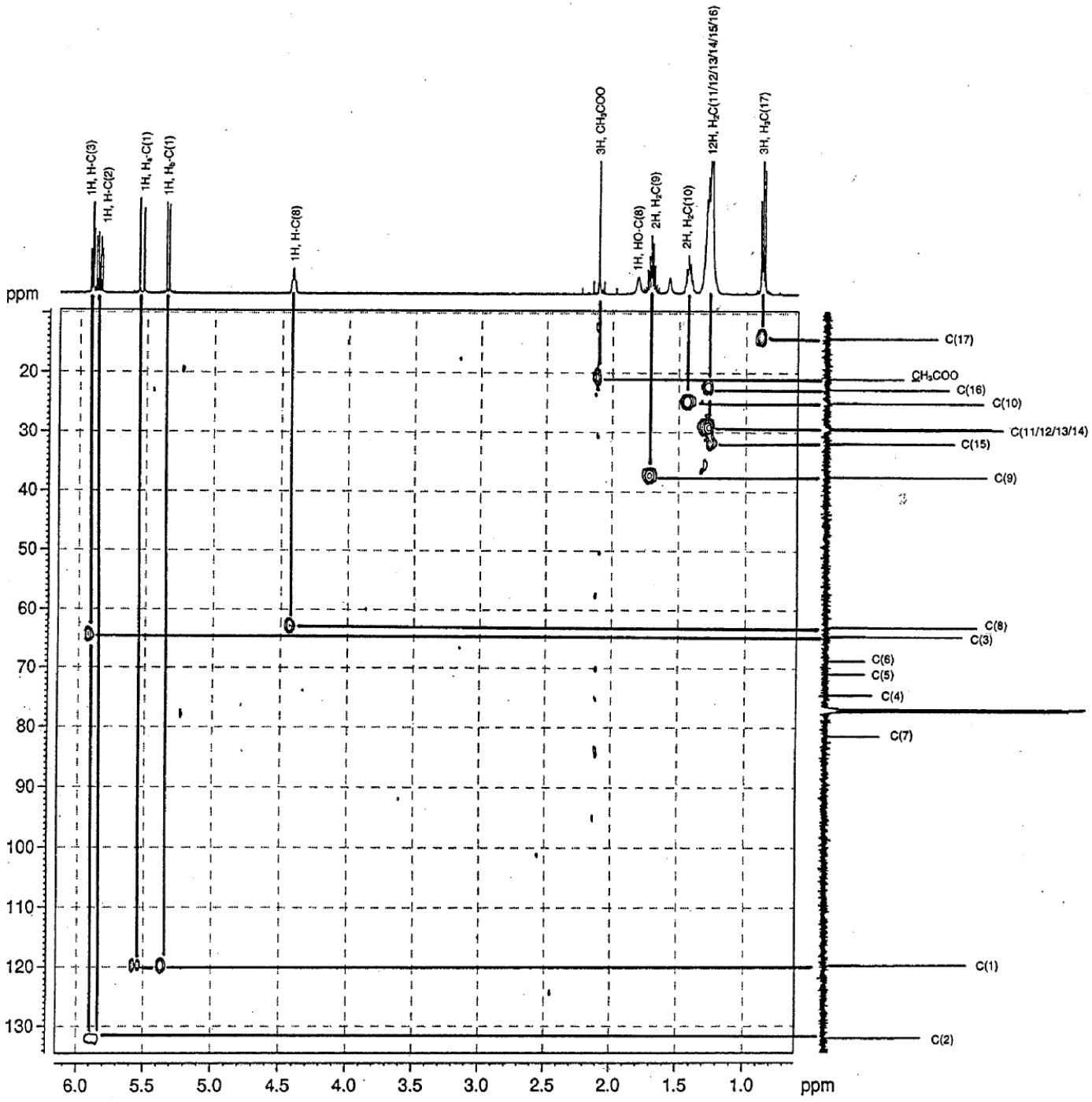

Figure 15 : HMQC of 8-hydroxyheptadeca-1-ene-4,6-diyn-3-yl acetate (MS-2 (**26**)) in $CDCl_3$.

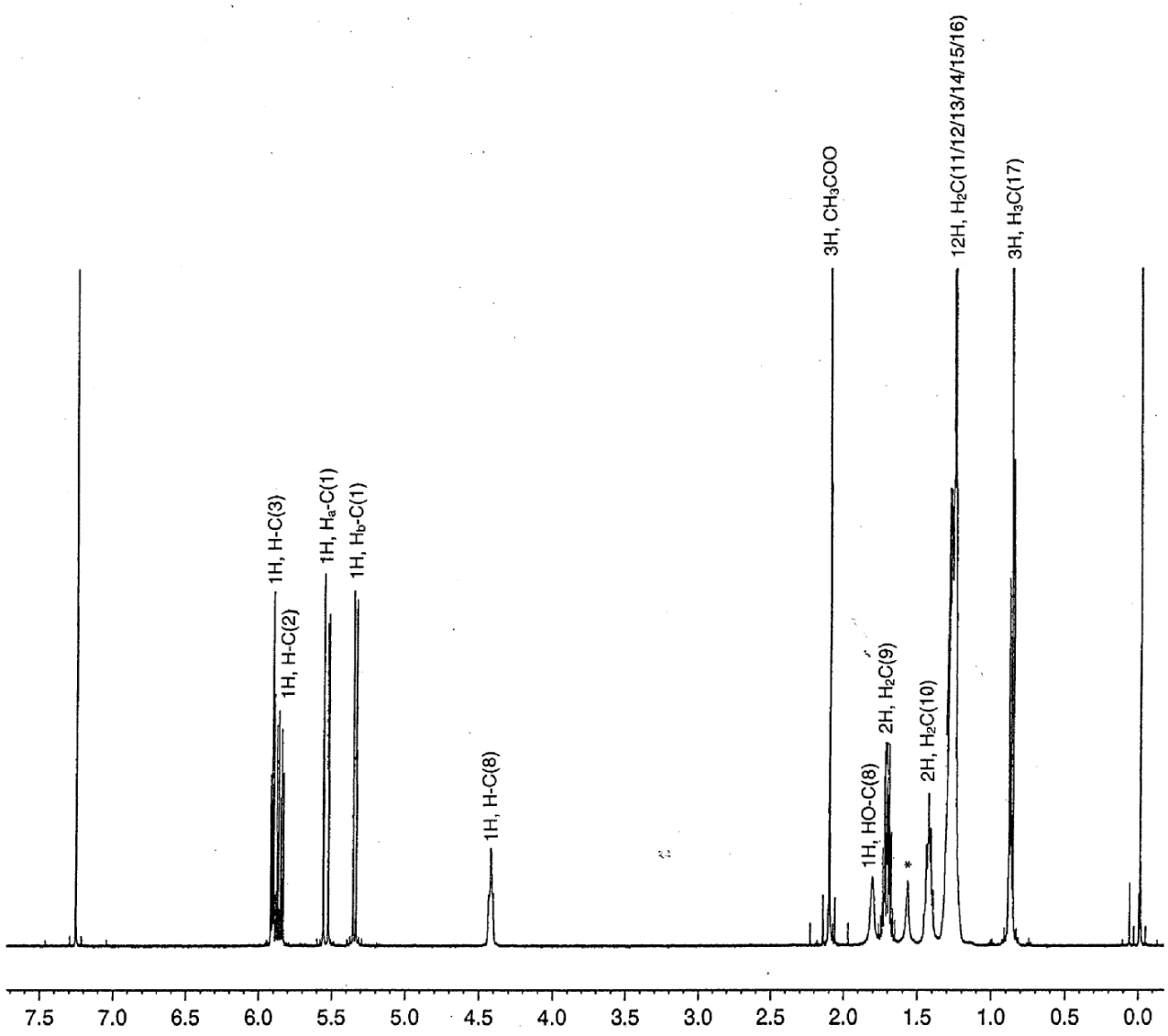

Figure 16 : ^{1}H-NMR of 8-hydroxyheptadeca-1-ene-4,6-diyn-3-yl acetate (MS-2 (**26**)) in $CDCl_3$.

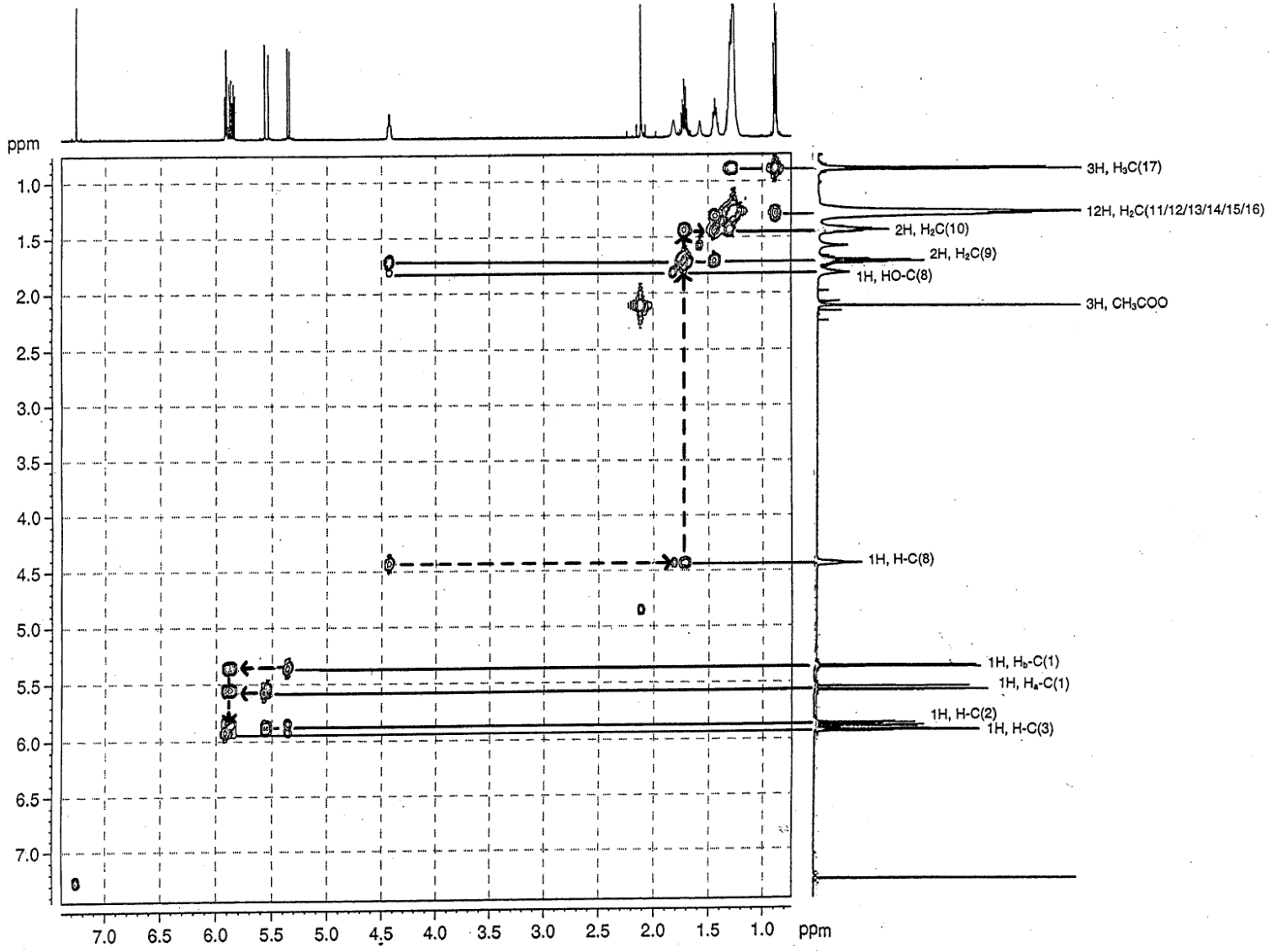

Figure 17 : ^{1}H-^{1}H COSY of 8-hydroxyheptadeca-1-ene-4,6-diyn-3-yl acetate (MS-2 (**26**)) in $CDCl_3$.

Then the ^{13}C resonances were correlated with the corresponding ^{1}H resonances by HMQC (figure 15) and the structure components were linked using an HMBC experiment (figure 18). Key correlations were that of the carbonyl carbon atom at δ_C 169.5 with the methyl protons at δ_H 2.11 which indicated an acetate. The correlation observed between the carbonyl carbon atom at δ_C 169.5 and the methine proton at δ_H 5.93-5.90 indicated an acetoxy group at the C-atom with δ_C 64.5. The acetylene carbon atom at δ_C 81.3 showed a correlation with the methylene protons at δ_H 1.75-1.66 but none with the protons of the hydroxyl-bearing methine (δ_H 4.43). After comparison with the data of MS-1 (**25**) the carbon atom with δ_C 62.9 had to be placed next to the acetylene-C at δ_C 81.3. On the opposite side of the diyne, a correlation was observed between the acetylene carbon atom at δ_C 74.4 and the methine protons at δ_H 5.93-5.90 and 5.89-5.84 which placed this acetylene-C adjacent to the C at δ_C 64.5. The position of the inner alkyne carbons could not been determined with certainty because both showed correlations with the same methine proton at δ_H 5.93-5.90 on the one side of the diyne and none with the protons of the hydroxyl-bearing methine (δ_H 4.43) on the other side of the diyne. But due to the comparison with the observed data of MS-1 (**25**) it could been suggested that the inner alkyne carbon at δ_C 70.8 was placed next to that at δ_C 74.4 and the other at δ_C 68.6 next to that at δ_C 81.3. The crosspeaks between the C at δ_C 64.5 and the olefinic methine proton at δ_H 5.89-5.84 and the olefinic methylene protons at δ_H 5.55 placed the olefinic methine at δ_C 131.9 adjacent to the C at δ_C 64.5 and the olefinic methylene at δ_C 119.8 next to the olefinic methine at δ_C 131.9. The hydroxyl-bearing methine at δ_C 62.9 showed crosspeaks with the methylene protons at δ_H 1.75-1.66 which placed the methylene-C at δ_C 37.4 next to the carbinol. This methylene-C correlated with a further methylene proton at δ_H 1.43 which placed that methylene-C next to the C with δ_C 25.0. Finaly the methylene-C at δ_C 31.9 showed strong correlations with the methyl protons at δ_H 0.88 and the protons of a methylene of the methylene envelope at δ_H 1.28. Another methylene-C at δ_C 22.7 showed also a strong correlation with the protons at δ_H 0.88 but only a weak correlation with protons of the methylene envelope at δ_H 1.26. That placed the methylene-C at δ_C 31.9 next to that at δ_C 22.7 and that adjacent to the terminal methyl group.

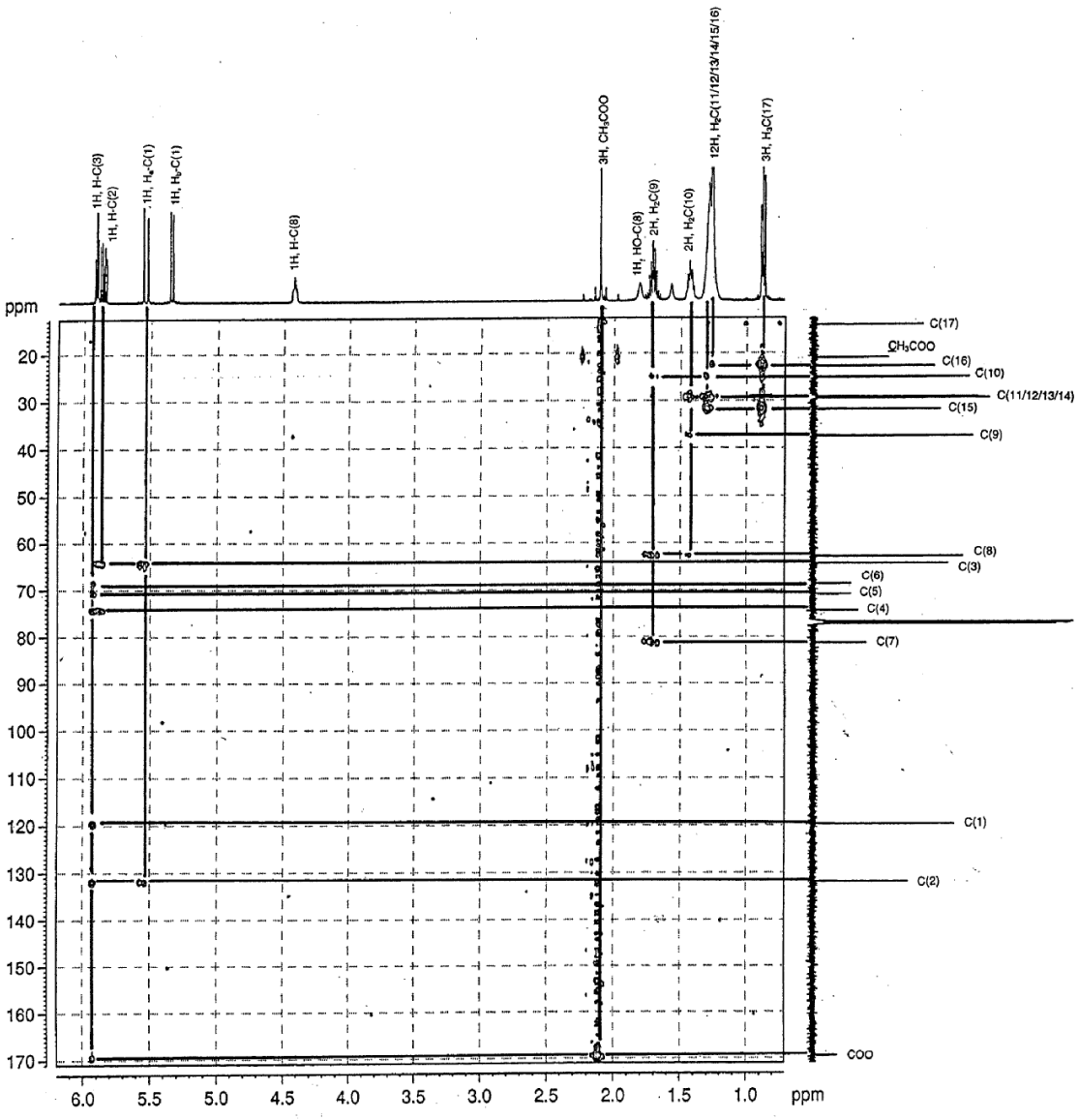

Figure 18 : HMBC of 8-hydroxyheptadeca-1-ene-4,6-diyn-3-yl acetate (MS-2 (**26**)) in $CDCl_3$.

The formula of MS-2 (**26**) with C→H correlations obtained from the HMBC experiment is shown in figure 19.

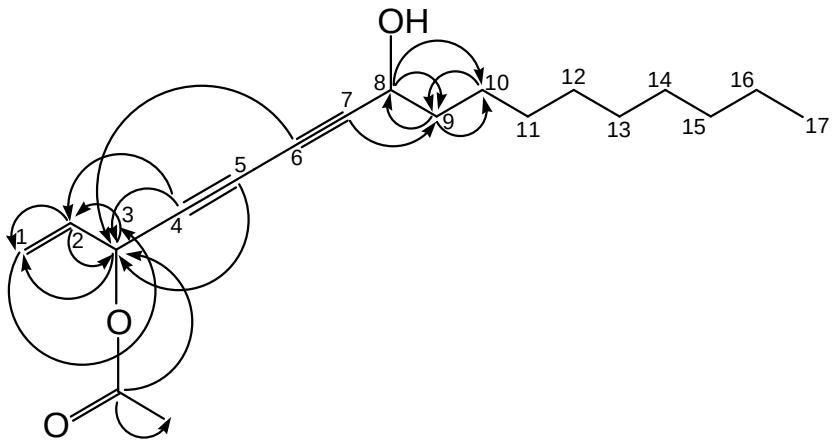

Figure 19 : C→H correlations obtained from the HMBC experiment of MS-2 (**26**) in $CDCl_3$.
(Optimized for ${}^{n}J_{CH}$ = 7 Hz (*n* = 2 or 3)).

On the basis of the above data MS-2 (**26**) was identified as 8-hydroxyheptadeca-1-ene-4,6-diyn-3-yl acetate. The comparison of the spectroscopic data with those of analogous structures from the literature : **43** [140]; **44**, **45**, **46** [168]; and **47** [169] showed good correspondance.

5.2.2.3 16-Acetoxy-11-hydroxyoctadeca-17-ene-12,14-diynyl acetate (MS-4 (**27**)), a novel diyne

Preparative HPLC (see scheme 13) yielded 221.7 mg of a yellowish viscous oil with a negative optical rotation ($[\alpha]_D$ –26.4). The oil was analyzed by FAB-MS (NBA + KCl), HR-EI-MS, UV/VIS- and IR-spectroscopy, ^{1}H-NMR, ^{13}C-NMR, DEPT135, ^{1}H-^{1}H COSY, HMQC and HMBC.

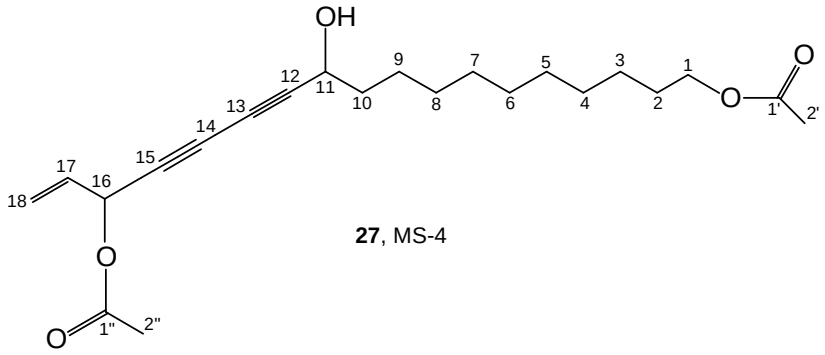

27, MS-4

The FAB-MS (NBA + KCl) measurement of MS-4 (**27**) showed a $[M+K]^+$ peak at *m*/*z* 415, therefore the molecular mass must have been 376. The molecular formula was determined as $C_{22}H_{32}O_5$ from its HR-EI-MS measurement (*m*/*z* $[M]^+$ calc.: 376.22497; found : 376.22369). The UV spectrum suggested a conjugated diyne [158]. IR absorption bands indicated the presence of hydroxyl groups (3444 cm^{-1}), alkenes (3086 cm^{-1}, 3031 cm^{-1} and 1644 cm^{-1}), alkanes (2922 cm^{-1}, 2844 cm^{-1}, 1467 cm^{-1} and 1367 cm^{-1}), acetylenes (2256 cm^{-1} and 2156 cm^{-1}) and esters/acetates (1739 cm^{-1} and 1233 cm^{-1}). The ^{13}C-NMR spectrum (figure 20) showed 22 resonances, which corresponded to the molecular formula derived from HR-EI-MS. The DEPT135 spectrum (figure 20) showed 16 resonances, five methyls or methines (δ_C 131.9, 64.5, 62.8, 21.0 and 20.9) and 11 methylenes (δ_C 119.7, 64.7, 37.4, 29.44, 29.41, 29.37, 29,21, 29.17, 28.6, 25.9 and 25.0). Therefore it could be concluded that the molecule must contain six quaternary carbon atoms (δ_C 171.3, 169.5, 81.4, 74.3, 70.9 and 68.5) which also was confirmed by HMQC. The quaternary carbon atoms at δ_C 171.3 and 169.5 were identified as those of ester carbonyl groups and the other four had to be connected by conjugated triple bonds due to the comparison with MS-1 (**25**). The suggestion of a diyne structure also was in agreement with the acetylene bands in the IR spectrum, the UV bands and the comparison with literature data [140].

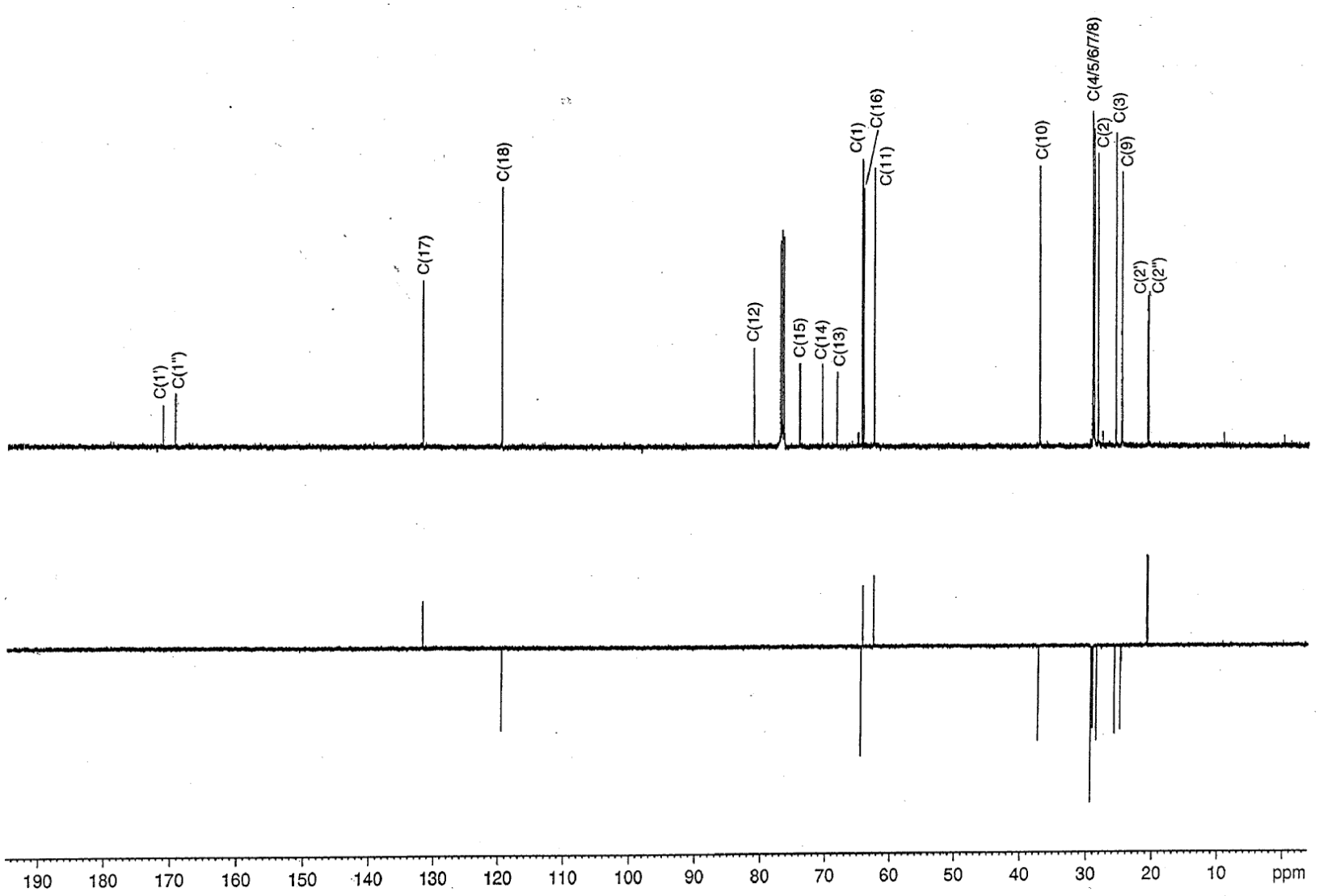

Figure 20 : ^{13}C-NMR and DEPT135 of 16-acetoxy-11-hydroxyoctadeca-17-ene-12,14-diynyl acetate (MS-4 (**27**)) in $CDCl_3$.

The crosspeaks in the HMQC spectrum (figure 21) and the corresponding integrals from the ^{1}H-NMR spectrum (figure 22) showed that the carbon atoms at δ_C 131.9, 64.5 and 62.8 were methines and those at δ_C 21.0 and 20.9 were methyls. Therefore the molecule must contain the following structure components :

2x COO

4x C (conjugated triple bonds)

3x CH

2x CH_3

11x CH_2

= $C_{22}H_{31}O_4$. The difference to the found molecular formula was OH which corresponded to the hydroxyl band in the IR spectrum.

Furthermore the carbon atoms at δ_C 64.7, 64.5 and 62.8 were identified as oxygen-bearing and those at δ_C 131.9 and 119.7 as a terminal olefin.

The ^{1}H-NMR spectrum (figure 22) showed signals for three olefinic protons at δ_H 5.88-5.83 (*m*), 5.54 (*d*, *J* = 16.8) and 5.34 (*d*, *J* = 10.0), three oxygen-bearing methines at δ_H 5.92-5.89 (*m*), 4.42 (*broad t*, *J* = 6.3) and 4.04 (*t*, *J* = 6.8), a hydroxyl at δ_H 2.02 (*broad s*), three methylenes at δ_H 1.73-1.68 (*m*), 1.61 (*q*, *J* = 7.2) and 1.43 (*broad q*, *J* = 7.2) and two methyls at δ_H 2.10 (*s*) and 2.04 (*s*). A ^{1}H-^{1}H COSY experiment (figure 23) showed three separate spin systems. The first began with an olefinic methylene at δ_H 5.54 (*d*) and 5.34 (*d*) which was coupled with an olefinic methine at δ_H 5.88-5.83 (*m*) that was further linked to an oxygen-bearing methine at δ_H 5.92-5.89 (*m*) marking the end of this spin system. The second spin system began at the second oxygen-bearing methine at δ_H 4.42 (*broad t*) which was coupled to a hydroxyl proton at δ_H 2.02 (*broad s*) and a methylene at δ_H 1.73-1.68 (*m*) that was coupled to a further methylene at δ_H 1.43 (*broad q*). Beyond this, the spin system extended to the overlapped methylene envelope at δ_H 1.34-1.24 (*m*) and could not be traced further with certainty. The third spin system showed a correlation between the third oxygen-bearing methine at δ_H 4.04 (*t*) and a methylene at δ_H 1.61 (*q*), beyond this the spin system also extended to the overlapped methylene envelope at δ_H 1.34-1.24 (*m*).

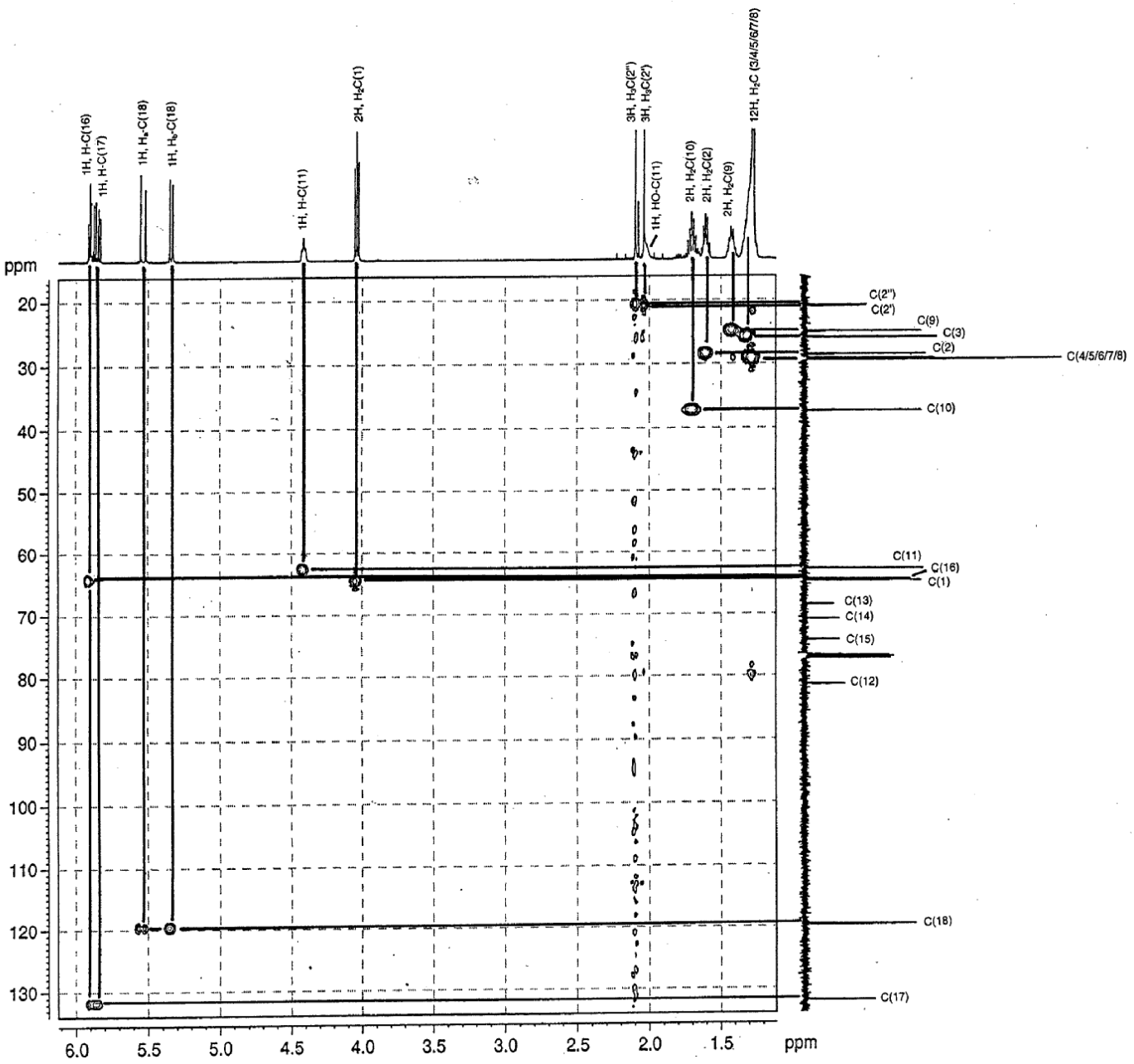

Figure 21 : HMQC of 16-acetoxy-11-hydroxyoctadeca-17-ene-12,14-diynyl acetate (MS-4 (**27**)) in $CDCl_3$.

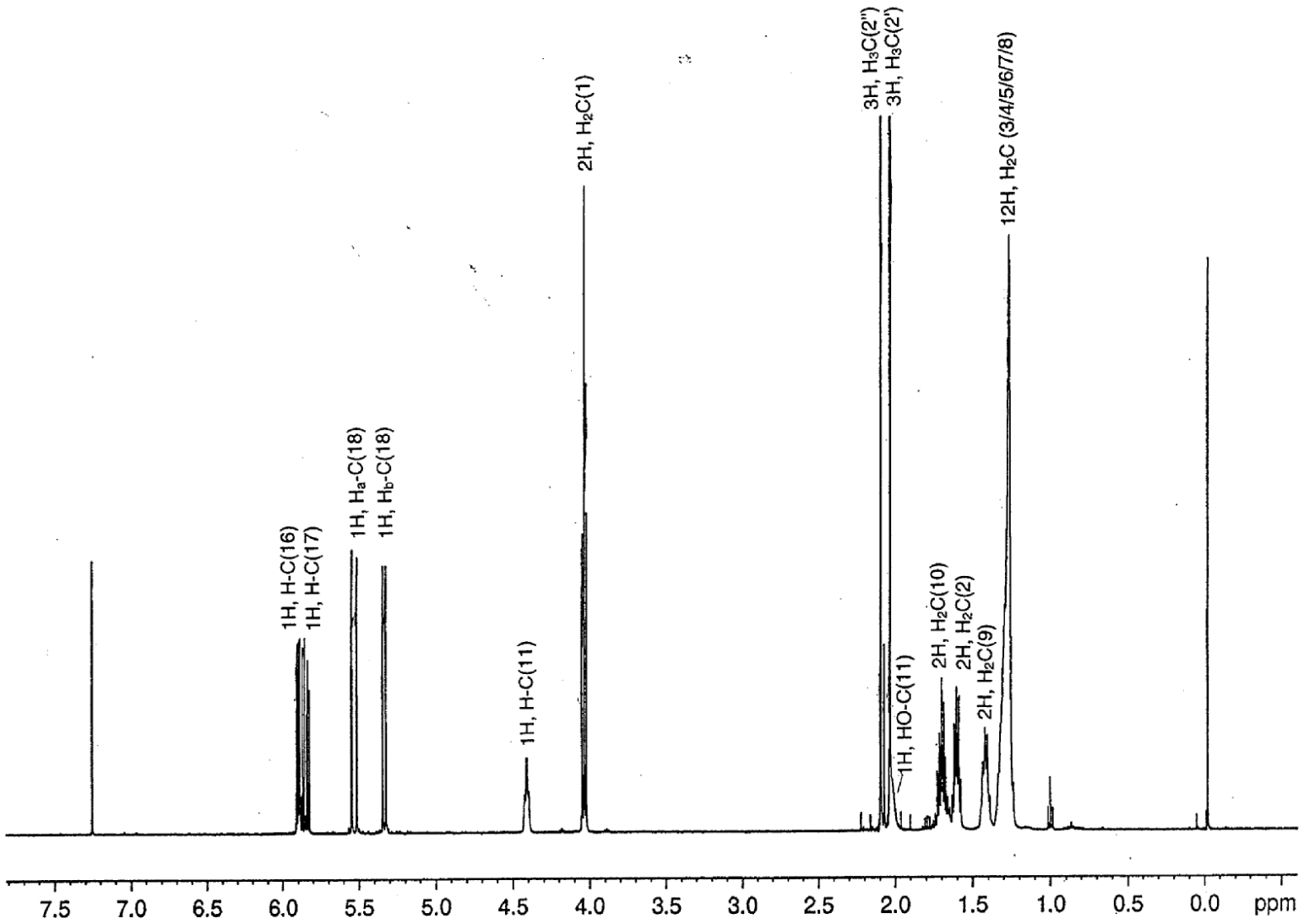

Figure 22 : ^{1}H-NMR of 16-acetoxy-11-hydroxyoctadeca-17-ene-12,14-diynyl acetate (MS-4 (**27**)) in $CDCl_3$.

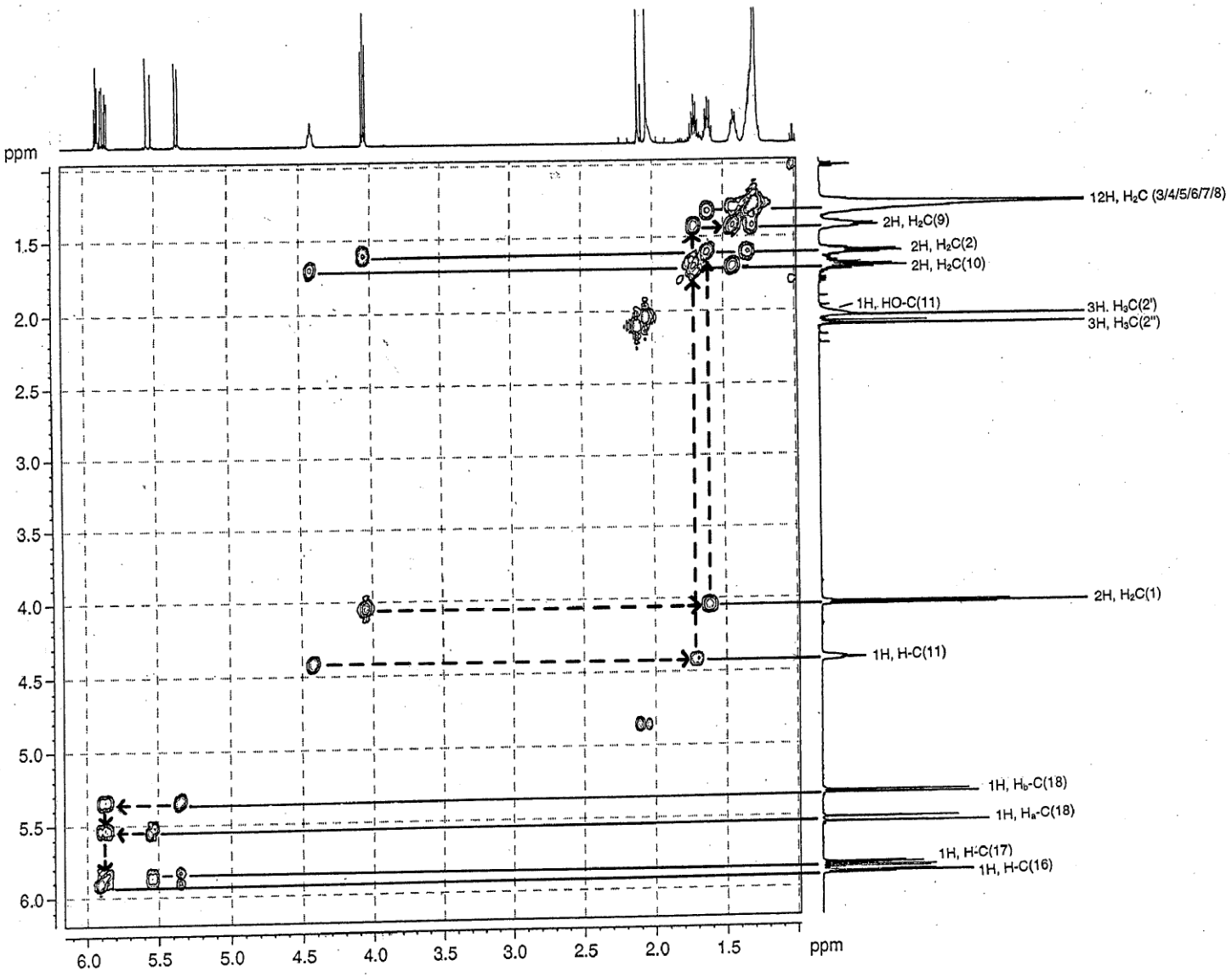

Figure 23 : ^{1}H-^{1}H COSY of 16-acetoxy-11-hydroxyoctadeca-17-ene-12,14-diynyl acetate (MS-4 (**27**)) in $CDCl_3$.

Then the ^{13}C resonances were correlated with the corresponding ^{1}H resonances by HMQC (figure 21) and the structure components were linked using an HMBC experiment (figure 24). Key correlations were that of the first carbonyl carbon atom at δ_C 171.3 with the methyl protons at δ_H 2.04 and the second carbonyl carbon atom at δ_C 169.5 with the methyl protons at δ_H 2.10 which indicated two acetates. The correlation observed between the carbonyl carbon atom at δ_C 171.3 and the methylene protons at δ_H 4.04 indicated a first acetoxy group at the C-atom with δ_C 64.7. The correlation observed between the carbonyl carbon atom at δ_C 169.5 and the methine proton at δ_H 5.92-5.89 indicated a second acetoxy group at the C-atom with δ_C 64.5. The acetylene carbon atom at δ_C 81.4 showed a correlation with the methylene protons at δ_H 1.73-1.68 and the proton of the hydroxyl-bearing methine at δ_H 4.42, which placed the carbinol-C with δ_C 62.8 adjacent to the acetylene carbon atom at δ_C 81.4. On the opposite side of the diyne, a correlation was observed between the acetylene carbon atom at δ_C 74.3 and the methine protons at δ_H 5.92-5.89 and 5.88-5.83 which placed this acetylene carbon next to the acetoxy-bearing C at δ_C 64.5. A strong correlation between one of the inner alkyne carbon atoms at δ_C 70.9 and the proton of the oxygen-bearing methine at δ_H 5.92-5.89 and a weak correlation with the proton of the hydroxyl-bearing methine at δ_H 4.42 placed this acetylene-C next to that at δ_C 74.3. The second inner alkyne carbon atom at δ_C 68.5 correlated with the proton of the hydroxyl-bearing methine at δ_H 4.42 and the proton of the oxygen-bearing methine at δ_H 5.92-5.89. Therefore its position could not been determined with certainty but due to the determined positions of the other three acetylene carbons and the comparison with MS-1 (**25**) the second inner alkyne carbon atom must have been placed next to that at δ_C 81.4. The crosspeaks between the carbon at δ_C 64.5 and the olefinic methine proton at δ_H 5.88-5.83 and the olefinic methylene protons at δ_H 5.54 placed the olefinic methine at δ_C 131.9 next to the acetate and the olefinic methylene at δ_C 119.7 next to the olefinic methine at δ_C 131.9. The hydroxyl-bearing methine at δ_C 62.8 showed crosspeaks with the methylene protons at δ_H 1.73-1.68 which placed the methylene-C at δ_C 37.4 next to the carbinol-C. This methylene-C correlated with further methylene protons at δ_H 1.43 which placed that methylene-C next at δ_C 25.0. The crosspeak between the acetate at δ_C 64.7 and the methylene-C at δ_H 1.61 together with the ^{1}H-^{1}H-COSY correlation between the acetate at δ_H 4.04 and the methylene protons at δ_H 1.61 placed that

methylene-C at δ_C 28.6 next to the acetate. Another crosspeak between the methylene-C at δ_C 25.9 and the methylene protons at δ_H 1.61 placed that methylene-C next to that at δ_C 28.6.

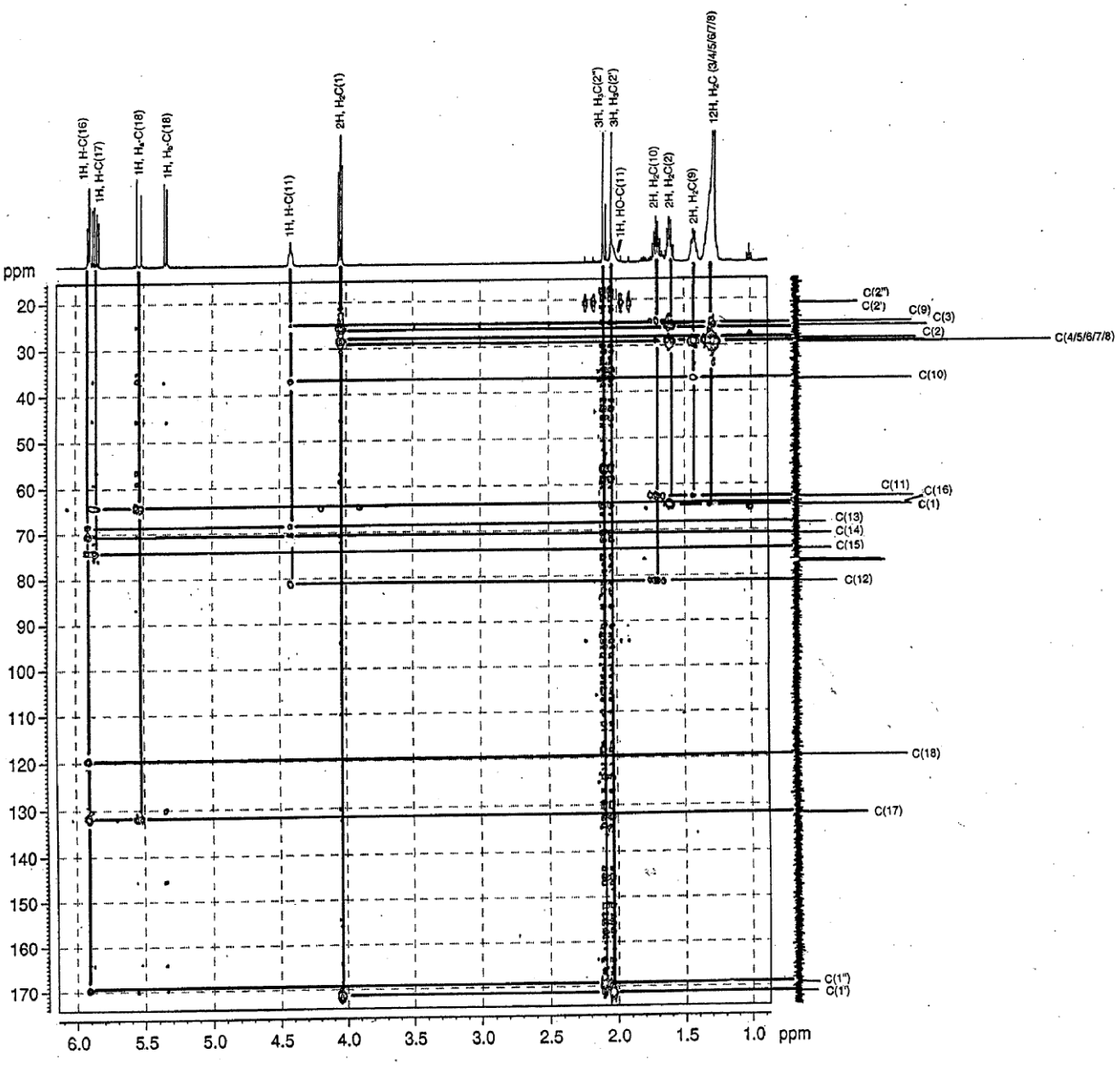

Figure 24 : HMBC of 16-acetoxy-11-hydroxyoctadeca-17-ene-12,14-diynyl acetate (MS-4 (**27**)) in $CDCl_3$.

The formula of MS-4 (**27**) with C→H correlations obtained from the HMBC experiment is shown in figure 25.

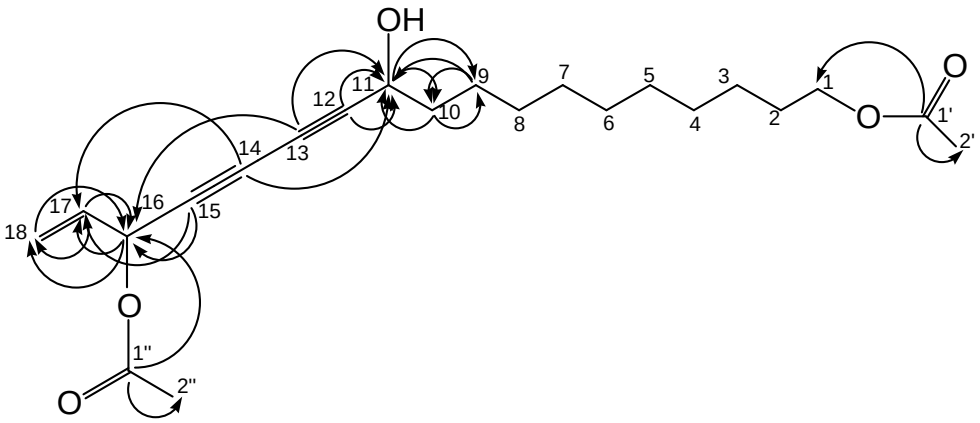

Figure 25 : C→H correlations obtained from the HMBC experiment of MS-4 (**27**) in $CDCl_3$. (Optimized for ${}^{n}J_{CH}$ = 7 Hz (*n* = 2 or 3)).

On the basis of the above data MS-4 (**27**) was identified as 16-acetoxy-11-hydroxyoctadeca-17-ene-12,14-diynyl acetate. The comparison of the spectroscopic data with those of analogous structures from the literature : **43** [140]; **44**, **45**, **46** [168]; and **47** [169] showed good correspondance.

5.2.2.3.1 Stereochemical analysis using the Mosher method

The Mosher technique is an empirically derived method to determine the absolute configuration of stereogenic centers of secondary alcohols by measuring the ^{1}H-NMR spectra [170] or ^{13}C-NMR spectra [171] of their MTPA esters. The method is based on the observation, that MTPA esters prefer a conformation in which the carbinyl proton, the C-O carbonyl bond, and the trifluoromethyl group are located in the same plane, called the "MTPA plane" (figure 26[A]). Protons and carbons on the same side as the phenyl group experience an upfield shift, due to the anisotropic effect of the phenyl group. Therefore, in an MTPA ester with the absolute configuration shown in figure 26[B], protons $H_{A,B,C}$ and carbons $C_{A,B,C}$ should have positive $\Delta\delta$ ($\Delta\delta = \delta_{(S)\text{-}ester} - \delta_{(R)\text{-}ester}$) values, and protons $H_{X,Y,Z}$ and carbons $C_{X,Y,Z}$ should have negative $\Delta\delta$ values.

The chiral alcohol is first coupled with each of the individual enantiomers of the Mosher acid chloride. The optically pure Mosher acid of *R* configuration [(*R*)-MTPA] is converted to the acid chloride of *S* configuration [(*S*)-MTPA-Cl] (**48**) and then to the MTPA ester of *R* configuration [(*R*)-MTPA-Cl] (**49**). The ^{1}H-NMR and ^{13}C-NMR spectra of the Mosher esters are then measured. The absolute configuration of the carbinol center can then be deduced from the $\Delta\delta$ values observed [172, 173].

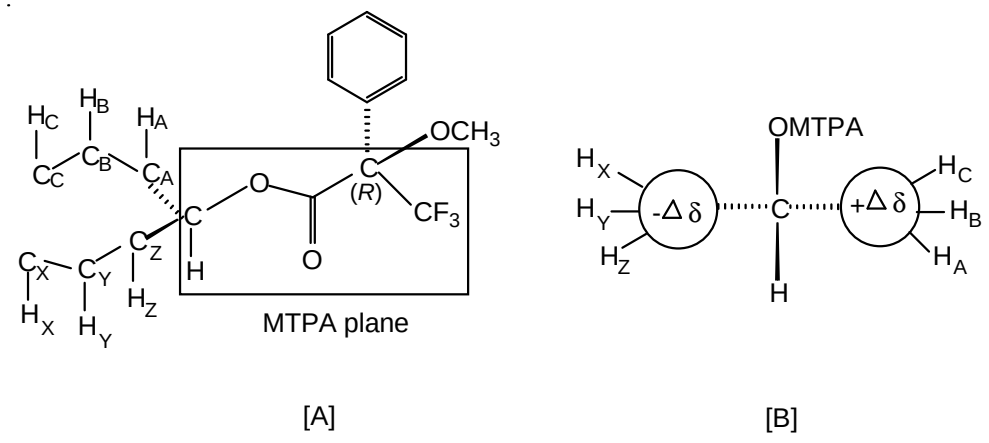

Figure 26 : [A] The MTPA plane of the (*R*)-MTPA ester of a secondary alcohol. [B] The rule for the determination of the absolute configurations of secondary alcohols ($\Delta\delta = \delta_{(S)\text{-}ester} - \delta_{(R)\text{-}ester}$).

5.2.2.3.2 Stereochemical analysis of MS-4 (**27**)

After the carrying out of the antiparasitic assays, the receptor binding studies and the electrophysiological investigations, only of MS-4 (**27**) the remaining amount was sufficient for stereochemical analysis.

The stereochemical analysis was performed by esterification of the OH at C(11) of MS-4 (**27**) according to the procedure outlined above (scheme 16). The results are shown in table 17.

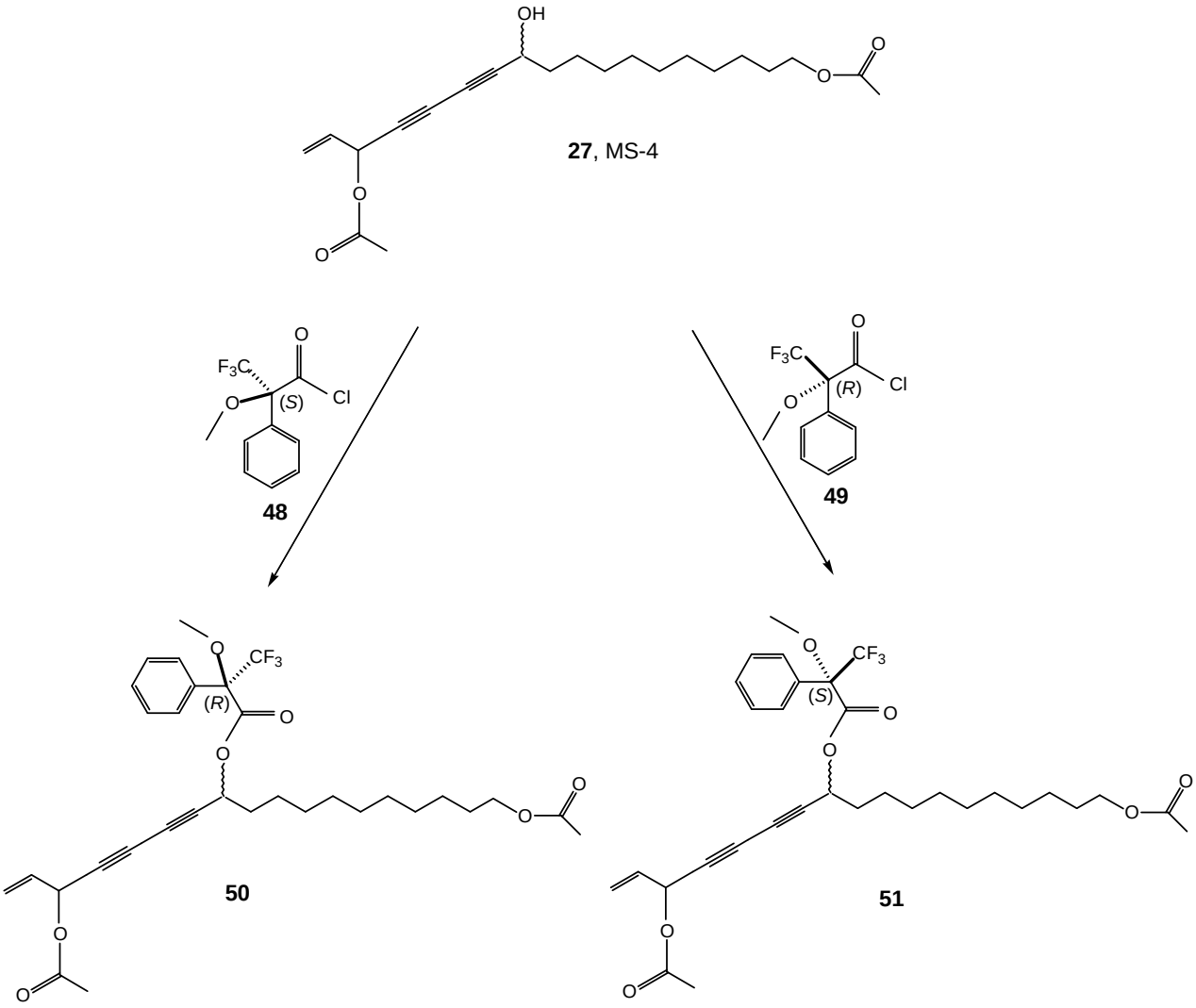

Scheme 16 : Synthesis procedure of the (*R*)-MTPA ester (**50**) and the (*S*)-MTPA ester (**51**) of MS-4 (**27**).

Table 17 : Results of the stereochemical analysis of the MTPA esters of MS-4 (**27**).

H no.	$\delta_{(S)\text{ - ester}}$	$\delta_{(R)\text{ - ester}}$	$\Delta\delta$ $(\delta_{(S)\text{ - ester}} - \delta_{(R)\text{ – ester}})$	C no.	$\delta_{(S)\text{ - ester}}$	$\delta_{(R)\text{ - ester}}$	$\Delta\delta$ $(\delta_{(S)\text{ – ester}} - \delta_{(R)\text{ – ester}})$
				12	76.03	75.88	+ 0.15
10	1.79	1.85	– 0.06	10	34.17	34.13	+ 0.04
9	1.29	1.43	– 0.14	9	24.61	24.88	– 0.27
8	*a*	*a*	-				

a : Resonances not assignable in overlapped multiplets.
$\Delta\delta$ measured in ppm at 500 MHz field strength.

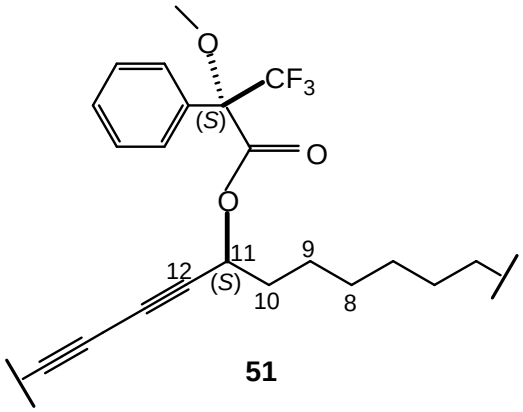

51

The MTPA esters thus obtained showed negative $\Delta\delta$ values for H-C(10) and H-C(9). This suggests the *S*-configuration for C(11) of MS-4 (**27**). The $\Delta\delta$ values for C(12), C(10), and C(9) were not consistent. C(12) and C(10) showed positive and C(9) showed negative $\Delta\delta$ values. Therefore, from the ^{13}C-NMR data the configuration for C(11) could not be determined.

For the determination of the absolute configuration at C(16) the Mosher method was not used because it was supposed that a deacetylation at C(16) would lead to a epimerization. Therefore the solid (*S*)-MTPA-ester (see p. 129) was recrystallized in order to elucidate the absolute configuration by X-ray structure determination. Only small crystals were obtained which could no be used for measurement.

5.2.2.4 11,16-Diacetoxyoctadeca-17-ene-12,14-diynyl acetate (MS-5 (**28**)), a novel diyne

Preparative HPLC yielded 1.4 mg of a yellowish viscous oil (see scheme 12). Because of its small quantity the structure was elucidated by FAB-MS (NBA + KCl) and mainly by comparison of its ^{1}H-NMR, ^{13}C-NMR, DEPT135, ^{1}H-^{1}H COSY, HMQC and HMBC data with that of MS-4 (**27**).

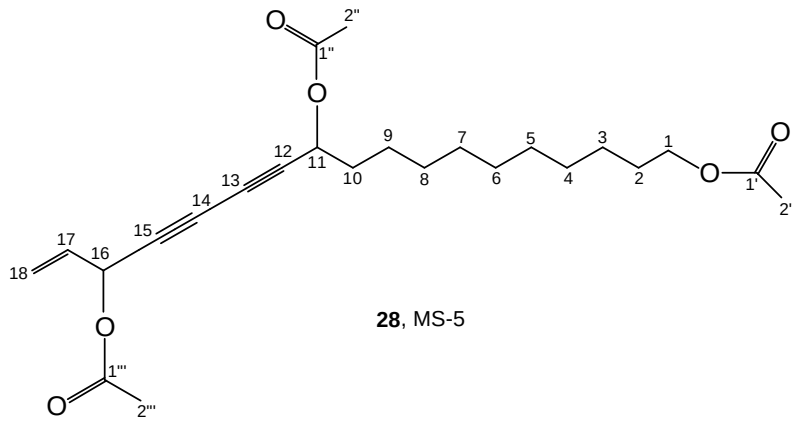

28, MS-5

The FAB-MS (NBA + KCl) measurement of MS-5 (**28**) showed a $[M+K]^{+}$ peak at *m*/*z* 457, therefore the molecular mass must have been 418. The ^{13}C-NMR spectrum (figure 27) showed 23 resonances, an additional resonance of a quaternary C-atom at δ_C 71.3 could only be seen in the HMBC (figure 27 detail). The DEPT135 spectrum (figure 27) showed 17 resonances, six methyls or methines (δ_C 131.8, 64.4, 64.1, 21.05, 20.90 and 20.88) and 11 methylenes (δ_C 119.8, 64.7, 34.4, 29.45, 29.42, 29.37, 29,22, 29.05, 28.6, 25.9 and 24.9). Therefore it could be concluded that the molecule must contain seven quaternary carbon atoms (δ_C 171.3, 169.8, 169.5, 77.7, 74.5, 70.7 and 69.0) which also was confirmed by HMQC (not shown). The quaternary carbon atoms at δ_C 171.3, 169.8 and 169.5 were identified as those of ester carbonyl groups and the other four had to be connected by conjugated triple bonds due to the comparison with MS-4 (**27**). The crosspeaks in the HMQC spectrum and the corresponding integrals from the ^{1}H-NMR spectrum (figure 28) showed that the carbon atoms at δ_C 131.8, 64.4 and 64.1 were methines and those at δ_C 21.05, 20.90 and 20.88 were methyls.

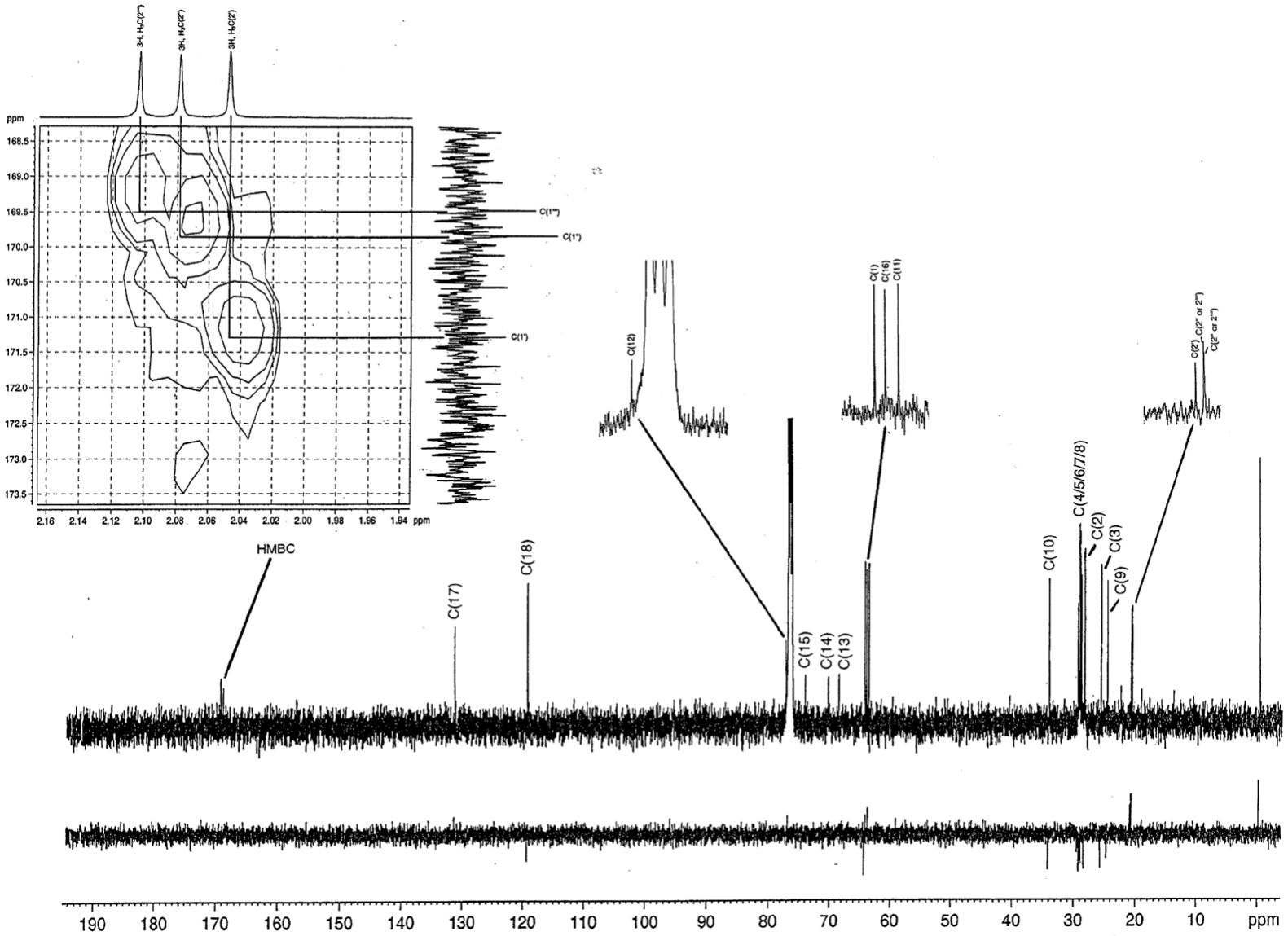

Figure 27 : ^{13}C-NMR, DEPT135 and HMBC (detail) of 11,16-diacetoxyoctadeca-17-ene-12,14-diynyl acetate (MS-5 (**28**)) in $CDCl_3$.

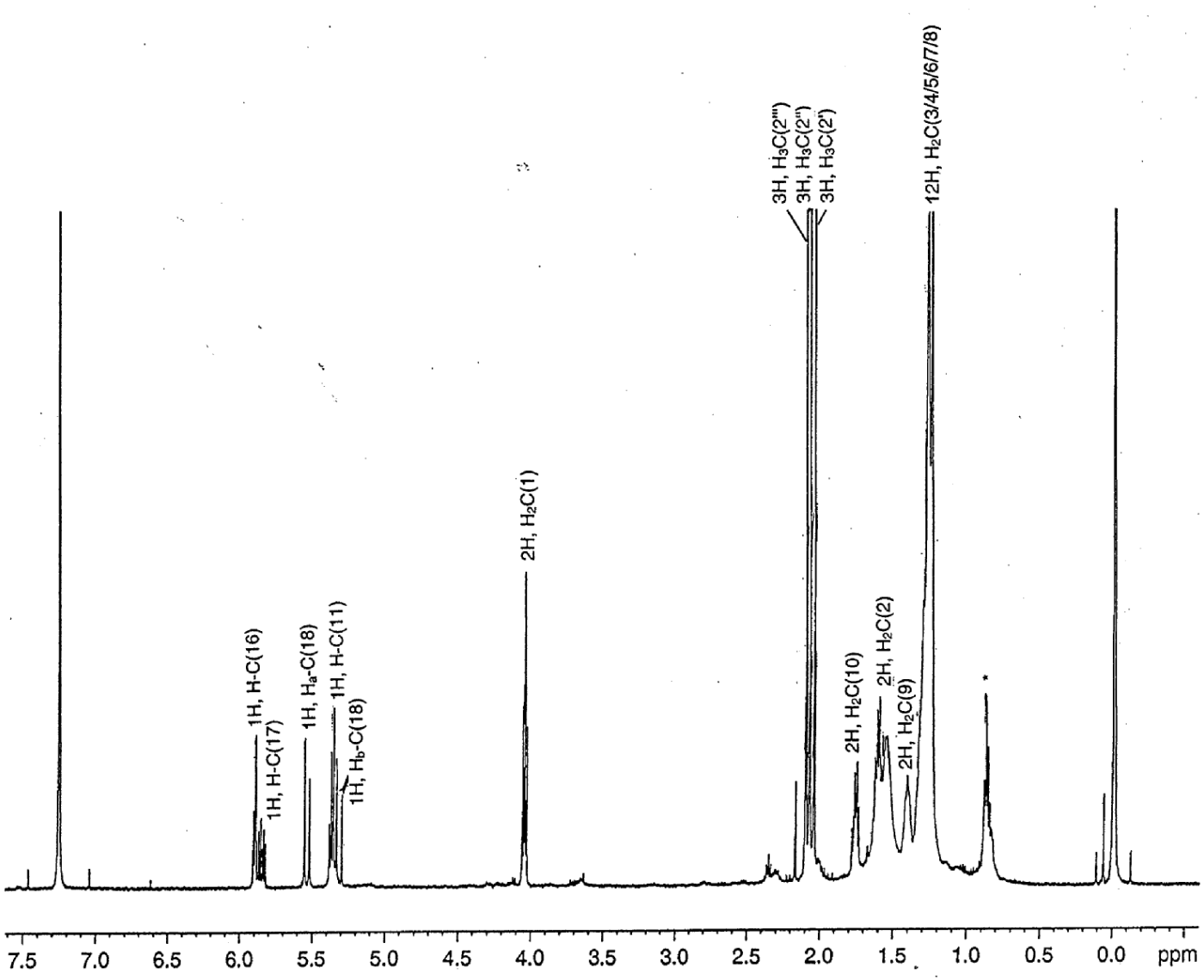

Figure 28 : ^{1}H-NMR of 11,16-diacetoxyoctadeca-17-ene-12,14-diynyl acetate (MS-5 (**28**)) in $CDCl_3$. (∗ impurity).

Therefore the molecule must contain the following structure components :

3x COO

4x C (conjugated triple bonds)

3x CH

3x CH_3

11x CH_2

= $C_{24}H_{34}O_6$

Furthermore the carbon atoms at δ_C 64.7, 64.4 and 64.1 were identified as oxygen-bearing and those at δ_C 131.8 and 119.8 as a terminal olefin.

In the ^{1}H-NMR spectrum (figure 28) the relevant differences to MS-4 (**27**) were a low field shift of the methine resonance at δ_H 5.37 (*t*, *J* = 7.4) (MS-4 (**27**) : δ_H 4.42 (*t*, *J* = 6.3)), an additional methyl singlet at δ_H 2.08, and the absence of the hydroxy proton (MS-4 (**27**) : δ_H 2.02 (*broad s*)).

The ^{13}C-NMR spectrum (figure 27) showed an additional quaternary carbon atom of a carbonyl group at δ_C 169.8. The HMBC experiment showed crosspeaks between the carbonyl carbon atom at δ_C 169.8 and the methine proton at δ_H 5.37 and the methyl protons at δ_H 2.08. Therefore it was concluded that in this molecule – in comparison to MS-4 (**27**) – the hydroxyl group at C(11) was acetylated.

The formula of MS-5 (**28**) with C→H correlations obtained from the HMBC experiment is shown in figure 29.

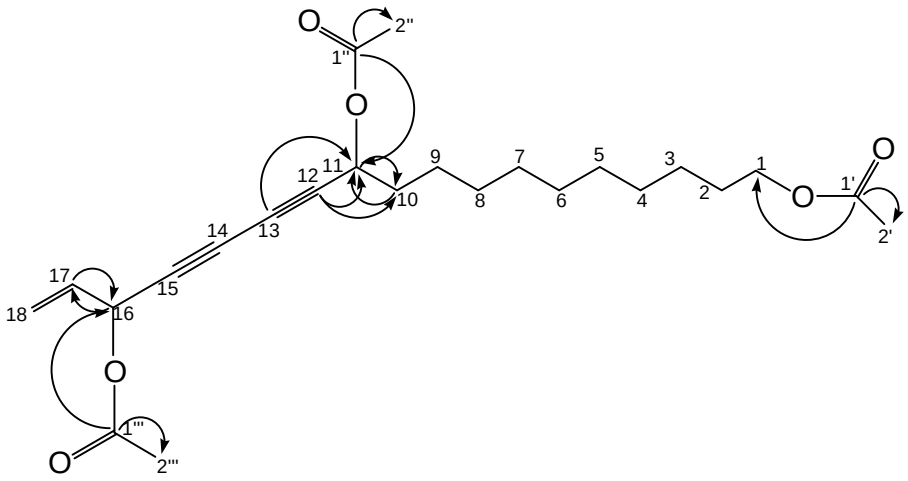

Figure 29 : C→H correlations obtained from the HMBC experiment of MS-5 (**28**) in $CDCl_3$.
(Optimized for ${}^{n}J_{CH}$ = 7 Hz (*n* = 2 or 3)).

On the basis of the above data and the comparison with MS-4 (**27**), MS-5 (**28**) was identified as 11,16-diacetoxyoctadec-17-ene-12,14-diynyl acetate. The comparison of the spectroscopic data with that of analogous structures from the literature : **43** [140]; **44**, **45**, **46** [168]; and **47** [169] showed good correspondance.

5.2.3 Identification of stigmasterol (**42**)

Preparative HPLC (see scheme 12) yielded 17.3 mg of a white powder. This powder, compound **42**, was identified as stigmasterol (24-ethyl-cholesta-5,22-dien-3β-ol) by comparison of its spectroscopic data (EI-MS, IR, ^{1}H-NMR, ^{13}C-NMR and DEPT135) with that of an authentic sample bought from Acros Organics. All spectroscopic data were in agreement. The ^{1}H-, and ^{13}C-NMR spectra of compound **42** and stigmasterol are shown in figure 30 and figure 31.

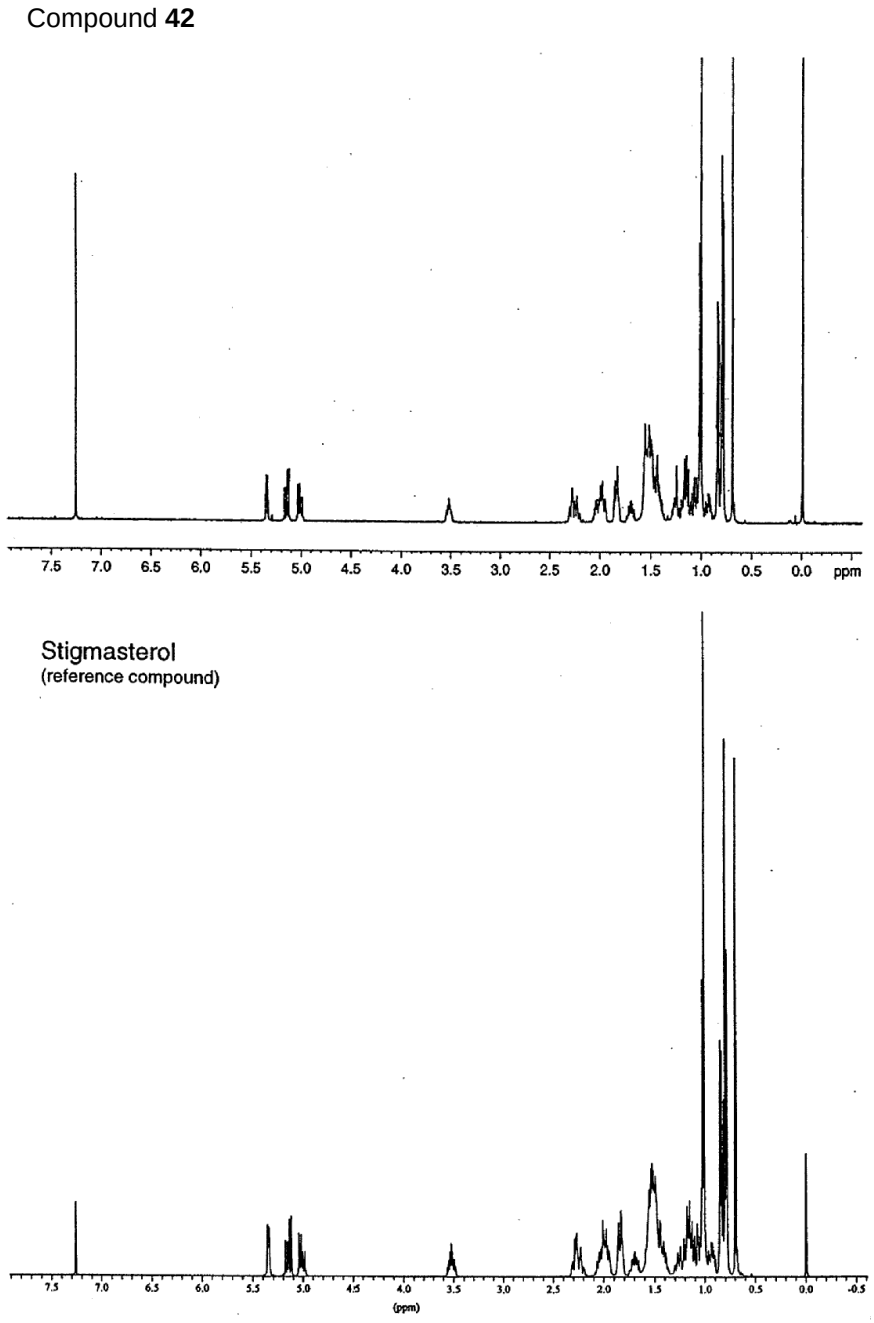

Figure 30 : ^{1}H-NMR spectra of compound **42** and stigmasterol (authentic sample).

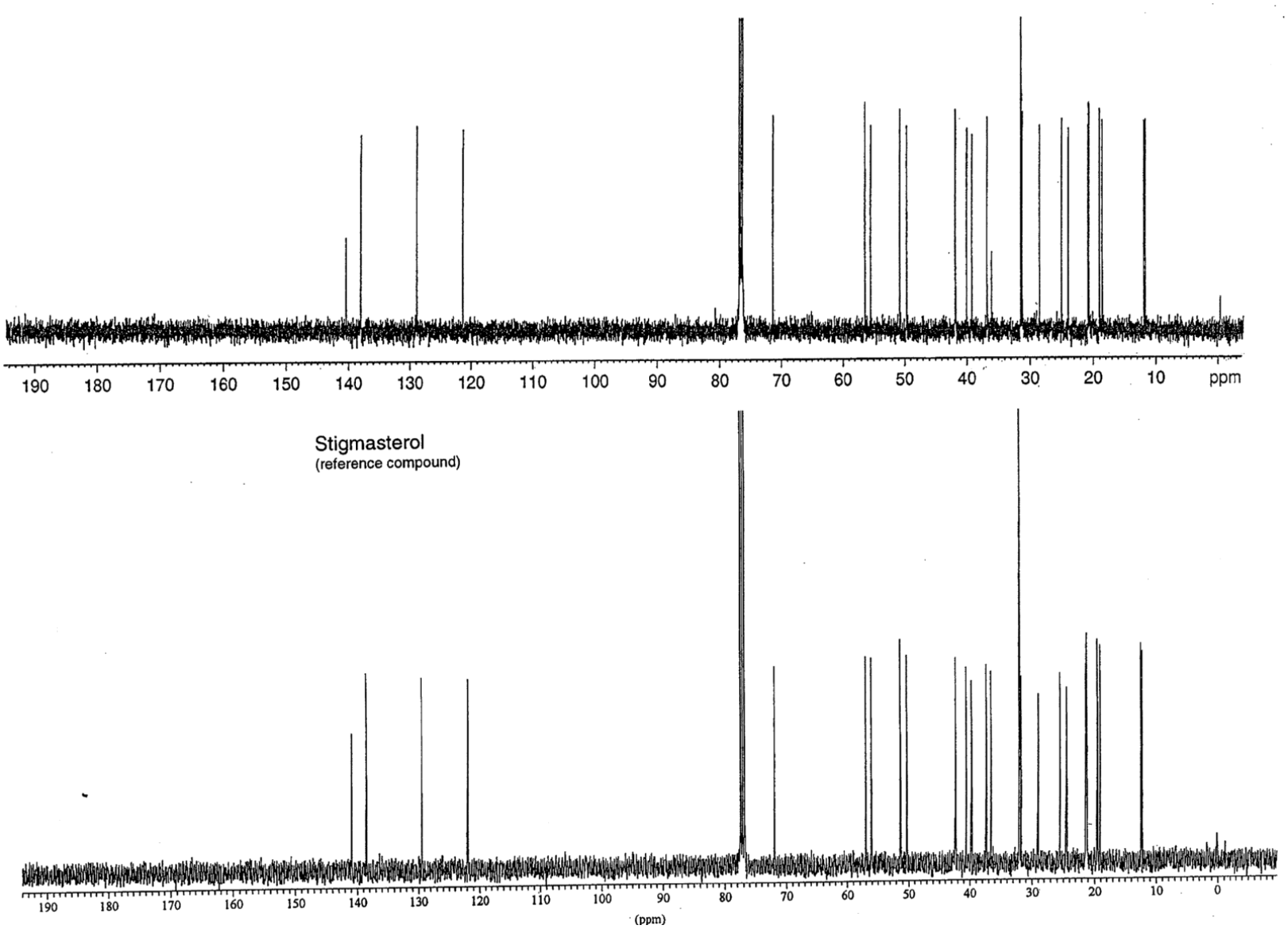

Figure 31 : ^{13}C-NMR spectra of compound **42** and stigmasterol (authentic sample).

6. *Commiphora fulvotomentosa* Engl.

6.1 Introduction

6.1.1 Botany

Commiphora fulvotomentosa Engl. belongs to the genus *Commiphora* of the family Burseraceae. Synonyms are *C. boiviniana* Engl., *C.* sp. near *C. trollii* Mattick sensu and *C. torrei* Mendes. It is a tree 4 - 12 m tall usually without spines on the branches, but sometimes with spines 4 - 7 cm long on the main stem. The trunk has up to 25 cm diameter, the bark is coppery grey, smooth, sometimes papery, sometimes horizontally folded. The exudate is clear and scented. Flowers appearing with the leaves along with brownish tomentose ovate-oblong or spathulate prophylls up to 13 mm long and 4 mm diameter on peduncles up to 5 cm long. The plant occurs in Tanzania (Kilosa-, Ulanga and Mikindani District) and Mozambique. It grows in woodland and dry forest, especially on rocky outcrops, 200 - 1050 m [123].

6.1.2 Use in traditional medicine

In the Tanga District the decoction of the roots of *C. boiviniana* Engl. (syn.) is drunk against gonorrhoe [13]. The bark which is said to contain a mucilaginous resin is a Zigula dysenterie remedy.

6.2 Fractionation

The procedure of the bioassay-guided fractionation of the petroleum ether extract from *Commiphora fulvotomentosa* Engl. stembark is shown in schemes 17-19. The footnotes stand for the following : bold frames : fractions investigated further and [1] : fractions with activity against *T. b. rhodesiense*. For the activities of the crude extract and the fractions see chapter 4.2.1.2. For the isolation methods see chapter 5.2 in the experimental part.

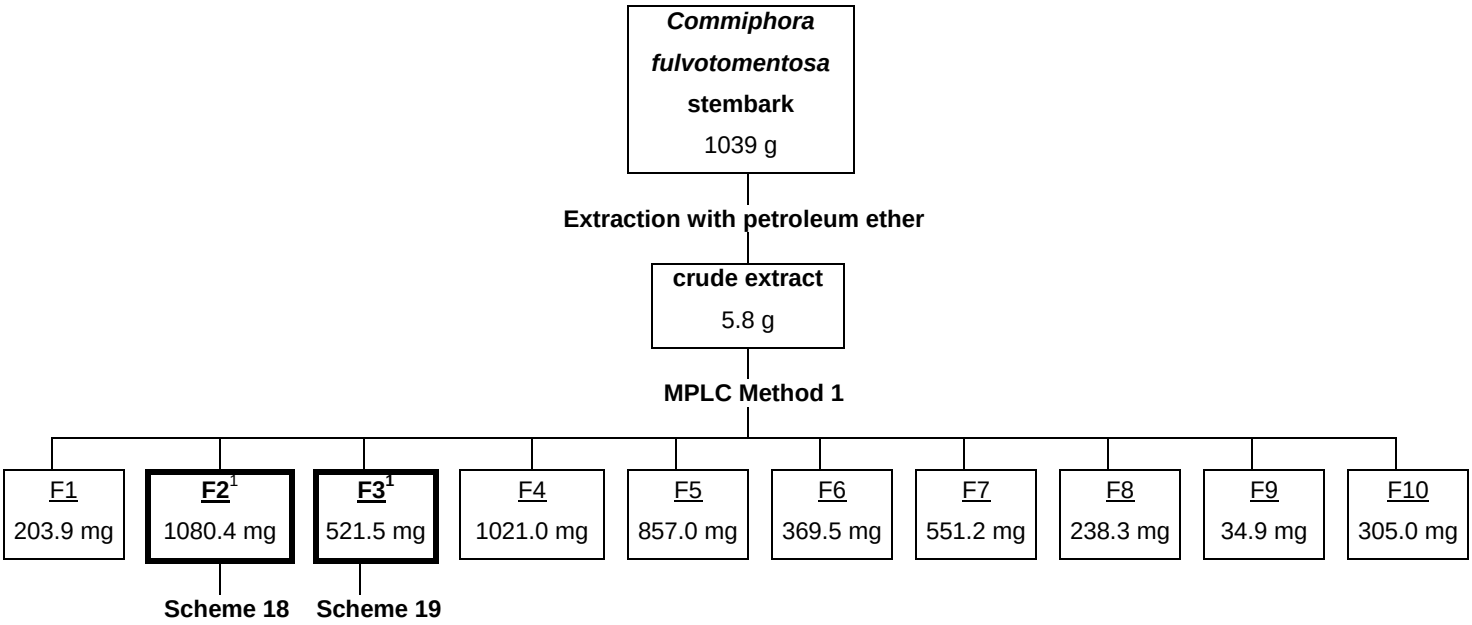

Scheme 17 : Procedure of the bioassay-guided fractionation of the petroleum ether extract from *Commiphora fulvotomentosa* Engl. stembark (from plant material to fraction F2 and F3).

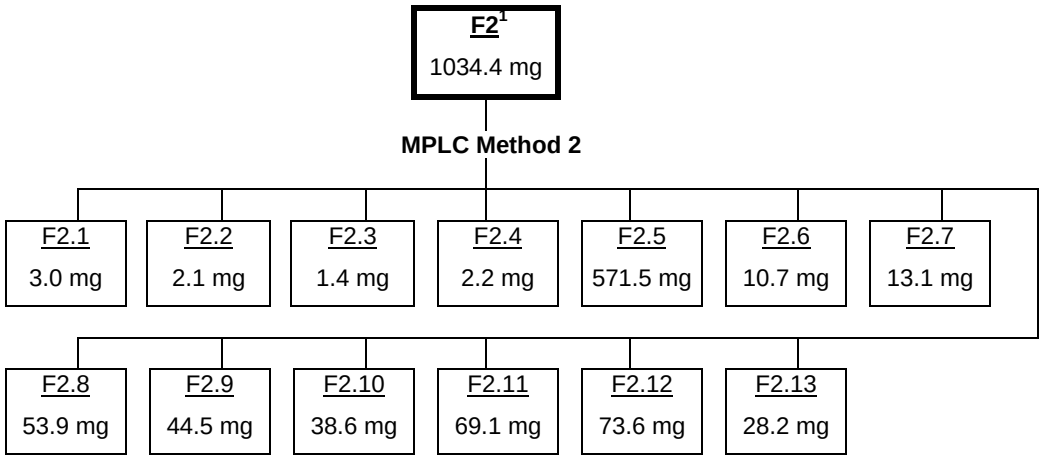

Scheme 18 : Procedure of the bioassay-guided fractionation of the petroleum ether extract from *Commiphora fulvotomentosa* Engl. stembark (from fraction F2 to fraction F2.1-F2.13).

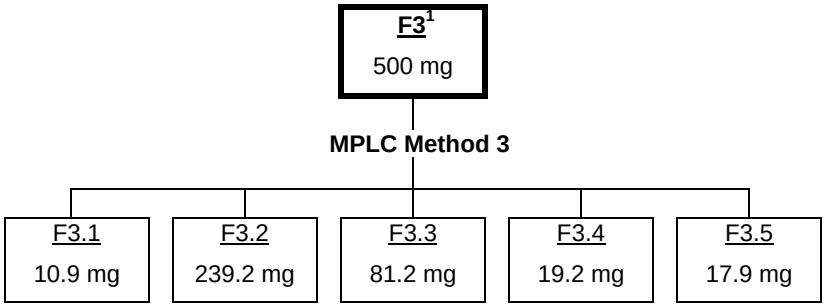

Scheme 19 : Procedure of the bioassay-guided fractionation of the petroleum ether extract from *Commiphora fulvotomentosa* Engl. stembark (from fraction F3 to fraction F3.1-F3.5).

B. Experimental Part

1. General

Hackling of dried plant material was performed with a Fuchs Mühle type MM 125 H.

Powdering of hackled plant material was performed with a Miostar coffee grinder.

Solvents used for extraction, MPLC and recrystallisation were technical, distilled solvents. Solvents used for extraction were distilled twice. Solvents used for analytical and preparative HPLC were of HPLC-quality.

Solvent concentrations were performed on a Büchi Rotavapor RE 111 with a water bath at 40 °C; final pressure was 14 mbar. The high vacuum drying process was performed with an Edwards vacuum pump, final pressure was $4x10^{-2}$ mbar.

MPLC was performed with a Büchi B-680 system, consisting of a Büchi B-688 chromatography pump, a Büchi B-687 gradient former, a Knauer variable wavelength monitor, a Knauer strip chart recorder and a Büchi B-684 fraction collector.

Adsorbents used for MPLC are described in the methods.

Freeze drying was performed with a LSL secfroid, Lyolab B freeze dryer.

Analytical HPLC was performed with a HP 1090 system from Hewlett Packard. The data were processed on a HP Chemstation from Hewlett Packard.

Preparative HPLC was performed with a Waters 600 system consisting of a Waters 600 multisolvent delivery system, a Waters 996 photodiode array detector, a Waters 600 controller and a Waters fraction collector. The spectra were processed with the software millenium V3.1. from Waters.

Columns used for analytical and preparative HPLC are described in the methods.

IR spectra were measured on a Perkin Elmer model 1600 FT-IR spectrophotometer using a substance film between NaCl plates or potassium bromide pellets. Resonance frequencies are given in cm^{-1}; intensities : *s* = strong, *m* = medium and *w* = weak.

UV/VIS spectra were obtained from a Perkin Elmer Lamda Bio 40 UV/VIS spectrometer.

Optical rotation was measured on a Perkin Elmer polarimeter 341 in a 10 cm cuvette at 20 °C.

Mass spectra were measured by Dr. H. Nadig at the Department of Chemistry of the University of Basel on a spectrometer VG 70S (EI) and a Finnigan MAT 312 (FAB). *M/z* values are reported with the corresponding relative intensities in parentheses.

NMR spectra were measured on a Bruker Avance 400 (^{1}H-NMR 400 MHz; ^{13}C-NMR 101 MHz) and a Bruker VRX 500 (^{1}H-NMR 500 MHz; ^{13}C-NMR 125 MHz) at the Department of Chemistry of the University of Basel with the assistance of Dr. K. Kulicke. The chemical shifts δ are given in ppm relative to the internal standard tetramethylsilane (δ = 0 ppm). The ^{13}C-NMR spectra were measured using broad band decoupling with $CDCl_3$ as the reference (δ = 77.0 ppm). The multiplicities derived from DEPT experiments are indicated as follow : *s* : singlet, *d* : doublet, *t* : triplet and *q* : quadruplet; *br* : broad. HMQC and HMBC experiments are reported as ^{13}C resonance $\rightarrow$ ^{1}H resonance and COSY experiments ^{1}H resonance $\rightarrow$ ^{1}H resonance (intensity), where (+) : weak, (++) : medium and (+++) : strong. HMBC experiments were carried out using delays optimized for $^nJ_{CH}$ = 7 Hz (*n* = 2 or 3).

Chemicals for derivatization were bought from Fluka AG. Stigmasterol (authentic sample) was bought from Acros Organics. Chemicals and materials used in the antiparasitic and cytotoxicity testings were standard materials used in the routine work of the laboratories of the Swiss Tropical Institute, Basel. Chemicals and materials for the performance of the $GABA_A$ receptor binding assays were standard materials in the routine work of the laboratories of the Institute of Pharmaceutical Biology of the University of Basel and the ones used for electrophysiological

investigations were standard materials in the routine work of the laboratories of the Institute of Pharmacology of the University of Bern.

2. Extraction

The dried plant material was hackled with a chaffcutter and then powdered with a coffee grinder. For the production of the crude extracts for primary biological *in vitro* screening, samples of about 35 g of the ground plant material were consecutively extracted by stirring with two portions each of petroleum ether (40-60 °C), dichloromethane, methanol and water (see scheme 2). A ten-fold quantity of solvent in relation to plant material was used. The extraction was carried out at room temperature under stirring for 24 h per portion. After each aliquot the mixture was left to stand and then filtered. Petroleum ether and dichloromethane mixtures were filtered under normal pressure and methanol and water mixtures were filtered under vacuum. The extraction procedure continued with the next solvent. Same solvent filtrates were combined and concentrated at 40 °C. Lipophilic filtrates were dried under high vacuum and aqueous filtrates were freeze dried. The solvent-free crude extracts obtained were weighed (results see table 5) and then stored at 4 °C until use.

3. Biological tests

3.1 Antiparasitic and cytotoxicity tests

3.1.1 General

The antiparasitic and the cytotoxicity assays were performed according to internal Standard Operation Procedures (SOP) of the Swiss Tropical Institute, Basel. Sample stock solutions of 10 mg/ml were prepared by dissolving the weighed samples in DMSO. The solutions were kept at room temperature until use. Each assay was performed in duplicate (n = 2). For the performance of the antiparasitic and cytotoxicity assays Costar™ 96-well microtiter plates were used (figure 32).

	1	2	3	4	5	6	7	8	9	10	11	12
A												
B												
C												
D												
E												
F												
G												
H												

Figure 32 : Representation of a Costar™ 96-well microtiter plate.

3.1.2 Antitrypanosomal tests

3.1.2.1 African trypanosomes

Crude plant extracts, fractions and the isolated pure compounds MS-1 (**25**), MS-2 (**26**), and MS-4 (**27**) were tested. The highest sample concentration tested was 100 µg/ml for extracts and fractions, 30 µg/ml for MS-1 (**25**) and 10 µg/ml for MS-2 (**26**) and MS-4 (**27**), respectively. Due to bacterial contamination of the crude plant extracts 1 % of an antibiotic mix, containing 6 mg/ml penicillin G, 10 mg/ml kanamycin sulfate, 5 mg/ml 5-fluorocytosin and 1 mg/ml chloramphenicol, 100 fold diluted with distilled water containing 1 % ethanol, was added to the background controls (no. 4 of the SOP), and to the trypanosome suspension (no. 5 of the SOP) so that the final volume (100 µl) contained an antibiotic mix-concentration of 0.5 %. After fractionation of the crude extracts, fractions and isolated pure compounds did not show any contamination. Therefore assays for fractions and pure compounds were performed without addition of antibiotic mix.

T. b. rhodesiense in vitro assay (LILIT: long incubation low inoculation test)

Standard parasite strain :	*T. b. rhodesiense*; STIB 900 (stage trypomastigotes)	
Standard drug :	Melarsoprol™ start. conc. : 72 ng/ml	
Standard conditions :	Medium :	MEM with Earle's salts 9.75 g/l
		HEPES 6.0 g/l
		Glucose 1.0 g/l
		$NaHCO_3$ 2.2 g/l
		MEM NEAA 10.0 ml/l
		Further supplemented with Baltz-Medium components :
		0.2 mM 2-mercaptoethanol
		2 mM Na-pyruvate
		0.1 mM hypoxanthine
		0.016 mM thymidine
		15 % heat inactivated horse serum
Incubation :	37 °C , 5 % CO_2	

Assay procedure

1. The trypanosomes were diluted to $4x10^4$ tryps. / ml medium. The trypanosome density was adjusted with a CASY (Cell Analysis System (Schaerfe System, Reutlingen, Germany)).
2. Into the wells of row H, 75 µl of medium that contained two times the highest sample concentration were added.
3. Serial sample dilutions were pepared by using a 12-channel multi-pipette. First, 25 µl were removed from wells of row H and put into row G and mixed well. Then 25 µl were taken out of row G and put into row F and so on until row C. The last 25 µl of row C were discarded. A serial dilution factor of 1:3 was thus obtained. Row A and B wells served as controls without samples.
4. 50 µl of medium without trypanosomes containing 1 % of antibiotic mix (only for assays with crude extracts) were added to columns 3, 6, 9 and 12 (background controls).

5. 50 µl of trypanosome suspension containing 1 % of antibiotic mix were added into the remaining wells.
6. The plates were incubated for 72 h.
7. 10 µl of the fluorescent dye Alamar Blue (Laboserv GmbH, Art. Nr. DAL 1100) were added to each well and incubation resumed for an additional 2-6 h.
8. The IC_{50} values were determined by reading the plates at excitation wavelength 530 nm and emission wavelength 590 nm. A sigmoidal inhibition curve was thus obtained.
9. IC_{50} values were calculated by linear interpolation between the two adjacent drug concentrations on the sigmoidal inhibition curve above and below the 50 % incorporation line.

3.1.2.2 American Trypanosomes

Only the isolated pure compounds MS-1 (**25**), MS-2 (**26**), and MS-4 (**27**) were tested. The highest sample concentration tested was 100 µg/ml for MS-1 (**25**) and 5 µg/ml for MS-2 (**26**) and MS-4 (**27**), respectively.

T. cruzi in vitro assay

Standard parasite strain :	*T. cruzi* Tulahuen C2C4
	transfected with the β-galactosidase gene
	(stage trypomastigotes)
Standard cell line :	L-6 cells (mouse muscle fibroblasts)
Standard drug :	Benznidazole
	Start conc. : 30 µg/ml
Standard conditions :	Medium : RPMI 1640 + 10 % FCS
	+ 1.7 µM L-Glutamine
Incubation :	37 °C , 5 % CO_2
Substrate :	2.5x CPRG/Nonidet solution : 5x stock = 500 µl Nonidet
	P40 + 30.38 mg CPRG in 100 ml 1x PBS
	The 5x stock was diluted 1:1 with 1x PBS

Assay procedure

Day 1 : All 96 wells were seeded with 100 µl of medium containing $2x10^3$ L6 cells / well.

Day 2 : 50 µl of a trypanosome suspension with a density of $5x10^3$ tryps. / ml were added into columns 1 and 2, 4 and 5, 7 and 8, and 10 and 11. In columns 3, 6, 9 and 12, 50 µl of medium were added.

Day 4 : Medium from wells in row A to G was removed with the aspirator and replaced with 100 µl of medium. Medium was removed from row H and replaced with 150 µl of the highest sample concentration. Serial sample dilutions were prepared by using a 12-channel multi-pipette. First, 50 µl were removed from wells of row H and put into row G and mixed well. Next, 50 µl were taken out of row G and put into row F and so on until row B. The last 50 µl of row B were discarded. A serial dilution factor of 1:3 was thus obtained. Wells in row A served as control wells without samples.

Day 8 : 50 µl of 2.5x CPRG/Nonidet were added to all wells. After 2-6 h the plates were read in an Absorbance Reader at 540 nm. A sigmoidal inhibition curve was thus obtained.

IC_{50} values were calculated by linear interpolation between the two adjacent drug concentrations on the sigmoidal inhibition curve above and below the 50 % incorporation line.

3.1.3 Antiplasmodial tests

Crude plant extracts, fractions and the isolated pure compounds MS-1 (**25**), MS-2 (**26**), and MS-4 (**27**) were tested. Because the medium itself contained an antibiotic, no antibiotic had to be added for the assays of the crude plant extracts. The highest sample concentration tested was 20 µg/ml for extracts, fractions and MS-1 (**25**), and 5 µg/ml for MS-2 (**26**) and MS-4 (**27**), respectively.

P. falciparum in vitro assay ([^{3}H]hypoxanthine incorporation)

Standard parasite strain :	*P. falciparum*, K1 strain (chloroquine and pyrimethamine resistant)	
Standard drugs :	Chloroquine :	start. conc. : 1000 ng/ml
	Artemisinin :	start. conc. : 10 ng/ml
Standard conditions :	Medium :	RPMI 1640 (without hypoxanthine) supplemented with : 5.94 g/l HEPES, 2.1 g/l $NaHCO_3$ 100 U/ml Neomycin 5 g/l Albumax® Human washed red blood cells (RBC) A+
Incubation :	48 h, followed by an additional 24 h in the presence of [^{3}H]hypoxanthine Gas mixture : 4 % CO_2, 3 % O_2, 93 % N_2, 37 °C	

Assay procedure

1. Smears of the stock cultures of the K1 strain were prepared and the parasitaemia was determined. The dilution factor was calculated to obtain the starting conditions for the assay :
   Concentration of red cells : 2.5 %
   Initial parasitaemia : 0.3 %
2. 100 µl of medium were added to each well.
3. 100 µl of medium, containing 4x the highest sample concentration, were added to wells in row B.
4. Serial sample dilutions were prepared by using a 12-channel multi-pipette. 100 µl were taken from wells of row B and transferred, after gentle mixing, to wells of row C. After mixing, 100 µl were transferred from wells of row C to wells of row D and so on until row H. The 100 µl removed from row H were discarded. A serial dilution factor of 1:2 was thus obtained. Wells of row A served as controls without samples.
5. 100 µl of a double-concentrated (5 %) red cell suspension with a parasitaemia of 0.3 % were added to each well with the exception of A9 -A12 (negative controls).

6. The plates were incubated for 48 h.
7. 50 µl [^{3}H]hypoxanthine (0.5 µCi) were added to each well and the plates were incubated for an additional 24 h.
8. The plates were harvested using a cell harvester (Wallac, Zürich, Switzerland), which transferred the red blood cells onto a glass fiber filter and washed with distilled water. The dried filters were inserted into a plastic foil with 10 ml of scintillation fluid, and counted in a liquid scintillation counter. A sigmoidal inhibition curve was thus obtained.
9. IC_{50} values were calculated by linear interpolation between the two adjacent drug concentrations on the sigmoidal inhibition curve above and below the 50 % incorporation line.

3.1.4 Antileishmanial tests

3.1.4.1 Axenic

Only the isolated pure compounds MS-1 (**25**), MS-2 (**26**), and MS-4 (**27**) were tested. The highest sample concentration tested was 30 µg/ml for MS-1 (**25**) and 1 µg/ml for MS-2 (**26**) and MS-4 (**27**), respectively.

Axenic *L. donovani in vitro* assay

Standard parasite strain :	*L. donovani* MHOM-ET-67/L82 (axenic amastigotes)	
Standard drug :	Miltefosine	
Standard conditions :	Medium :	SM + SDM (1:1), pH 5.4 + 10 % FCS, heat inactivated HEPES and MOPS are substituted with MES (40 mM final conc.)
Incubation :	72 h at 37 °C and 5 % CO_2	

Assay procedure

1. 50 µl of medium were added to all wells, except in row H. Row H received 75 µl, in triplicate, of two times the highest sample concentration. Serial sample dilutions were prepared in triplicate by using a 12-channel multi-pipette. First, 25 µl were removed from wells of row H and put into row G and mixed well. Then 25 µl were taken out of row G and put into row F and so on until row C. The last 25 µl of row C were discarded. A serial dilution factor of 1:3 was thus obtained. Row A and B served as controls with no samples but parasites.
2. 50 µl of amastigote suspension ($1x10^5$/well ; $2x10^6$/ml) were added to the sample dilutions in columns 1 and 2, 4 and 5, 7 and 8, and 10 and 11. Columns 3, 6, 9 and 12 received medium only and served as controls with samples but no parasites.
3. The plates were incubated for 72 h.
4. 10 µl of Alamar Blue were added to each well and incubation was continued for another 3-4 h.
5. Plates were read in the Cytofluor at excitation wavelength 530 nm and emission wavelength 590 nm. A sigmoidal inhibition curve was thus obtained.
6. IC_{50} values were calculated by linear interpolation between the two adjacent drug concentrations on the sigmoidal inhibition curve above and below the 50 % incorporation line.

3.1.4.2 In infected macrophages

Only the isolated pure compounds MS-1 (**25**), MS-2 (**26**), and MS-4 (**27**) were tested. The highest sample concentration tested was 30 µg/ml for MS-1 (**25**) and MS-4 (**27**) and 1 µg/ml for MS-2 (**26**), respectively.

L. donovani in vitro assay using macrophages infected with axenically grown amastigotes containing the Lac-Z gene marker

Standard parasite strain : *L. donovani* MHOM-ET-67/L82-Lac Z
Standard drug : Miltefosine

Standard conditions :	Stock :	Axenic amastigote stock in SM/SDM (1:1) pH 5.4, 20 % FCS
		37 °C, 5 % CO_2 in Falcon 12.5 cm^2 flasks
	Assay :	RPMI 1640 without phenol red, 10 % FCS, pH 7.4
Incubation :		37 °C, 5 % CO_2
		96 h (4 days) sample exposure

Assay procedure

Day 1 : Two mice were injected i.p. with 2 ml each of a 2 % starch in H_2O suspension.

Day 2 : Macrophages were harvested by peritoneal lavage. All wells were seeded with 50 µl containing $5x10^3$ cells.

Day 3 : An axenically growing amastigote culture was passed through a 26 gauge needle to break up clumps and counted by CASY (Cell Analysis System (Schärfe System, Reutlingen, Germany)). The macrophages on the plates were infected at a ratio of 1:3 (macrophgs. : amastig.) in columns 1 and 2, 4 and 5, 7 and 8, and 10 and 11. Columns 3, 6, 9 and 12 served as controls of uninfected macrophages. After 6 h of infection excess amastigotes were washed away.

Day 4 : The medium was removed from all wells and replaced with 100 µl of fresh RPMI, 10 % FCS in rows A to G. Row H received 150 µl of the highest sample concentration (in duplicate + background). Serial sample dilutions were made with 50 µl from row H into row G, then into row F etc. The last 50 µl from row C were discarded. A serial dilution factor of 1:3 was thus obtained. Row A and B served as controls (infected cells with no samples).

Day 8 : The plates were inspected visually to determine possible toxicity of the sample for the host cells in columns 3, 6, 9 and 12 (uninfected host cells + samples). 50 µl of CPRG/Nonidet (1:1 in PBS) were added to each well and the plates were incubated for another 2-6 h.

The plates were read in an Eliza reader. A sigmoidal inhibition curve was thus obtained.

IC_{50} values were calculated by linear regression analysis.

3.1.5 Cytotoxicity tests

Only extracts, which showed significant activity in the antitrypanosomal (African trypanosomes) and/or in the antiplasmodial testings (IC_{50} *T. b. rhodesiense* ≤ 10 µg/ml, IC_{50} *P. falciparum* ≤ 5 µg/ml) and the isolated pure compounds MS-1 (**25**), MS-2 (**26**), and MS-4 (**27**) were tested for cytotoxicity. The highest sample concentration tested was 100 µg/ml. The antibiotic mix (see chapter 3.1.2.1) was used for cytotoxicity assays with crude plant extracts. It was added to the fresh medium (no. 2 of the SOP), and to the medium containing the highest sample concentration (no. 3 of the SOP). Fractions and isolated pure compounds were testet without addition of antibiotic mix.

In vitro cytotoxicity assay

Standard cell line :	L-6 cells (mouse muscle fibroblasts)	
Standard drug :	Mefloquine	
Standard conditions :	Medium :	RPMI 1640
		+ 10 % FBS
		+ 1 % L-Glutamine (200 mM)
Incubation :	37 °C, 5 % CO_2 in air	

Assay procedure

1. 100 µl of a cell suspension containing $4x10^4$ cells / ml medium were added into columns 1 and 2, 4 and 5, 7 and 8, and 10 and 11. Cells were allowed to attach over night.
2. The next morning the medium was removed completely, using the aspirator, and 100 µl of fresh medium containing 0.5 % of antibiotic mix (only for assays with crude plant extracts) were added to all wells of the plate, except in row H.
3. 150 µl of medium containing the highest sample concentration (100 µg/ml) and 0.5 % of antibiotic mix were added to the wells of row H.
4. Serial sample dilutions were prepared by using a 12-channel multi-pipette. First, 50 µl were taken from wells of row H and put into row G, mixed well, then 50 µl were taken out of row G and put into row F and so on until row C. The last 50 µl

of row C were discarded. A serial dilution factor of 1:3 was thus obtained. Wells in row A and B served as control wells without samples.

5. The plates were incubated vor 72 h.
6. 10 µl of Alamar Blue were added to each well and the plates were incubated for another 2 h.
7. The plates were read at excitation wavelength 530 nm and emmision wavelength 590 nm. A sigmoidal inhibition curve was thus obtained.
8. IC_{50} values were calculated by linear interpolation between the two adjacent drug concentrations on the sigmoidal inhibition curve above and below the 50 % incorporation line.

3.2 $GABA_A$- receptor binding studies

The $GABA_A$-receptor binding studies were performed by Dr. U. Simmen and co-workers in the laboratories of the Institute of Pharmaceutical Biology of the University of Basel.

[^{3}H]Flunitrazepam binding assay to rat cortex membranes

Frozen cortex derived from rats was used to prepare membrane fractions. After separation of the cerebellum, cortex material was homogenised on ice with 50 mM Tris/HCl pH 7.4, 120 mM NaCl, 5 mM KCl using a Polytron homogeniser. The homogenate was centrifuged at 31'000 g for 10 min at 4 °C. The pellet was resuspended with 50 mM Tris/HCl pH 7.4 and centrifuged as described above for a total of three washing steps. The membrane fraction was stored at –80 °C. Binding equilibrium was performed under the following conditions: 200 µg of cortex membranes (determined with the BCA protein assay), 1 nM [^{3}H]flunitrazepam in 50 mM Tris/HCl pH 7.4, incubation for 1 h at r.t. in a total volume of 0.5 ml. Non-specific binding was defined in the presence of 100 µM diazepam. Stock solutions of crude plant extracts (20 mg/ml 50 % MeOH) and of the isolated pure compounds MS-1 (**25**), MS-2 (**26**), and MS-4 (**27**) (5 mg/ml MeOH) were prepared. Binding was terminated by rapid filtration with GF/C filters under reduced pressure and three washes with cold 5 mM Tris/HCl buffer, pH 7.4. Radioactivity on filters was

determined by liquid scintillation counting (TRI-CARB 2100TR, Packard). Results are given by means ± S.D. of triplicates.

3.3 Electrophysiological investigations

The electrophysiological investigations were performed by Prof. E. Sigel and co-workers in the laboratories of the Institute of Pharmacology of the University of Bern.

Xenopus laevis oocytes

Briefly, oocytes were injected with 50 nl of capped, polyadenylated cRNA dissolved in 5 mM K-HEPES (pH 6.8). For dual subunit combinations a concentration of 75 nM was used for each transcript. For triple subunit combinations 10 nM of the cRNA coding for the different α subunits (α_1, α_2, α_3, α_5, or α_6), 10 nM for β_2 and 50 nM for γ_2 were used. RNA transcripts were synthesized from linearized plasmids encoding the desired protein using the message machine kit (Ambion) according to the recommendations of the manufacturer. A poly (A) tail of ~300 residues was added to the transcripts by using yeast poly (A) polymerase (Amersham). The cRNA combinations were co-precipitated in ethanol and stored at –20 °C. Transcripts were quantified on agarose gels after staining with Radiant Red RNA Stain (Bio-Rad) by comparing staining intensities with various amounts of molecular weight markers (RNA Ladder, GibcoBRL). Electrophysiological experiments were performed by the two-electrode voltage clamp method at a holding potential of –80 mV. The medium contained 90 mM NaCl, 1 mM KCl, 1mM $CaCl_2$, 1 mM $MgCl_2$ and 5 mM HEPES-NaOH (pH 7.4). GABA, diazepam, and test drugs were applied for 20 s and a washout period of 3-15 min was allowed to ensure full recovery from desensitization. Current responses have been fitted to the Hill equation: $I = I_{max} / (1 + (EC_{50} / [\mathbf{A}])^n)$ where I is the peak current at a given concentration of GABA [**A**], I_{max} is the maximum current, EC_{50} is the concentration of agonist eliciting half maximal current, and n is the Hill coefficient. Currents were measured using a modified OC-725 amplifier (Warner Instruments Corp.) in combination with a xy-recorder or digitized using a MacLab/200 (AD Instruments).

The isolated pure compounds MS-1 (**25**), MS-2 (**26**), and MS-4 (**27**) were dissolved in DMSO. To minimize precipitation of the compounds the assay medium was complemented with 0.5 % DMSO. At this concentration DMSO had no significant effect on the current amplitude elicited by GABA. Relative current stimulation by the compounds was determined at a GABA concentration evoking 2-5 % of the maximal current amplitude in combination with increasing concentrations of compounds and expressed as $((I_{(GABA+MS)} / I_{(GABA)}) - 1) \times 100$ %. Only one cumulative concentration response curve was performed using the same oocyte, to avoid contamination, and the perfusion system was cleaned by washing with DMSO for the same reason.

4. Constituents of *Cussonia zimmermannii* Harms

4.1 The polyacetylenes and stigmasterol

4.1.1 Isolation

4.1.1.1 Extraction

717 g of ground rootbark of *Cussonia zimmermannii* Harms were extracted by stirring with three portions of petroleum ether (40-60 °C). A five-fold quantity of solvent in relation to plant material was used. The extraction was carried out at room temperature under stirring for 24 h per portion. After each aliquot the mixture was left to stand and then filtered under normal pressure. The filtrates were combined, evaporated at 40 °C and dried under high vacuum.

4.1.1.2 Chromatography

The isolation of the components from the crude plant extract was then carried out by MPLC followed by preparative scale HPLC. Fractions obtained with organic solvents were evaporated at 40 °C and then dried under high vacuum. From fractions obtained with organic solvent-water mixtures the organic solvent was removed by evaporation at 40 °C and the aquous residue was then freeze dried. After each fractionation step the fractions were checked for purity by analytical HPLC.

MPLC Method 1 (*crude extract*)

Column : LiChroprep® Si 60 (Merck), 15-25 µm, 460 x 36 mm ID
Detection : UV 254 nm
Flow rate : 15 ml/min
Fraction collecting : 1 fraction every min
Gradient table :

Time [min]	% Hexane	% Ethyl acetate	% MeOH
Initial	100	0	0
10	100	0	0
240	70	30	0
360	70	30	0
480	0	0	100

MPLC Method 2 (*F3*)

Column : LiChroprep® Si 60 (Merck), 15-25 µm, 460 x 26 mm ID

Detection : UV 254 nm

Flow rate : 15 ml/min

Fraction collecting : 1 fraction every min

Gradient table :

Time [min]	% Hexane	% Ethyl acetate	% MeOH
Initial	100	0	0
240	90	10	0
300	70	30	0
360	70	30	0
420	0	0	100

Prep. HPLC Method 1 (*F3.4.1*)

Column : Eurospher 100 C18 (Knauer), 7 µm, 250 x 16.0 mm ID

Detection : DAD Waters 996

Flow rate : 12 ml/min

Fraction collecting : 1 fraction every min

Gradient table :

Time [min]	% Acetonitrile	% Water
Initial	10	90
20	50	50
80	50	50
85	65	35
110	65	35
115	90	10
120	90	10

MPLC Method 3 (*F3.6*)

Column : Eurosil Bioselect 100-20 Diol 20 µm, 460 x 15 mm ID

Detection : UV 254 nm

Flow rate : 10 ml/min

Fraction collecting : 1 fraction every min

Gradient table :

Time [min]	% Hexane	% Ethyl acetate
Initial	98	2
480	98	2
540	90	10

Prep. HPLC Method 2 (*F3.6.5*)

Column : Eurospher 100 C18 (Knauer), 7 µm, 250 x 16.0 mm ID

Detection : DAD Waters 996

Flow rate : 12 ml/min

Fraction collecting : 1 fraction every min

Gradient table :

Time [min]	% Acetonitrile	% Water
Initial	60	40
80	60	40
95	80	20
115	80	20

Prep. HPLC Method 3 (*F3.6.5.6*)

Column : Eurospher 100 C18 (Knauer), 7 µm, 250 x 16.0 mm ID

Detection : DAD Waters 996

Flow rate : 12 ml/min

Fraction collecting : 1 fraction every min

Gradient table :

Time [min]	% Acetonitrile	% Water
Initial	65	35
50	65	35
60	90	10
70	90	10

Prep. HPLC Method 4 (*F3.6.5.7*)

Column : Eurospher 100 C18 (Knauer), 7 µm, 250 x 16.0 mm ID

Detection : DAD Waters 996

Flow rate : 12 ml/min

Fraction collecting : 1 fraction every min

Gradient table :

Time [min]	% Acetonitrile	% Water
Initial	70	30
50	70	30
60	90	10
70	90	10

MPLC Method 4 (*F3.7*)

Column : LiChroprep® Si 60 (Merck), 15-25 µm, 460 x 15 mm ID

Detection : UV 254 nm

Flow rate : 10 ml/min

Fraction collecting : 1 fraction every min

Gradient table :

Time [min]	% Hexane	% Ethyl acetate
Initial	95	5
480	95	5
600	50	50

Prep. HPLC Method 5 (*F3.7.3*)

Column : Eurospher 100 C18 (Knauer), 5 µm, 250 x 16.0 mm ID

Detection : DAD Waters 996

Flow rate : 12 ml/min

Fraction collecting : 1 fraction every min

Gradient table :

Time [min]	% Acetonitrile	% Water
Initial	60	40
65	60	40
70	70	30
110	70	30
115	90	10
120	90	10

Prep. HPLC Method 6 (*F3.7.3.5*)

Column : Eurospher 100 C18 (Knauer), 5 µm, 250 x 16.0 mm ID

Detection : DAD Waters 996

Flow rate : 12 ml/min

Fraction collecting : 1 fraction every min

Gradient table :

Time [min]	% Methanol	% Water
Initial	75	25
60	75	25
65	100	0
75	100	0

Prep. HPLC Method 7 (*F3.7.4.1*)

Column : Eurospher 100 C18 (Knauer), 5 µm, 250 x 16.0 mm ID

Detection : DAD Waters 996

Flow rate : 12 ml/min

Fraction collecting : 1 fraction every min

Gradient table :

Time [min]	**% Methanol**	**% Water**
Initial	10	90
5	10	90
15	20	80
35	20	80
45	45	55
55	45	55
65	98	2
120	98	2

Prep. HPLC Method 8 (*F3.7.4.2*)

Column : Eurospher 100 C18 (Knauer), 5 µm, 250 x 16.0 mm ID

Detection : DAD Waters 996

Flow rate : 12 ml/min

Fraction collecting : 1 fraction every min

Gradient table :

Time [min]	**% Acetonitrile**	**% Water**
Initial	55	45
80	55	45
90	70	30
105	70	30
110	90	10
120	90	10

MPLC Method 5 (*F4*)

Column : LiChroprep® Si 60 (Merck), 15-25 μm, 460 x 26 mm ID

Detection : UV 254 nm

Flow rate : 15 ml/min

Fraction collecting : 1 fraction every min

Gradient table :

Time [min]	% Hexane	% Ethyl acetate	% MeOH
Initial	100	0	0
240	80	20	0
360	80	20	0
420	50	50	0
480	50	50	0
540	0	0	100

Prep. HPLC Method 9 (*F4.7*)

Column : Eurospher 100 C18 (Knauer), 5 μm, 250 x 16.0 mm ID

Detection : DAD Waters 996

Flow rate : 12 ml/min

Fraction collecting : 1 fraction every min

Gradient table :

Time [min]	% Acetonitrile	% Water
Initial	55	45
65	55	45
70	65	35
105	65	35
110	100	0
120	100	0

Prep. HPLC Method 10 (*F4.7.7*)

Column : LiChrospher 100 DIOL (Knauer), 10 μm, 250 x 16.0 mm ID

Detection : DAD Waters 996

Flow rate : 12 ml/min

Fraction collecting : 1 fraction every min

Gradient table :

Time [min]	% Hexane	% CH_2Cl_2
Initial	50	50
20	50	50
25	0	100
35	0	100

MPLC Method 6 (*F5*)

Column : LiChroprep® Si 60 (Merck), 15-25 μm, 460 x 26 mm ID

Detection : UV 254 nm

Flow rate : 15 ml/min

Fraction collecting : 1 fraction every min

Gradient table :

Time [min]	% Hexane	% Ethyl acetate	% MeOH
Initial	100	0	0
180	80	20	0
360	80	20	0
420	50	50	0
480	50	50	0
540	0	0	100

MPLC Method 7 (*F6*)

Column : LiChroprep® Si 60 (Merck), 15-25 μm, 460 x 26 mm ID

Detection : UV 254 nm

Flow rate : 15 ml/min

Fraction collecting : 1 fraction every min

Gradient table :

Time [min]	% Hexane	% Ethyl acetate	% MeOH
Initial	100	0	0
120	70	30	0
240	70	30	0
300	50	50	0
360	50	50	0
420	0	0	100

4.1.2 8-Hydroxyheptadeca-4,6-diyn-3-yl acetate (MS-1 (**25**))

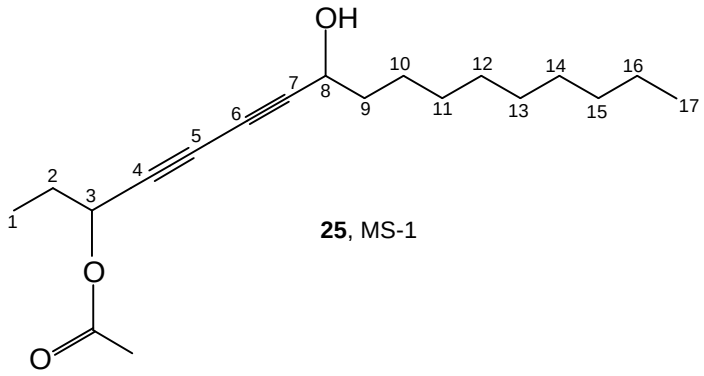

25, MS-1

t_R : 32.9 min (prep. HPLC method 4).

$[\alpha]^{20}_D$ = –94.5 (*c* = 0.78, $CHCl_3$/0.75 % ethanol).

UV/Vis ($CHCl_3$/0.75 % ethanol) : λ_{max} (ε) : 201.9 (282), 207.0 (308), 209.0 (350), 219.8 (395), 223.9 (440), 244.7 (848), 258.3 (589), 281.8 (196).

IR (NaCl) : 3424*m*, 2926*s*, 2855*s*, 2253*w*, 2156*w*, 1746*s*, 1464*m*, 1372*m*, 1231*s*.

^{1}H-NMR (500 MHz, $CDCl_3$) : 5.35 (*t*, *J* = 6.5, 1 H, H-C(3)); 4.42 (*t*, *J* = 6.6, 1 H, H-C(8)); 2.09 (*s*, 3 H, CH_3COO); 1.82-1.77 (*m*, 2 H, $H_2C(2)$); 1.75 (*d*, *J* = 5.8, 1 H, HO-C(8)); 1.72-1.69 (*m*, 2 H, $H_2C(9)$); 1.43 (*br. quintet*, *J* = 7.3, 2 H, $H_2C(10)$); 1.31-1.26 (*m*, 12 H, $H_2C(11/12/13/14/15/16)$); 1.02 (*t*, *J* = 7.4, 3 H, $H_3C(1)$); 0.88 (*t*, *J* = 7.0, 3 H, $H_3C(17)$).

^{13}C-NMR (125 MHz, $CDCl_3$) : 169.9 (*s*, COO); 80.6 (*s*, C(7)); 76.7 (*s*, C(4)); 69.3 (*s*, C(5)); 68.8 (*s*, C(6)); 65.3 (*d*, C(3)); 62.9 (*d*, C(8)); 37.5 (*t*, C(9)); 31.9 (*t*, C(15)); 29.51, 29.48, 29.29, 29.21 (4*t*, C(11/12/13/14)); 27.8 (*t*, C(2)); 25.0 (*t*, C(10)); 22.7 (*t*, C(16)); 20.9 (*q*, $\underline{C}H_3COO$); 14.1 (*q*, C(17)); 9.3 (*q*, C(1)).

COSY (500 MHz, $CDCl_3$) : 5.35 → 1.82-1.77 (+++); 4.42 → 1.75 (+++) and 1.72-1.69 (++); 1.82-1.77 → 1.02 (+++); 1.72-1.69 → 1.43 (+++); 1.43 → 1.31-1.26 (+++); 1.31-1.26 → 0.88 (+++).

HMQC (125 MHz, $CDCl_3$) : 65.3 → 5.35 (++); 62.9 → 4.42 (++); 37.5 → 1.72-1.69 (+++); 31.9 → 1.26 (++); 29.51-29.21 → 1.31-1.26 (+++); 27.8 → 1.82-1.77 (+++); 25.0 → 1.43 (+++); 22.7 → 1.28 (+++); 20.9 → 2.09 (+++); 14.1 → 0.88 (+++); 9.3 → 1.02 (+++).

HMBC (125 MHz, $CDCl_3$) : 169.9 → 5.35 (+) and 2.09 (+++); 80.6 → 4.42 (+++) and 1.72-1.69 (++); 76.7 → 5.35 (+++) and 1.82-1.77 (+++); 69.3 → 5.35 (+++) and 4.42 (+); 68.8 → 5.35 (+) and 4.42 (+++); 65.3 → 1.82-1.77 (+++) and 1.02 (+++); 62.9 → 1.72-1.69 (++); 37.5 → 4.42 (++); 31.9 → 1.28 (+++) and 0.88 (+++); 29.51-29.21 → 1.43 (++) and 1.31-1.26 (++); 27.8 → 5.35 (++) and 1.02 (+++); 25.0 → 4.42 (+), 1.72-1.69 (+) and 1.31-1.26 (+); 22.7 → 1.26 (+) and 0.88 (+++); 9.3 → 5.35 (+) and 1.82-1.77 (+++).

EI-MS (70 eV, ca. 200 °C) : 306 (84), M^+; 291 (20), $[M\text{-}15]^+$; 264 (6); 249 (26); 217 (10); 175 (17); 161 (32); 133 (33); 119 (50); 91 (68); 57 (33); 55 (36); 43 (100).

HR-EI-MS : 306.21971, M^+; calc. for $[C_{19}H_{30}O_3]^+$: 306.21950.

4.1.3 8-Hydroxyheptadeca-1-ene-4,6-diyn-3-yl acetate (MS-2 (**26**))

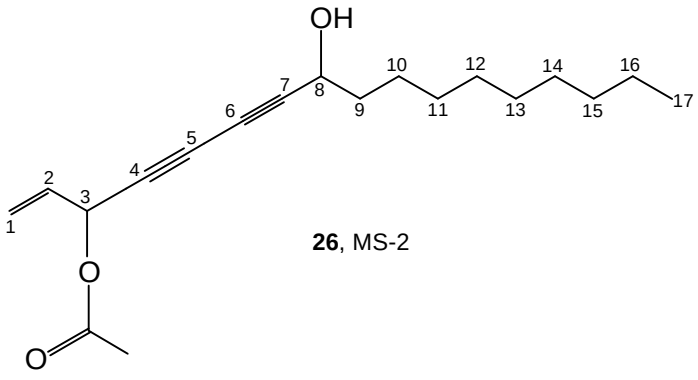

26, MS-2

t_R : 40.0 min (prep. HPLC method 3).

$[\alpha]^{20}_D$ = –28.0 (*c* = 0.85, $CHCl_3$/0.75 % ethanol).

UV/Vis ($CHCl_3$/0.75 % ethanol) : λ_{max} (ε) : 201.1 (369), 204.0 (351), 208.0 (495), 209.9 (455), 214.0 (567), 216.0 (548), 219.1 (527), 222.1 (642), 245.9 (1245), 259.6 (955), 283.1 (456).

IR (NaCl) : 3426*m*, 3088*w*, 2926*s*, 2856*s*, 2255*w*, 2157*w*, 1746*s*, 1650*w*, 1461*m*, 1372*m*, 1225s.

^{1}H-NMR (500 MHz, $CDCl_3$) : 5.93-5.90 (*m*, 1 H, H-C(3)); 5.89-5.84 (*m*, 1 H, H-C(2)); 5.55 (*d*, *J* = 16.8, 1 H, H_a-C(1)); 5.35 (*d*, *J* = 10.0, 1 H, H_b-C(1)); 4.43 (*br. t*, *J* = 6.5, 1 H, H-C(8)); 2.11 (*s*, 3 H, CH_3COO); 1.81 (*br. s*, 1 H, HO-C(8)); 1.75-1.66 (*m*, 2 H, H_2C(9)); 1.43 (*br. quintet*, *J* = 7.5, 2 H, H_2C(10)); 1.31-1.22 (*m*, 12 H, H_2C(11/12/13/14/15/16)); 0.88 (*t*, *J* = 7.0, 3 H, H_3C(17)).

^{13}C-NMR (125 MHz, $CDCl_3$) : 169.5 (*s*, COO); 131.9 (*d*, C(2)); 119.8 (*t*, C(1)); 81.3 (*s*, C(7)); 74.4 (*s*, C(4)); 70.8 (*s*, C(5)); 68.6 (6)); 64.5 (*d*, C(3)); 62.9 (*d*, C(8)); 37.4 (*t*, C(9)); 31.9 (*t*, C(15)); 29.51, 29.48, 29.29, 29.20 (4*t*, C(11/12/13/14)); 25.0 (*t*, C(10)); 22.7 (*t*, C(16)); 20.9 (*q*, $\underline{C}H_3COO$); 14.1 (*q*, C(17)).

COSY (500 MHz, $CDCl_3$) : 5.93-5.90 → 5.89-5.84 (+++); 5.89-5.84 → 5.55 (+++) and 5.35 (+++); 4.43 → 1.81 (+) and 1.75-1.66 (+++); 1.75-1.66 → 1.43 (+++); 1.43 → 1.31-1.22 (+++); 1.31-1.22 → 0.88 (+++).

HMQC (125 MHz, $CDCl_3$) : 131.9 → 5.93-5.90 (+) and 5.89-5.84 (+); 119.8 → 5.55 (++) and 5.35 (++); 64.5 → 5.93-5.90 (+++); 62.9 → 4.43 (+++); 37.4 → 1.75-1.66 (+++); 31.9 → 1.26 (+++); 29.51-29.20 → 1.31-1.22 (+++); 25.0 → 1.43 (+++); 22.7 → 1.28 (+++); 20.9 → 2.11 (+++); 14.1 → 0.88 (+++).

HMBC (125 MHz, $CDCl_3$) : 169.5 → 5.93-5.90 (++) and 2.11 (+++); 131.9 → 5.93-5.90 (+++) and 5.55 (++); 119.8 → 5.93-5.90 (+++); 81.3 → 1.75-1.66 (+++); 74.4 → 5.93-5.90 (++) and 5.89-5.84 (+++); 70.8 → 5.93-5.90 (+++); 68.6 → 5.93-5.90 (++); 64.5 → 5.89-5.84 (++) and 5.55 (+++); 62.9 → 1.75-1.66 (+++) and 1.43 (+); 37.4 → 1.43 (+); 31.9 → 1.28 (+++) and 0.88 (+++); 29.51-29.20 → 1.43 (+++) and 1.31-1.22 (+++); 25.0 → 1.75-1.66 (+) and 1.30 (++); 22.7 → 1.26 (+) and 0.88 (+++).

FAB-MS (NBA + KCl) : 343 (36), $[M+K]^+$; 287 (12); 245 (12); 227 (8); 137 (17); 91 (33); 43 (100).

EI-MS : 303 (20), $[M\text{-}1]^+$; 201 (14); 178 (78); 159 (44); 135 (47); 107 (65); 79 (38); 43 (100).

HR-EI-MS : 303.19530, $[M\text{-}1]^+$; calc. for $[C_{19}H_{27}O_3]^+$: 303.19602.

4.1.4 16-Acetoxy-11-hydroxyoctadeca-17-ene-12,14-diynyl acetate (MS-4 (**27**))

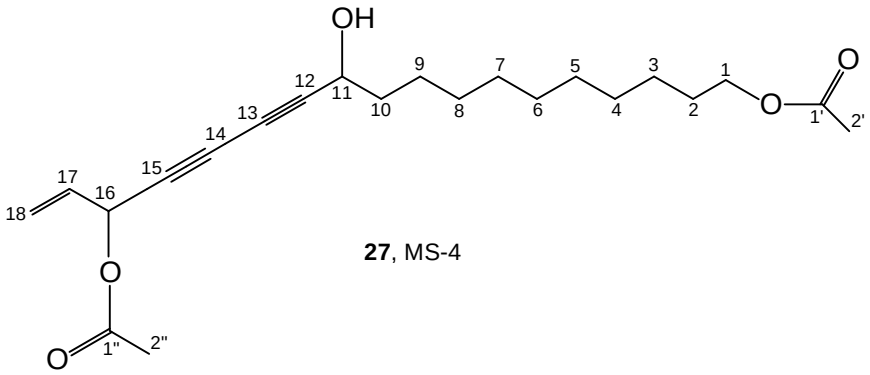

27, MS-4

t_R : 11.0 min (prep. HPLC method 10).

$[\alpha]^{20}_D$ = –26.4 (*c* = 0.81, $CHCl_3$/0.75 % ethanol).

UV/Vis ($CHCl_3$/0.75 % ethanol) : λ_{max} (ε) : 202.0 (254), 207.0 (302), 209.1 (353), 212.9 (352), 245.8 (984), 259.7 (601).

IR (NaCl) : 3444*m*, 3086*w*, 3031*w*, 2922*s*, 2844*s*, 2256*w*, 2156*w*, 1739*s*, 1644*w*, 1467*w*, 1367*w*, 1233*s*.

^{1}H-NMR (500 MHz, $CDCl_3$) : 5.92-5.89 (*m*, 1 H, H-C(16)); 5.88-5.83 (*m*, 1 H, H-C(17)); 5.54 (*d*, *J* = 16.8, 1 H, H_a-C(18)); 5.34 (*d*, *J* = 10.0, 1 H, H_b-C(18)); 4.42 (*br. t*, *J* = 6.3, 1 H, H-C(11)); 4.04 (*t*, *J* = 6.8, 2 H, H_2C(1)); 2.10 (*s*, 3 H, H_3C(2")); 2.04 (*s*, 3 H, H_3C(2')); 2.02 (*br. s*, 1 H, HO-C(11)); 1.73-1.68 (*m*, 2 H, H_2C(10)); 1.61 (*quintet*, *J* = 7.2, 2 H, H_2C(2)); 1.43 (*br. quintet*, *J* = 7.2, 2 H, H_2C(9)); 1.34-1.24 (*m*, 12 H, H_2C (3/4/5/6/7/8)).

^{13}C-NMR (125 MHz, $CDCl_3$) : 171.3 (*s*, C(1')); 169.5 (*s*, C(1")); 131.9 (*d*, C(17)); 119.7 (*t*, C(18)); 81.4 (*s*, C(12)); 74.3 (*s*, C(15)); 70.9 (*s*, C(14)); 68.5 (*s*, C(13)); 64.7 (*t*, C(1)); 64.5 (*d*, C(16)); 62.8 (*d*, C(11)); 37.4 (*t*, C(10)); 29.44, 29.41, 29.37, 29.21, 29.17 (5*t*, C(4/5/6/7/8)); 28.6 (*t*, C(2)); 25.9 (*t*, C(3)); 25.0 (*t*, C(9)); 21.0 (*q*, C(2')); 20.9 (*q*, C(2")).

COSY (500 MHz, $CDCl_3$) : 5.92-5.89 → 5.88-5.83 (++); 5.88-5.83 → 5.54 (++) and 5.34 (++), 4.42 → 2.02 (+) and 1.73-1.68 (+++); 4.04 → 1.61 (+++); 1.73-1.68 → 1.43 (++); 1.61 → 1.34-1.24 (+++); 1.43 → 1.34-1.24 (+++).

HMQC (125 MHz, $CDCl_3$) : 131.9 → 5.92-5.89 (++) and 5.88-5.83 (++); 119.7 → 5.54 (+++) and 5.34 (+++); 64.7 → 4.04 (+++); 64.5 → 5.92-5.89 (+++); 62.8 → 4.42 (+++); 37.4 → 1.73-1.68 (+++); 29.44-29.17 → 1.34-1.24 (+++); 28.6 → 1.61 (+++); 25.9 → 1.32 (+++); 25.0 → 1.43 (+++); 21.0 → 2.04 (+++); 20.9 → 2.10 (+++).

HMBC (125 MHz, $CDCl_3$) : 171.3 → 4.04 (+++) and 2.04 (+++); 169.5 → 5.92-5.89 (++) and 2.10 (+++); 131.9 → 5.92-5.89 (++) and 5.54 (++); 119.7 → 5.92-5.89 (++); 81.4 → 4.42 (++) and 1.73-1.68 (+++); 74.3 → 5.92-5.89 (+++) and 5.88-5.83 (+++); 70.9 → 5.92-5.89 (+++) and 4.42 (+); 68.5 → 5.92-5.89 (++) and 4.42 (++); 64.7 → 1.61 (+++) and 1.31 (+); 64.5 → 5.88-5.83 (++) and 5.54 (+++); 62.8 → 1.73-1.68 (+++) and 1.43 (+); 37.4 → 4.42 (++) and 1.43 (+); 29.44-29.17 → 4.04 (++), 1.73-1.68 (+), 1.61 (+++), 1.43 (+++) and 1.34-1.24 (+++); 28.6 → 4.04 (+++) and 1.34-1.24 (+++); 25.9 → 4.04 (+++), 1.61 (+++) and 1.34-1.24 (+++); 25.0 → 4.42 (++), 1.73-1.68 (++) and 1.34-1.24 (++).

FAB-MS (NBA + KCl) : 415 (32), $[M+K]^+$; 377 (2); 359 (5); 317 (11); 299 (12); 136 (13); 91 (24); 55 (35); 43 (100).

HR-EI-MS : 376.22369, M^+; calc. for $[C_{22}H_{32}O_5]^+$: 376.22497.

4.1.4.1 Stereochemical analysis of MS-4 (**27**) using the Mosher method

Both the (*R*)-MTPA ester (**50**) from (*S*)-MTPA-Cl (**48**) and (*S*)-MTPA ester (**51**) from (*R*)-MTPA-Cl (**49**) were prepared from 16-Acetoxy-11-hydroxyoctadeca-17-ene-12,14-diynyl acetate (MS-4 (**27**)).

*(R)-MTPA ester (**50**)*

A granule (4 mg) of catalytic DMAP was dissolved in 500 µl of absolute pyridine at r.t. This solution was added to 5.4 mg (0.0144 mmol) of MS-4 (**27**) under argon. To this solution 14.5 mg (0.0574 mmol, 4 eq.) of (*S*)-MTPA-Cl (**48**) were added and the mixture was stirred at r.t. for 24 h under argon. After the addition of 5 ml diethyl ether, the solution was washed with water. After separation, the resulting organic phase was dried over $MgSO_4$, filtered and the solvent evaporated. Preparative HPLC purification afforded 4.9 mg (0.0083 mmol, 58 %) of **50** as a pale yellow oil.

Prep. HPLC purification

Column : Eurospher 100 Si (Knauer), 5 µm, 250 x 16.0 mm ID

Detection : DAD Waters 996

Flow rate : 12 ml/min

Fraction collecting : 1 fraction every 30 seconds

Gradient table :

Time [min]	**% CH_2Cl_2**	**% MeOH**
Initial	100	0
15	100	0
25	80	20
40	80	20

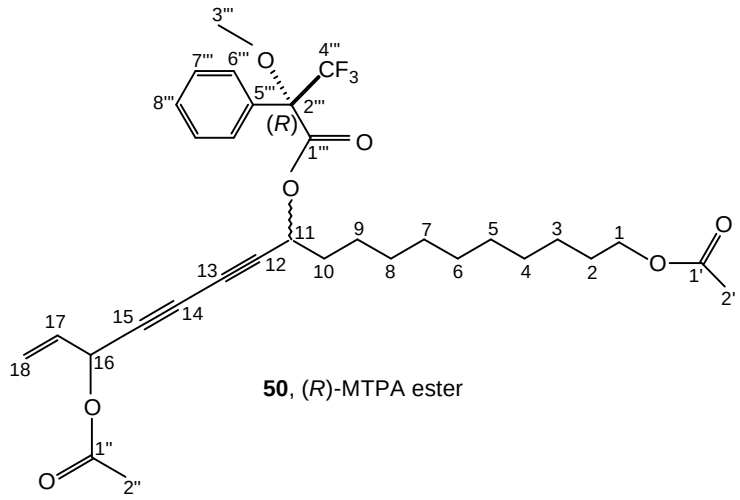

50, (*R*)-MTPA ester

^{1}H-NMR (500 MHz, $CDCl_3$) : 7.52-7.51 (*m*, 2 H, H-C(6''')); 7.43-7.40 (*m*, 3 H, H-C(7'''), H-C(8''')); 5.92-5.90 (*m*, 1 H, H-C(16)); 5.88-5.84 (*m*, 1 H, H-C(17)); 5.55 (*t*, *J* = 6.7, 1 H, H-C(11)); 5.54 (*d*, *J* = 16.4, 1 H, H_a-C(18)); 5.36 (*d*, *J* = 9.7, 1 H, H_b-C(18)); 4.05 (*t*, *J* = 6.8, 2 H, H_2C(1)); 3.55 (*s*, 3 H, H-C(3''')); 2.11 (*s*, 3 H, H_3C(2'')); 2.04 (*s*, 3 H, H_3C(2')); 1.87-1.83 (*m*, 2 H, H_2C(10)); 1.63-1.59 (*m*, 2 H, H_2C(2)); 1.43 (*m*, 2 H, H_2C(9)); 1.34-1.27 (*m*, 12 H, H_2C(3/4/5/6/7/8)).

^{13}C-NMR (125 MHz, $CDCl_3$) : 171.3 (*s*, C(1')); 169.4 (*s*, C(1'')); 165.6 (*s*, C(1''')); 131.8 (*s*, C(5''')); 131.7 (*d*, C(17)); 129.7-127.4 (3*d*, C(6'''/7'''/8''')); 123.2 (*q*, C(4'''), J^{CF} = 289); 119.9 (*t*, C(18)); 84.5 (*s*, C(2''')); 75.88 (*s*, C(12)); 75.2 (*s*, C(15)); 70.4 (*s*, C(14)); 70.2 (*s*, C(13)); 66.38 (*d*, C(11)); 64.6 (*t*, C(1)); 64.3 (*d*, C(16)); 55.6 (*q*, C(3''')); 34.13 (*t*, C(10)); 29.42, 29.37, 29.30, 29.22, 28.90 (5*t*, C(4/5/6/7/8)); 28.6 (*t*, C(2)); 25.9 (*t*, C(3)); 24.88 (*t*, C(9)); 21.05 (*q*, C(2')); 20.88 (*q*, C(2'')).

*(S)-MTPA ester (**51**)*

A granule (3 mg) of catalytic DMAP was dissolved in 500 µl of absolute pyridine at r.t. This solution was added to 7.8 mg (0.0207 mmol) of MS-4 (**27**) under argon. To that solution 21.0 mg (0.083 mmol, 4 eq.) of (*R*)-MTPA-Cl (**49**) were added and the mixture was stirred at r.t. for 24 h under argon. After the addition of 5 ml diethyl ether, the solution was washed with water. After separation, the resulting organic phase was dried over $MgSO_4$, filtered and the solvent evaporated. Preparative HPLC purification (see above) afforded 6.8 mg (0.0115 mmol, 55 %) of **51** as a pale yellow solid.

The two derivatives were analyzed by 500 MHz ^{1}H- and 125 MHz ^{13}C NMR. The absolute konfiguration at C(11) was determined according to the formula $\Delta\delta = \delta_{(S)\text{-ester}} - \delta_{(R)\text{-ester}}$. Results are summarized under 5.2.2.3.2 in the theoretical part.

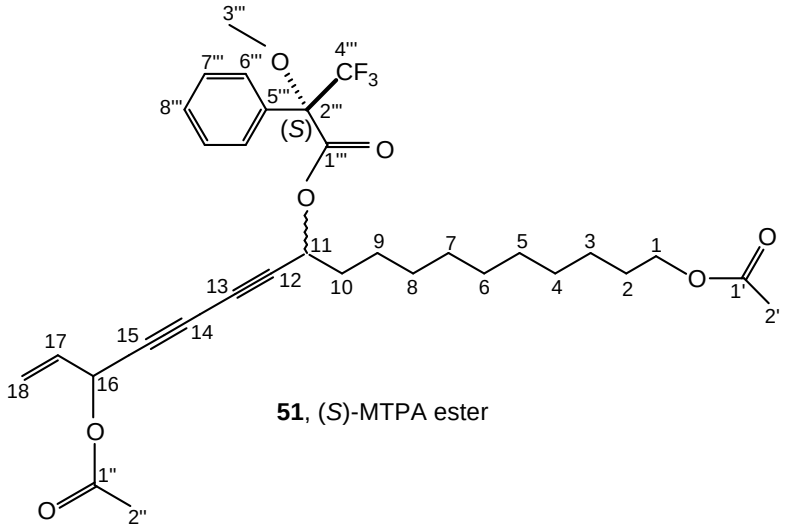

51, (*S*)-MTPA ester

^{1}H-NMR (500 MHz, $CDCl_3$) : 7.53-7.51 (*m*, 2 H, H-C(6''')); 7.42-7.39 (*m*, 3 H, H-C(7'''), H-C(8''')); 5.92-5.90 (*m*, 1 H, H-C(16)); 5.89-5.84 (*m*, 1 H, H-C(17)); 5.59 (*t*, *J* = 6.7, 1 H, H-C(11)); 5.55 (*d*, *J* = 16.3, 1 H, H_a-C(18)); 5.36 (*d*, *J* = 9.8, 1 H, H_b-C(18)); 4.05 (*t*, *J* = 6.8, 2 H, H_2C(1)); 3.58 (*s*, 3 H, H-C(3''')); 2.11 (*s*, 3 H, H_3C(2")); 2.05 (*s*, 3 H, H_3C(2')); 1.81-1.76 (*m*, 2 H, H_2C(10)); 1.65-1.56 (*m*, 2 H, H_2C(2)); 1.33-1.22 (*m*, 12 H, H_2C(3/4/5/6/7/8)); 1.29 (*m*, 2 H, H_2C(9)).

^{13}C-NMR (125 MHz, $CDCl_3$) : 171.3 (*s*, C(1')); 169.5 (*s*, C(1")); 165.7 (*s*, C(1''')); 132.1 (*s*, C(5''')); 131.7 (*d*, C(17)); 129.7-127.3 (3*d*, C(6'''/7'''/8''')); 123.2 (*q*, C(4'''), J^{CF} = 288); 119.9 (*t*, C(18)); 84.5 (*s*, C(2''')); 76.03 (*s*, C(12)); 75.3 (*s*, C(15)); 70.4 (*s*, C(14)); 70.2 (*s*, C(13)); 65.97 (*d*, C(11)); 64.7 (*t*, C(1)); 64.3 (*d*, C(16)); 55.6 (*q*, C(3''')); 34.17 (*t*, C(10)); 29.71, 29.42, 29.33, 29.25, 29.22 (5*t*, C(4/5/6/7/8)); 28.8 (*t*, C(2)); 25.9 (*t*, C(3)); 24.61 (*t*, C(9)); 21.05 (*q*, C(2')); 20.88 (*q*, C(2")).

4.1.5 11,16-Diacetoxyoctadeca-17-ene-12,14-diynyl acetate (MS-5 (**28**))

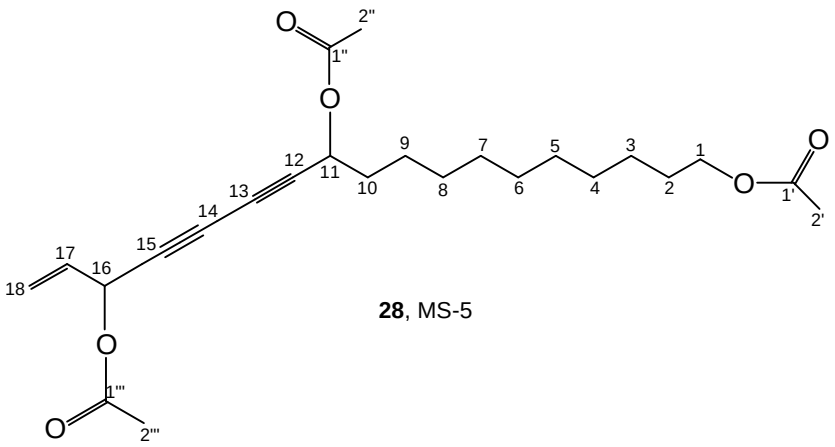

28, MS-5

t_R : 105.0 min (prep. HPLC method 8).

^{1}H-NMR (500 MHz, $CDCl_3$) : 5.91-5.89 (*m*, 1 H, H-C(16)); 5.87-5.83 (*m*, 1 H, H-C(17)); 5.54 (*d*, *J* = 16.4, 1 H, H_a-C(18)); 5.37 (*t*, *J* = 7.4, 1 H, H-C(11)); 5.35 (*d*, *J* = 9.7, 1 H, H_b-C(18)); 4.05 (*t*, *J* = 6.8, 2 H, $H_2C(1)$); 2.10 (*s*, 3 H, $H_3C(2''')$); 2.08 (*s*, 3 H, $H_3C(2'')$); 2.05 (*s*, 3 H, $H_3C(2')$); 1.78-1.74 (*m*, 2 H, $H_2C(10)$); 1.63-1.59 (*m*, 2 H, $H_2C(2)$); 1.46-1.37 (*m*, 2 H, $H_2C(9)$); 1.33-1.23 (*m*, 12 H, H_2C (3/4/5/6/7/8)).

^{13}C-NMR (125 MHz, $CDCl_3$) : 171.3 (*s*, C(1')); 169.8 (*s*, C(1'')); 169.5 (*s*, C(1''')); 131.8 (*d*, C(17)); 119.8 (*t*, C(18)); 77.7 (*s*, C(12)); 74.5 (*s*, C(15)); 70.7 (*s*, C(14)); 69.0 (*s*, C(13)); 64.7 (*t*, C(1)); 64.4 (*d*, C(16)); 64.1 (*d*, C(11)); 34.4 (*t*, C(10)); 29.45, 29.42, 29.37, 29.22, 29.05 (5*t*, C(4/5/6/7/8)); 28.6 (*t*, C(2)); 25.9 (*t*, C(3)); 24.9 (*t*, C(9)); 21.05 (*q*, C(2')); 20.90 (*q*, C(2'' or 2''')); 20.88 (*q*, C(2'' or 2''')).

COSY (500 MHz, $CDCl_3$) : 5.91-5.89 → 5.87-5.83 (++); 5.87-5.83 → 5.54 (++) and 5.35 (++); 5.37 → 1.78-1.74 (+++); 4.05 → 1.63-1.59 (+++); 1.78-1.74 → 1.46-1.37 (+++); 1.63-1.59 → 1.33-1.23 (+++); 1.46-1.37 → 1.33-1.23 (++).

HMQC (125 MHz, $CDCl_3$) : 119.8 → 5.54 (+) and 5.35 (+); 64.7 → 4.05 (++); 64.4 → 5.91-5.89 (+); 64.1 → 5.37 (++); 34.4 → 1.78-1.74 (+); 29.45-29.05 → 1.33-1.23 (+++); 28.6 → 1.63-1.59 (+); 25.9 → 1.33 (+); 24.9 → 1.46-1.37 (+); 21.05 → 2.05 (+++); 20.90 or 20.88 → 2.10 (+++); 20.88 or 20.90 → 2.08 (+++).

HMBC (125 MHz, $CDCl_3$) : 171.3 → 4.05 (++) and 2.05 (+++); 169.8 → 5.37 (+) and 2.08 (+++); 169.5 → 5.91-5.89 (+) and 2.10 (+++); 131.8 → 5.91-5.89 (+); 77.7 → 5.37 (++) and 1.78-1.74 (+); 69.0 → 5.37 (+); 64.7 → 1.63-1.59 (+); 64.4 → 5.87-5.83 (+); 64.1 → 1.78-1.74 (+); 34.4 → 5.37 (+); 29.45-29.05 → 1.78-1.74 (+), 1.63-1.59 (+) and 1.33-1.23 (++); 28.6 → 4.05 (++) and 1.33-1.23 (+); 25.9 → 4.05 (+++) and 1.63-1.59 (+).

FAB-MS (NBA + KCl) : 457 (94), $[M+K]^+$; 419 (8), $[M+1]^+$; 359 (99); 317 (19); 171 (9); 115 (15); 55 (35); 43 (100).

4.1.6 Stigmasterol (**42**)

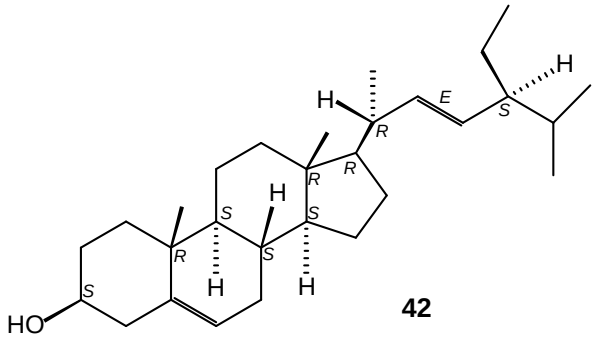

42

Table 18 : Comparison of the spectroscopic data of compound **42** with stigmasterol (authentic sample).

Analytical method	Compound 42	Authentic sample
EI-MS (70 eV, ca. 200 °C)	412 (90), $[M]^+$; 369 (23); 351 (39); 300 (40); 271 (53); 255 (83); 213 (32); 159 (56); 133 (52); 83 (89); 55 (100).	412 (100), $[M]^+$; 369 (25); 351 (38); 300 (40); 271 (50); 255 (74); 213 (28); 159 (45); 133 (40); 83 (57); 55 (59).
IR (KBr pellet)	3346*m*, 2935*s*, 2866*s*, 1458*m*, 1440*m*, 1382*m*, 1368*m*, 1331*w*, 1193*w*, 1055*m*, 1022*w*, 970*m*, 961*m*, 838*w*, 799*w*.	3346*m*, 2935*s*, 2867*s*, 1458*m*, 1442*m*, 1382*m*, 1368*m*, 1331*w*, 1193*w*, 1054*m*, 1022*w*, 971*m*, 960*m*, 838*w*, 799*w*.
^{1}H-NMR* (500/400 MHz, $CDCl_3$)	5.35-5.34 (*m*); 5.15 (*dd*, *J* = 8.6, 8.7); 5.01 (*dd*, *J* = 8.8, 8.7); 3.54-3.50 (*m*); 2.31-2.23 (*m*); 2.06-1.94 (*m*); 1.87-1.82 (*m*); 1.72-1.66 (*m*); 1.58-1.39 (*m*); 1.30-1.25 (*m*); 1.23-1.14 (*m*); 1.12-1.04 (*m*); 1.03 (*s*); 1.01 (*s*); 1.00-0.91 (*m*); 0.85 (*d*, *J* = 6.4); 0.80 (*t*, *J* = 7.5); 0.70 (*s*).	5.36-5.34 (*m*); 5.15 (*dd*, *J* = 8.6, 8.7); 5.01 (*dd*, *J* = 8.6, 8.6); 3.56-3.48 (*m*); 2.32-2.23 (*m*); 2.07-1.95 (*m*); 1.87-1.81 (*m*); 1.73-1.66 (*m*); 1.59-1.38 (*m*); 1.30-1.24 (*m*); 1.22-1.13 (*m*); 1.11-1.05 (*m*); 1.03 (*s*); 1.01 (*s*); 1.00-0.90 (*m*); 0.85 (*d*, *J* = 6.6); 0.80 (*t*, *J* = 7.2); 0.70 (*s*).
^{13}C-NMR** (125/101 MHz, $CDCl_3$)	140.8; 138.3; 129.3; 121.7; 71.8; 56.9; 55.9; 51.2; 50.2; 42.3; 42.2; 40.5; 39.7; 37.3; 36.5; 31.90; 31.90; 31.7; 28.9; 25.4; 24.4; 21.2; 21.1; 21.08; 19.4; 19.0; 12.3; 12.1.	140.9; 138.5; 129.4; 121.9; 71.9; 57.0; 56.1; 51.4; 50.3; 42.4; 42.3; 40.7; 39.8; 37.4; 36.7; 32.0; 32.0; 31.8; 29.1; 25.6; 24.5; 21.4; 21.24; 21.21; 19.5; 19.1; 12.4; 12.2.

* : 500 MHz ^{1}H-NMR spectrum of compound **42** / 400 MHz ^{1}H-NMR spectrum of authentic sample
** : 125 MHz ^{13}C-NMR spectrum of compound **42** / 101 MHz ^{1}H-NMR spectrum of authentic sample

5. Fractionation of *Commiphora fulvotomentosa* Engl. extract

5.1 Extraction

1039 g of ground stembark of *Commiphora fulvotomentosa* Engl. were extracted by stirring with three portions of petroleum ether (40-60 °C). A five-fold quantity of solvent in relation to plant material was used. The extraction was carried out at room temperature under stirring for 24 h per portion. After each aliquot the mixture was left to stand and then filtered under normal pressure. The filtrates were combined, evaporated at 40 °C and dried under high vacuum.

5.2 Chromatography

The fractionation of the crude plant extract was carried out by MPLC followed by preparative scale HPLC. After each fractionation step the fractions were checked for purity by analytical HPLC.

MPLC Method 1 (*crude extract*)

Column : LiChroprep® Si 60 (Merck), 15-25 µm, 460 x 36 mm ID
Detection : UV 254 nm
Flow rate : 15 ml/min
Fraction collecting : 1 fraction every min
Gradient table :

Time [min]	% Hexane	% Ethyl acetate	% MeOH
Initial	100	0	0
10	100	0	0
240	50	50	0
360	50	50	0
480	0	0	100

MPLC Method 2 (*F2*)

Column : LiChroprep® Si 60 (Merck), 15-25 µm, 460 x 26 mm ID

Detection : UV 254 nm

Flow rate : 15 ml/min

Fraction collecting : 1 fraction every min

Gradient table :

Time [min]	% Hexane	% Ethyl acetate	% MeOH
Initial	100	0	0
240	95	5	0
360	95	5	0
420	80	20	0
480	80	20	0
540	0	0	100

MPLC Method 3 (*F3*)

Column : LiChroprep® Si 60 (Merck), 15-25 µm, 460 x 26 mm ID

Detection : UV 254 nm

Flow rate : 15 ml/min

Fraction collecting : 1 fraction every min

Gradient table :

Time [min]	% Hexane	% Ethyl acetate	% MeOH
Initial	100	0	0
240	90	10	0
360	90	10	0
420	70	30	0
480	70	30	0
540	0	0	100

C. Summary

For the present thesis 22 samples of seven African medicinal plants, the extracts of which had previously proved to possess an *in vitro* activity against *T. b. rhodesiense* and/or *P. falciparum* and 13 samples of six randomly selected plant species based on availability were collected in Tanzania.

Of these 35 samples, 140 crude extracts were produced with four solvents of different polarity, and the extracts were tested for *in vitro* antitrypanosomal and antiplasmodial activity and for cytotoxicity. In addition the extracts were tested for the affinity to the $GABA_A$ receptor performed by radioligand binding experiments.

Based on the considerable antitrypanosomal and antiplasmodial activity and the affinity to the $GABA_A$ receptor, two extracts were selected for bioassay-guided fractionation : the petroleum ether extract of the stembark of *Commiphora fulvotomentosa* Engl. because of its promising IC_{50} value of 2.1 μg/ml against *T. b. rhodesiense* and the high selectivity index of 21.4, and the petroleum ether extract of the rootbark of *Cussonia zimmermannii* Harms because of its IC_{50} value of 4.8 μg/ml against *T. b. rhodesiense*, its IC_{50} value of 3.3 μg/ml against *P. falciparum*, and the potent modulatory effect at the $GABA_A$ receptor of 151 %.

After three fractionation steps the fractions of the petroleum ether extract of the stembark of *Commiphora fulvotomentosa* Engl. did not show any inhibitory activity against *T. b. rhodesiense* and were therefore not investigated further.

Bioassay-guided fractionation of the petroleum ether extract of the rootbark of *Cussonia zimmermannii* Harms lead to the isolation of four polyacetylenes. By the application of MS, HR-MS, UV/VIS and IR methods and NMR experiments (^{1}H-NMR, ^{13}C-NMR, DEPT135, ^{1}H-^{1}H COSY, HMQC and HMBC) the structures of the four novel diynes were established : 8-Hydroxyheptadeca-4,6-diyn-3-yl acetate (MS-1 (**25**)), 8-Hydroxyheptadeca-1-ene-4,6-diyn-3-yl acetate (MS-2 (**26**)), 16-Acetoxy-11-hydroxyoctadeca-17-ene-12,14-diynyl acetate (MS-4 (**27**)), and 11,16-Diacetoxyoctadeca-17-ene-12,14-diynyl acetate (MS-5 (**28**)).

Additionally, stigmasterol (**42**) was isolated and identified by comparison of its spectroscopic data with those of an authentic sample.

For the determination of the absolute configuration of MS-4 (**27**) at C(11) the Mosher method was used. The negative $\Delta\delta$ values for the neighbouring protons suggested the *S*-configuration. But this result could not be confirmed by the ^{13}C-NMR data since both positive and negative $\Delta\delta$ values were obtained for the neighbouring carbons. Due to the fact, that the results for the protons and the carbons were not consistent the *S*-configuration for C(11) of MS-4 (**27**) could not be assigned with certainty.

The isolated compounds MS-1 (**25**), MS-2 (**26**), and MS-4 (**27**) were tested for *in vitro* inhibitory activity against additional parasites like *T. cruzi* and *L. donovani* (axenic and in infected macrophages). **42** was not tested because it was a well known phytosterol which is ubiquitous in plants. Neither was MS-5 (**28**) tested, since the isolated amount was not sufficient.

It was found that MS-1 (**25**) showed in all antiparasitic *in vitro* assays no higher inhibitory activity than the crude extract. MS-2 (**26**) showed promising activities in the *T. cruzi* and *L. donovani* (axenic and in infected macrophages) assay with IC_{50} values of 0.2, 0.039, and 0.098 μg/ml, respectively. The respective IC_{50} values of the standard drugs were 0.62, 0.18, and 0.29. The cytotoxicity was relatively high; therefore the selectivity with SI values of 18.0 and 36.7, respectively (*T. cruzi*, *L. donovani* in inf. mac.), was in a moderate range. MS-4 (**27**) showed also interesting activities in the *T. cruzi* and *L. donovani* (axenic) assays with IC_{50} values of 0.15 and 0.054 μg/ml. The SI value of 145.3 (*T. cruzi*) was high. Compared with the standard drugs the activities of MS-2 (**26**) and MS-4 (**27**) against *T. b. rhodesiense* and *P. falciparum* were in a moderate range.

MS-1 (**25**), MS-2 (**26**), and MS-4 (**27**) were also tested in the $GABA_A$ receptor binding assay. Here MS-4 (**27**) showed the highest relative specific binding of 158 % at a concentration of 20 μg/ml, followed by MS-2 (**26**) with 152 % and MS-1 (**25**) with 138 %.

In order to investigate whether the modulatory effect at the $GABA_A$ receptor leads to a chanel opening, the isolated compounds were investigated electrophysiologically. It was found that MS-1 (**25**), MS-2 (**26**), and MS-4 (**27**) act as potent positive allosteric modulators at $GABA_A$ receptors with a half maximal stimulation at a concentration of 0.6-3.5 μM and a maximal stimulation of 110-450 %. The compounds also showed unique subunit selectivity profiles, the stimulation was independend from the presence of the γ subunit and resistant to the benzodiazepine antagonist Ro15-1788.

These *in vitro* data suggested that MS-1 (**25**), MS-2 (**26**), and MS-4 (**27**) may be used to treat diseases of the central nervous system, specifically they may be used to treat states of anxiety, as sedatives/hypnotics, as muscle relaxants and as anticonvulsives (e.g. in epilepsy), and in the treatment of drug addiction. Therefore it was decided to patent the compounds for these indications [174].

All data are on the *in vitro* level. For a pharmaceutical application *in vivo* data are needed. Therefore MS-1 (**25**), MS-2 (**26**), and MS-4 (**27**) need to be synthesized in order to get more material for subsequent *in vivo* experiments.

D. Bibliography

[1] G. M. Cragg, D. J. Newman, in `Ethnomedicine and drug discovery´, Ed. M. M. Iwu, J. C. Wootton, Elsevier, Amsterdam, London, New York, 2002, p. 23-38.

[2] A. D. Buss, R. D. Waigh, in `Burgers medicinal chemistry and drug discovery´, Ed. M. E. Wolff, Wiley, New York, 1995, Vol. 1, p. 983-1033.

[3] N. Neuss, M. N. Neuss, in `The Alkaloids´, Ed. A. Brossi, M. Suffness, Academic Press, New York, 1990, p. 229-240.

[4] D. L. Klayman, in `Human medicinal agents from plants´, Ed. A. D. Kinghorn, M. F. Balandrin, American Chemical Society, Washington DC, 1993, p. 242-255.

[5] K. Hostettmann, A. Marston, J.-L. Wolfender, in `Phytochemistry of plants used in traditional medicine´, Ed. K. Hostettmann, A. Marston, M. Maillard, M. Hamburger, Clarendon Press, Oxford, 1995, p. 17-45.

[6] M. Hamburger, K. Hostettmann, *Phytochem.*, **1991**, *30*, 3864-3874.

[7] M. M. Iwu, in `Ethnomedicine and drug discovery´, Ed. M. M. Iwu, J. C. Wootton, Elsevier, Amsterdam, 2002, p. 309-320.

[8] M. J. O'Neill, J. A. Lewis, in `Human medicinal agents from plants´, Ed. A. D. Kinghorn, M. F. Balandrin, American Chemical Society, Washington DC, 1993, p. 48-55.

[9] J. G. Bruhn, F. Sandberg, in `The medical plant industry´, Ed. R. O. B. Wijesekera, CRC Press, Ann Arbor, 1991, p. 223.

[10] O. Akerele, *Int. Trad. Health. New.*, **1985**, *1*, 1.

[11] F. Haerdi, in `Afrikanische Heilpflanzen´ Ed. A. Buehler, R. Geigy, A. Gigon, F. Meier, Acta Tropica, 1964, Supplement 8.

[12] J. O. Kokwaro, `Medicinal plants of East Africa´, East African Literature Bureau, Kampala, 1976.

[13] I. Hedberg, O. Hedberg, P. J. Madati, K. E. Mshigeni, E. N. Mshiu, G. Samuelsson, *J. Ethnopharm.*, **1982**, *6*, 29-60.

[14] I. Hedberg, O. Hedberg, P. J. Madati, K. E. Mshigeni, E. N. Mshiu, G. Samuelsson, *J. Ethnopharm.*, **1983**, *9*, 105-128.

[15] I. Hedberg, O. Hedberg, P. J. Madati, K. E. Mshigeni, E. N. Mshiu, G. Samuelsson, *J. Ethnopharm.*, **1983**, *9*, 237-260.

[16] S. C. Chhabra, R. L. Mahunnah, E. N. Mshiu, *J. Ethnopharm.*, **1987**, *21*, 253-277.

[17] S. C. Chhabra, R. L. Mahunnah, E. N. Mshiu, *J. Ethnopharm.*, **1989**, *25*, 339-359.

[18] H. Weenen, M. H. H. Nkunya, D. H. Bray, L. B. Mwasumbi, L. S. Kinabo, V. A. E. B. Kilimali, *Plant. Med.,* **1990**, *56*, 368-370.

[19] H. Weenen, M. H. H. Nkunya, D. H. Bray, L. B. Mwasumbi, L. S. Kinabo, V. A. E. B. Kilimali, *Plant. Med.,* **1990**, *56*, 371-373.

[20] M. Gessler, `The antimalarial potential of medicinal plants traditionally used in Tanzania, and their use in the treatment of Malaria by traditional healers´, Ph.D. Thesis, University of Basel, 1995.

[21] F. Freiburghaus, `African medicinal plants used in the treatment of sleeping sickness – an evaluation´, Ph.D. Thesis, University of Basel, 1996.

[22] B. Räz, `Isolation and evaluation of antiparasitic lead compounds from African medicinal plants´, Ph.D. Thesis, University of Basel, 1998.

[23] J. D. Phillipson, C. W. Wright, G. C. Kirby, D. C. Warhurst, in `Phytochemistry of Plants Used in Traditional Medicine´, Ed. K. Hostettmann, A. Marston, M. Maillard, M. Hamburger, Clarendon Press, Oxford, 1995, p. 94-135.

[24] P. I. Trigg, in `Economic and medicinal plant research´, Ed. H. Wagner, H. Hikino, N. R. Farnsworth, Academic Press, London, 1989, Vol. 3, p. 1-56.

[25] J. D. Phillipson, M. J. O'Neill, in `Biologically active natural products, Proceedings of the Phytochemical Society of Europe´, Ed. K. Hostettmann, P. J. Lea, Clarendon Press, Oxford, 1987, Vol. 27, p. 49-64.

[26] M. H. H. Nkunya, `Progress in the search for antimalarials´, NAPRECA Monograph Series, NAPRECA, Addis Ababa University, Addis Ababa, 1992, No. 4, p. 1-36.

[27] G. L. Sharma, K. K. Bhutani, *Plant. Med.*, **1988**, *54*, 120-122.

[28] M. Hooper, G. C. Kirby, M. M. Kulkarni, S. N. Kulkarni, B. A. Nagasampagi, M. J. O'Neill, J. D. Phillipson, S. R. Rojatkar, D. C. Warhurst, *J. Med. Chem.*, **1990**, *25*, 717-723.

[29] A. Fournet, V. Muñoz, F. Roblot, R. Hocquemiller, A. Cave, J. C. Gantier, *Phyto. Res.*, **1993**, *7*, 111-115.

[30] J. D. Phillipson, C. W. Wright, G. C. Kirby, D. C. Warhurst, in `Phytochemical potential of tropical plants´, Ed. K. R. Downum, J. T. Romeo, H. A. Stafford, Plenum Press, New York, 1993, p. 1-40.

[31] L. -Z. Lin, H. -L. Shieh, C. K. Angerhofer, J. M. Pezzuto, G. A. Cordell, L. Xue, M. E. Johnson, N. Ruangrungsi, *J. Nat. Prod.*, **1993**, *56*, 22-29.

[32] J. C. Cavin, S. M. Krassner, E. Rodriguez, *J. Ethnopharm.*, **1987**, *19*, 89-94.

[33] M. Sauvin, J. -P. Dedet, N. Kunesch, J. Poisson, J. C. Gantier, P. Gayral, G. Kunesch, *Phyto. Res.*, **1993**, *7*, 167-171.

[34] K. C. Liu, S. -L. Yang, M. F. Roberts, B. C. Elford, J. D. Phillipson, *Plant Cell Rep.*, **1992**, *11*, 637-640.

[35] World Health Organisation, `Fighting disease, fostering development´, Report WHO, Geneva, 1996b, Fact sheet no. 134.

[36] D. T. Okpako, *Trends pharmacol. Sci.*, **1999**, *20*, 482-485.

[37] D. T. Okpako, `Principles of Pharmacology. A tropical approach´, Cambridge University Press, New York, 1991.

[38] World Health Organisation, `Fighting disease, fostering development´, Report WHO, Geneva, 1996.

[39] World Health Organisation, `Life in the 21st Century – A vision for all´, Report WHO, Geneva, 1998.

[40] K. Vickermann, *Int. J. Parasitol.*, **1994**, *24*, 1317-1331.

[41] A. Stich, M. P. Barrett, S. Krishna, *Trends Pharmacol.*, **2003**, *19*, 195-197.

[42] D. Legros, G. Ollivier, M. Gestellu-Etchegorry, C. Paquet, C. Burri, J. Jannin, P. Buescher, *The Lancet Infect. Dis.*, **2002**, *2*, 437-440.

[43] World Health Organisation, *WHO Tech. Rep. Ser. 881,* **1998**, 1-114.

[44] E. K. Markell, M. Voge, `Medical Parasitology´, W. B. Saunders Comp., Philadelphia, 1981.

[45] D. D. Despommier, J. W. Karapelou, `Parasite Life Cycles´, Springer-Verlag, Berlin, 1987.

[46] H. Mehlhorn, `Encyclopedic Reference of Parasitology, Diseases, Treatment, Therapy´, Springer-Verlag, Berlin, 2001.

[47] A. H. Fairlamb, *Trends Parasito.*, **2003**, *19*, 488-494.

[48] J. Pépin, F. Milford, *Adv. Parasitol.*, **1994**, *33*, 1-47.

[49] N. S. Carter, *J. Biol. Chem.*, **1995**, *270*, 28153-28157.

[50] H. P. De Koning, *Mol. Pharmacol.*, **2001**, *59*, 586-592.

[51] T. A. Shapiro, P. T. Englund, *Proc. Natl. Acad. Sci. USA*, **1990**, *87*, 950-954.

[52] O. Heby, *Biochem. Soc. Trans.*, **2003**, *31*, 415-419.

[53] P. G. Bray, *Mol. Biochem. Parasitol.*, **1994**, *63*, 87-94.

[54] J. A. Urbina, R. Docampo, *Tr. Parasitol.*, **2003**, *19*, 495-501.

[55] World Health Organisation, *WHO Tech. Rep. Ser. 905*, **2002**, 1-109.

[56] C. M. Morel, *Parasitol. Today*, **2000**, *16*, 522-525.

[57] G. A. Schmuñis, in `Trypanosoma cruzi e Doença de Chagas´, Ed. Z. Brener et al., Guanabara Koogan, Rio de Janeiro, 2000, p. 1-15.

[58] A. Prata, *The Lancet Inf. Dis.*, **2001**, *1*, 92-100.

[59] D. S. Fries, A. H. Fairlamb in `Burgers medicinal chemistry and drug discovery´, Ed. D. J. Abraham, Wiley, New York, 2003, p. 1033-1087.

[60] R. Docampo, *Chem. Biol. Interact.*, **1990**, *73*, 1-27.

[61] J. R. Cançado, *Mem. Inst. Oswaldo Cruz*, **1999**, *94*, 331-336.

[62] L. V. Kirchhoff, in `Emergin Infections 3´, Ed. W. M. Scheld, ASM Press, Boston, 1999, p. 111-134.

[63] S. G. Andrade, *Trans. R. Soc. Trop. Med. Hyg.*, **1992**, *86*, 624-626.

[64] J. Sachs, P. Malaney, *Nature*, **2002**, *415*, 680-685.

[65] P. J. Guerin, P. Olliaro, F. Nosten, P. Druilhe, R. Laxminarayan, F. Binka, W. L. Kilama, N. Ford, N. J. White, *The Lancet Infect. Dis.*, **2002**, *2*, 564-573.

[66] R. W. Snow, M. H. Craig, U. Deichmann, U. Marsh, *Bull. WHO*, **1999**, *77*, 624-640.

[67] J. G. Breman, *Am. J. Trop. Med. Hyg.*, **2001**, *64*, 1-11.

[68] K. Marsh, *Lancet*, **1998**, *352*, 924-925.

[69] F. M. A. Ukoli, `Introduction to Parasitology in Tropical Africa´, John Wiley, Chichester, 1984.

[70] P. A. Nogueira, *Res. Microbiol.*, **2001**, *152*, 141-147.

[71] C. G. Nevill, *Soc. Sci. Med.*, **1990**, *6*, 667-669.

[72] W. A. Krotoski, *Am. J. Trop. Med. Hyg.*, **1982**, *31*, 1291-1293.

[73] World Health Organisation, *Trans. R. Soc. Trop. Med. Hyg.*, **1990**, *84*, 1-65.

[74] K. Marsh, *Parasitol.*, **1992**, *104*, 53-69.

[75] S. R. Meshnick, *Med. Trop.*, **1998**, *58*, 13-17.

[76] M. Korsinczky, N. Chen, B. Kotecka, A. Saul, K. Rieckmann, Q. Cheng, *Antimic. A. Chemo.*, **2000**, *44*, 2100-2108.

[77] A. Sabchareon, P. Attanath, P. Phanuaksook, *Trans. R. Soc. Trop. Med. Hyg.*, **1998**, *92*, 201-206.

[78] P. Winstanley, *The Lancet Infect. Dis.*, **2001**, *1*, 242-250.

[79] P. M. O'Neill, P. G. Bray, S. R. Hawley, S. A. Ward, B. K. Park, *Pharmacol. Ther.*, **1998**, *77*, 29-58.

[80] P. A. Phillips-Howard, F. O. ter Kuile, *Drug. Saf.*, **1995**, *12*, 370-383.

[81] A. L. Bittencourt, A. Barral, *Mem. Inst. Oswaldo Cruz Rio J.*, **1991**, *86*, 51-56.

[82] World Health Organisation, `Zoonoses and veterinary public health´, 2005.

[83] M. Siddig, H. Galid, D. Shillington, A. Petesen, S. Khidir, *Trop. Geogr. Med.*, **1990**, *42*, 107-112.

[84] K. S. Warren, A. A. F. Mahmoud, `Tropical and Geographical Medicine´, McGraw-Hill, New York, 1990.

[85] S. F. Moody, *Acta. Trop. Basal*, **1993**, *53*, 185-205.

[86] D. G. Russel, T. Talamas-Rhoana, *Immunol. Today*, **1989**, *10*, 328-334.

[87] S. J. Turco, *Biochem.*, **1990**, *118*, 74-78.

[88] M. K. Wasseff, D. M. Dywer, *J. Biol. Chem.*, **1985**, *264*, 6711-6715.

[89] E. Braunwald, F. C. Isselbacher, R. G. Petersdor, J. D. Wilson, `Harrison's Principals of Internal Medicine´, McGraw-Hill, New York, 1987.

[90] D. T. Hart, `Leishmaniasis, The Currant Status and New Strategies for Control´, Plenum Press, New York, 1987.

[91] B. C. Walton, L. L. Valvuerde, *Ann. Trop. Med. Parasitol.*, **1979**, *73*, 23-27.

[92] S. L. Croft, *Mol. Biochem. Parasitol.*, **2003**, *126*, 165-172.

[93] World Health Organisation, `WHO Model prescribing information : drugs used in parasitic disease´, WHO, Geneva, 1995.

[94] C. P. Thakur, *Trans. R. Soc. Trop. Med. Hyg.*, **1999**, *93*, 319-323.

[95] W. Sieghart, *Pharmacol. Rev.*, **1995**, *47*, 182-234.

[96] G. B. Smith, R. W. Olsen, *Trends Pharmacol. Sci.*, **1995**, *16*, 162-168.

[97] D. R. Burt, G. L. Kamatchi, *FASEB J.*, **1991**, *5*, 2916-2923.

[98] R. L. Mcdonald, T. P., *Cell Physiol. Biochem.*, **1993**, *3*, 352-373.

[99] P. J. Whiting, R. M. McKernan, K. A. Wafford, *Int. Rev. Neurobiol.*, **1995**, *38*, 95-138.

[100] I. Mody, Y. DeKoninck, T. S. Otis, I. Soltesz, *Trends. Neurosci.*, **1994**, *17*, 517-525.

[101] Y. Okada, H. Taniguchi, C. Shimada, *Science*, **1976**, *194*, 620-622.

[102] H. Taniguchi, Y. Okada, H. Seguchi, C. Shimada, M. Seki, A. Tsutou, S. Baba, *Diabetes*, **1979**, *28*, 629-633.

[103] H. Betz, *Neuron*, **1990**, *5*, 383-392.

[104] J. L. Galzi, J. P. Changeux, *Curr. Opin. Struct. Biol.*, **1994**, *4*, 554-565.

[105] H. Moehler, J. M. Fritschy, B. Luescher, U. Rudolph, J. Benson, D. Benke, in `Ion Channels´, Ed. T. Narahashi, Plenum, New York, 1995, vol. 4, p. 89-113.

[106] S. Mertens, D. Benke, H. Moehler, *J. Biol. Chem.*, **1993**, *268*, 5965-5973.

[107] S. Bohlhalter, O. Weinmann, H. Moehler, J. M. Fritschy, *J. Neurosci.*, **1996**, *16*, 283-297.

[108] K. H. Backus, M. Arigoni, U. Drescher, L. Scheurer, P. Malherbe, H. Moehler, *Neuroreport*, **1993**, *5*, 285-288.

[109] E. A. Barnard, in `$GABA_A$ Receptors and Anxiety. From Neurobiology to Treatment, Advances in Biochemical Psychopharmacology´, Ed. G. Biggio, E. Sanna, M. Serra, E. Costa, Raven, New York, 1995, vol. 48, p. 1-16.

[110] G. Richards, P. Schoch, W. Haefely, *Semin. Neurosci.*, **1991**, *3*, 191-203.

[111] W. Haefely, in `The Challenge of Neuropharmacology. A Tribute to the Memory of Willy Haefely´, Ed. H. Moehler, M. Da Prada, Editiones Roche, Basel, 1994, p. 15-40.

[112] R. E. Study, J. L. Baker, *Neurons. Proc. Natl. Acad. Sci. USA*, **1981**, *78*, 7180-7184.

[113] E. Sigel, A. Buhr, *Trends Pharmacolog. Sci.*, **1997**, *18*, 425-429.

[114] M. D. Majewska, *Prog. Neurobiol.*, **1992**, *38*, 379-395.

[115] K. A. Wafford, D. M. Burnett, T. V. Dunwiddie, R. A. Harris, *Science*, **1990**, *249*, 291-293.

[116] E. Sigel, R. Baur, P. Malherbe, *FEBS Lett.*, **1993**, *324*, 140-142.

[117] A. R. Smith, `Flora of tropical East Africa. Euphorbiaceae (Part 1)´, A. A. Balkema, Rotterdam, Boston, 1988.

[118] J. P. M Brenan, `Flora of tropical East Africa. Leguminosae, subfamily Mimosoideae´, Crown agents for oversea governments and administrations, Millbank, London, 1959.

[119] B. Verdcourt, *Kew Bulletin*, **1985**, *40*, 635-636.

[120] N. K. B., Robson, B. Mathew, `Flora of tropical East Africa. Celastraceae´, A. A. Balkema, Rotterdam, Brookfield, 1994.

[121] B. Verdcourt, `Flora of tropical East Africa. Annonaceae´, Crown agents for oversea governments and administrations, Millbank, London, 1971.

[122] J. R. Tennant, `Flora of tropical East Africa. Araliaceae´, Crown agents for oversea governments and administrations, Millbank, London, 1968.

[123] J. B. Gillett, `Flora of tropical East Africa. Araliaceae´, A. A. Balkema, Rotterdam, Brookfield, 1991.

[124] B. Verdcourt, `Flora of tropical East Africa. Rubiaceae (Part 3)´, A. A. Balkema, Rotterdam, Brookfield, 1991.

[125] L. B. Mwasumbi, University of Dar Es Salaam, Tanzania, personal communication.

[126] R. Brun, Z. V. Lun, *Vet. Parasitol.*,**1994**, *52*, 37-46.

[127] B. Raez, M. Iten, B. Y. Grether, R. Kaminsky, R. Brun, *Act. Trop.*, **1997**, *68*, 139-147.

[128] R. Kaminsky, R. Brun, *Antimicrob. Agents Chemother.*, **1998**, *42*, 2858-2862.

[129] M. Hills, C. Hudson, P. G. Smith, `WHO working paper no. 2.8.5´, WHO, 1986, Geneva.

[130] R. E. Desjardins, C. J. Canfield, J. D. Haynes, J. D. Chulay, *Antimicrob. Agents Chemother.*, **1979**, *16*, 710-718.

[131] R. A. Neal, S. L. Croft, *Antimicrob. Agents Chemother.*, **1984**, *14*, 463-475.

[132] B. Pagé, M. Pagé, C. Noel, *C. Int. J. Oncol.*, **1993**, *3*, 473-476.

[133] S. A. Ahmed, R. M. Gogal, J. E. Walsh, *J. Immunol. Methods*, **1994**, *170*, 211-224.

[134] M. Karobath, G. Sperk, *Proc. Natl. Acad. Sci USA*, **1979**, *76*, 1004-1006.

[135] U. Simmen, C. Saladin, P. Kaufmann, M. Poddar, C. Wallimann, W. Schaffner, *Plant. Med.*, **2005**. *In press*.

[136] E. Sigel, *J. Physiol.*, **1987**, *386*, 73-90.

[137] E. Sigel, R. Baur, G. Trube, H. Moehler, P. Halherbe, *Neuron*, **1990**, *5*, 703-711.

[138] P. B. Wingrove, K. A. Wafford, C. Bain, P. J. Whiting, *Proc. Natl. Acad. Sci. USA*, **1994,** *91*, 4569-4573.

[139] E. Sigel, R. Baur, R. Furtmueller, R. Razet, R. H. Dodd, W. Sieghart, *Mol. Pharmacol.*, **2001**, *59*, 1470-1477.

[140] S. Papajewski, `Isolierung und Strukturaufklärung von biologisch aktiven Pflanzeninhaltsstoffen aus *Cussonia barteri* Seemann (Araliaceae)´, Ph.D. Thesis, University of Hohenheim, 2000.

[141] S. Papajewski, B. Vogler, J. Conrad, I. Klaiber, G. Roos, C. U. Walter, R. Suessmuth, W. Kraus, *Plant. Med.*, **2001**, *67*, 732-736.

[142] L. A. Tapondjou, D. Lontsi, B. L. Sondengam, F. Shaheen, M. I. Choudhary, R. Atta-ur, F. R. Van Heerden, H. -J. Park, K. -J. Lee, *J. Nat. Prod.*, **2003**, *66*, 1266-1269.

[143] L. A. Tapondjou, D. Lontsi, H. Bouda, B. L. Sondengam, R. Atta-ur, M. I. Choudhary, F. R. Van Heerden, *Chem. Res. Comm.*, **2002**, *15*, 11-19.

[144] L. Harinantenaina, R. Kasai, K. Yamasaki, *Chem. Pharm. Bull.*, **2002**, *50*, 1290-1293.

[145] J. Gunzinger, J. D. Msonthi, K. Hostettmann, *Phytochem.*, **1986**, *25*, 2501-2503.

[146] M. A. Dubois, M. Ilyas, H. Wagner, *Plant. Med.*, **1986**, *2*, 80-83.

[147] T. G. Fourie, E. Matthee, F. O. Snyckers, *Phytochem.*, **1989**, *28*, 2851-2852.

[148] H. Weidong, L. Van Puyvelde, L. Maes, J. Bosselaers, N. De Kimpe, *Nat. Prod. Res.*, **2003**, *17*, 127-133.

[149] F. Trotin, L. Bezanger-Beauquesne, M. Pinkas, A. Robelet, *Ann. Pharm. Franc.*, **1972**, *30*, 555-560.

[150] H. Dadoun, A. Cave, *Plant. Med. Phyto.*, **1972**, *6*, 223-227.

[151] L. Harinantenaina, R. Kasai, K. Yamasaki, *Phytochem.*, **2002**, *61*, 367-372.

[152] L. Harinantenaina, R. Kasai, K. Yamasaki, *Chem. Pharm. Bull.*, **2002**, *50*, 1122-1123.

[153] L. Harinantenaina, R. Rakotondraibe, R. Kasai, K. Yamasaki, *Chem. Pharm. Bull.*, **2002**, *50*, 268-271.

[154] L. Harinantenaina, R. Kasai, K. Yamasaki, *Phytochem.*, **2002**, *60*, 339-343.

[155] `Roempp encyclopedia natural products´, Ed. W. Steglich, B. Fugmann, S. Lang-Fugmann, Thieme, Stuttgart, 2000.

[156] J. Bruneton, `Pharmacognosy, Phytochemistry, Medicinal Plants´, Intercept Ltd., Andover, 1995.

[157] R. Haensel, O. Sticher, E. Steinegger, `Pharmakognosie – Phytopharmazie´, Springer, Berlin, 1999.

[158] F. Bohlmann, T. Burkhardt, C. Zdero, `Naturally Occuring Acetylenes´, Academic Press, London, 1973.

[159] P. B. Kaufman, L. J. Cseke, S. Warber, J. A. Duke, H. L. Brielmann, `Natural Products from Plants´, CRC Press, Boca Raton, 1999.

[160] L. Hansen, P. M. Boll, *Phytochem.*, **1985**, *25*, 285-293.

[161] B. M. Hausen, J. Broehan, W. A. Koenig, H. Faasch, H. Hahn, G. Bruhn, *Contact Derm.*, **1987**, *17*, 1-9.

[162] J-M. Kim, J-E. Shin, M. J. Han, N-I. Baek, D-H. Kim, *Nat. Prod. Sci.*, **2003**, *9*, 158-160.

[163] J. Lutomski, T. C. Luan, T. T. Hoa, *Herb. Polon.*, **1992**, *38*, 137-140.

[164] J. H. Liu, S. Zschocke, E. Reininger, R. Bauer, *Pharma. Biol.*, **1998**, *36*, 207-216.

[165] J. Lutomski, T. C. Luan, *Herb. Polon.*, **1991**, *37*, 113-123.

[166] A. F. Magalhaes, E. G. Magalhaes, H. F. Leitao Filho, V. Nunes Junior, *Biochem. Syst. Ecol.*, **1992**, *20*, 783-784.

[167] D. Chapman, M. T. Kramers, C. J. Restall, in `Sterols and Bile Acids´, Ed. H. Danielsson, J. Sjoevall, Elsevier, New York, 1985, p. 151-174.

[168] M. Kobaisy, Z. Abramowski, L. Lermer, G. Saxena, R. E. Hancock, G. H. Towers, *J. Nat. Prod.*, **1997**, 1210-1213.

[169] B-Y. Park, B-S. Min, S-R. Oh, J-H. Kim, T-J. Kim, D-H. Kim, K-H. Bae, H-K. Lee, *J. Ethnopharm.*, **2004**, 404-408.

[170] J. A. Dale, H. S. Mosher, *J. Am. Chem. Soc.* **1973**, *95*, 512-519.

[171] G. L. Lemière, J. J. Willaert, R. A. Dommisse, J. A. Lepoivre, F. C. Alderweireldt, *Chirality*, **1990**, *2*, 175-184.

[172] M. J. Rieser, Y. Hui, K. K. Rupprecht, J. F. Kozlowski, K. V. Wood, J. L. McLaughlin, P. R. Hanson, Z. Zhuang, T. R. Hoye, *J. Am. Chem. Soc.*, **1992**, *114*, 10203-10213.

[173] I. Ohtani, T. Kusumi, Y. Kashman, H. Kakisawa, *J. Org. Chem.*, **1991**, *56*, 1296-1298.

[174] M. Senn, U. Simmen, E. Sigel, U. Séquin, R. Brun, U.K. Pat. 04 281 64.8, 2004.

E. Curriculum vitae

Personal data

Name :	Senn Martin Werner
Date and place of birth :	April, 17th 1968 in Dornach (SO)
Place of origine :	Buus (BL)
Nationality :	Swiss
Marital status :	married (2 children)

School education

1975 - 1980	Primary school, Reinach (BL)
1980 - 1984	Secundary school, Reinach (BL)
4/1984 - 4/1987	Apprenticeship as laboratory technician
1989 - 1992	Eidg. Matura in Economy

University education (University of Basel, Switzerland)

1993 - 1994	Basic studies I in Pharmaceutical Sciences
1994 - 1995	Basic studies in Medicine
1995 - 1996	Basic studies II in Pharmaceutical Sciences
9/1996 - 11/1996	Practical training at the hospital pharmacy of Kantonsspital Aarau (as part of the studies in Pharmaceutical Sciences)
12/1996 - 9/1997	Practical training at Kronen-Apotheke, Binningen (as part of the studies in Pharmaceutical Sciences)
9/1997	Federal diploma as assistant pharmacist
1997 - 1999	Specialised studies in Pharmaceutical Sciences
11/1999	Federal diploma in Pharmaceutical Sciences
9/2000 - 12/2004	Ph.D. thesis in Phytochemistry and Medicinal Parasitology : *'Structures and Evaluation of Biologically Active Constituents of Cussonia zimmermannii Harms',* supervised by Prof. U. Séquin, Department of Chemistry, University of Basel and Prof. R. Brun, Swiss Tropical Institute, Basel.

Professional experience

4/1987 - 12/1988	Employment as laboratory technician
1/1989 - 7/1989	Employment as laboratory technician
1997 - 1999	Deputyship as assistant pharmacist
2000 - 2004	Deputyships as pharmacist

Teaching experience

2002 - 2004	Teaching assistant Department of Chemistry, University of Basel

Lectures and courses of the following professors were attended during the pharmaceutical education at the University of Basel :

J-P. Barras, H. Durrer, J. Drewe, U. Eppenberger, A. Fahr, T. Günthert, D. Haag, A. Hädener, W. Häfeli, K. Hersberger, R. Hof, A. Kress, L. Landmann, H. Leuenberger, B. Meier, J. Meier, P. Oelhafen, H.-R. Olpe, M. Rüegg, H. Seiler, W. Schaffner, A. Scholer, U. Séquin, I. Sick, H. Sigel, P. Strazewski, P. Wolf, A. Zuberbühler.

Lectures and courses of the following professors were attended during the medicinal education at the University of Basel :

R. Baur, L. Hösli, Th. Kaden, D. Ladewig, L. Landmann, H. Mäcke, P. Oelhafen, U. Séquin, H. Sigel, W. Weber.

Lectures and courses of the following professors were attended during the post-graduate education at the University of Basel :

Th. Boller, H. Gampp, B. Giese, J. Meier, M. Oehme, U. Séquin, M. Tanner, N. Weiss, W. Woggon.